University of Kerbala

College of Science

Department of Chemistry

Study of Enzymatic Substitution Reactions of Phosphatidyl Derivative with Alcohol and Acidic Medium

A Thesis

Submitted to the Council of the College of Science - University of Kerbala

in Partial Fulfillment of the Requirements for the Master Degree in Chemistry Science

Written By

Ikram Salem Hussein

B.Sc. Chemistry (2012) / University of Kerbala

Supervised By

Assistant Prof. Dr. -Thaer Mahdi Madlool

December \ 2023 A.D **Jumada II \1445 A.H**

Supervisor Certification

I Certify examining that this thesis is conducted under my supervision at the department of chemistry, college of science university of Kerbala, as partial fulfillment of the requirement for the degree of M.Sc.in chemistry.

Signature 

Name: **Assistant Prof. Dr. Thaer Mahdi Madlool**

Address: University of Kerbala / College of Science

Date: 31/12/2023

Report of the Head of Chemistry Department

According to the recommendation presented by the Chairman of the Postgraduate Studies Committee, I forward this thesis for discussion.

Signature: 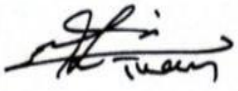

Head of Chemistry Department: **Assistant Prof. Dr. Thaer Mahdi Madlool**

Address: University of Kerbala / College of Science

Date: 31/ 12/2023

Examination Committee Certification

We the examining certify committee that we read this thesis and examined the student (Ikram Salem Hussein) in its contents and in our opinion, it is adequate as a thesis for the degree of Master of Science in Chemistry.

Signature
Prof Dr. **Narjis Hadi Al-Saadi**
Date: 15/ 1/2024
(Chairman)

Signature
Prof Dr. **Hanaa Addai Ali**
Date: 15/1/2024
(Member)

Signature
Assist. Prof Dr. **Rehab Jassim Mohammed**
Date: / /2024
(Member)

Signature
Assist. Pro. Dr. **Thaer Mahdi Madlool**
Date: 15/1/2024
Member (Supervisor)

I have certified upon the discussion of the examining committee.

Name: Prof .Dr. **Hassan Jameel Jawad Al-Fatlawy**
Date: Date: / /2024
Address: Dean the College of Sciences
University of Karbala

Dedication

To the Awaited Beloved and the Savior of Humanity ... Imam Mahdi may Allah hasten his reappearance

To whom the words race to express themselves to the one who taught me and suffered hardships to get to what I am ... To my mother

To my husband, beloved sons Zahraa,

Mohammed and Baraa

To my sister and all my family

To everyone who taught me a letter, light the way in front of me

To science and its pioneers and students

To you I dedicate the result of my research effort and my humble message, hoping from Allah Almighty finds acceptance and success

Ikram Salem Hussein

Acknowledgments

First and foremost, praises and thanks to the Allah, the Almighty, for His showers of blessings throughout my research work to complete the research successfully.

My supervisor, Assistant Prof. Dr. - Thaer Mahdi Madlool, deserves recognition and my sincere gratitude for making this work possible. His direction and counsel saw me through the entire project writing process. In addition, I want to express my gratitude to my committee members for making my defence a fun experience and for their insightful remarks and recommendations.

Additionally, I want to express my gratitude to my husband and my entire family for their unwavering support and tolerance as I conducted my research and wrote my project.

As well I thank the management of the chemistry department and its staff, for their support to do this work and complete this thesis successfully.

Finally, my thanks go to all the people who have supported me to complete the research work directly or indirectly.

Ikram Salem Hussein

Summary

The phospholipids (PLs) play an important role in building up all the cells membrane of the animals. In addition, PLs are amphiphilic compounds that are widely found in the living system. In general, PLs can be divided into two groups: sphingomyelin and glycerophospholipids, which include phosphatidylcholine (PC), phosphatidylserine (PS), phosphatidylethanolamine (PE), phosphatidylglycerol and phosphatidylinositol.

The hydrolysis of the PLs is the main reaction for lipolysis that catalyzes in presence of specific enzymes known as phospholipases. In *vitro*, there are many studies to understand the mechanism of the phospholipolytic PLs and what the effect of the environment on this reaction.

The current study focused on monitoring of the hydrolysis reaction of PC in acidic medium and compared of the same reaction in alcoholic medium to find the effect of alcoholic environment on this reaction. In addition, this work focuses on the enzymatic hydrolysis reactions of the two PLs derivatives, which are phosphatidylcholine and phosphatidylserine, in water as well as in ethanol catalyzing by phospholipase D to find the impact of the toxic concentration of ethanol that may lead to damage to the cell membrane. The study shows that there is clear impact of the change of the nitrogen bases of phospholipids and the environment of the hydrolysis on the activity of the enzymatic catalyzing.

All products for the hydrolysis of PC in both the acidic and alcoholic environments were isolated and characterized using the GC-Mass, NMR, and FTIR spectroscopy.

Depending on the results, the mechanisms of the hydrolysis of PC in acidic and alcoholic environments were suggested. The final products of the hydrolysis of PC in acidic medium were choline chloride, palmitic acid, octadeca-9,12-dienoic acid, and glycerol-3-phospate. However, the hydrolysis of PC in ethanol provided the following products: choline chloride, ethyl palmitate, ethyl octadeca-9,12-dienoate, and glycerol-3-ethylphospate. It can be noted that the glycerol-3-phosphate was formed in both reactions as backbone of the PC also the choline chloride was produced during the dissociation from the phosphate group of the PC.

The same reactions above were repeated for two phospholipids, which were the PC and PS, respectively, in presence of phospholipase D (PLD) as catalyst. The kinetics of dissociation of the choline from the phosphate-group in presence of PLD were studied by applying the Michaelis-Menten equation. The maximum velocity (V_{max}) and the Michaelis-Menten constant (K_m) for all the enzymatic hydrolysis of PC and PS in presence of PLD at the acidic and alcoholic environments were determined. The affinity between the phospholipid PC and the enzyme in the case of using ethanol as a solvent was the least among the other reactions because it had the highest K_m value of 3.664. However, the enzymatic hydrolysis reaction of PS was the highest affinity among others by having the lowest K_m value.

In addition, the optimization of the enzymatic hydrolysis reactions which were included the concentration of the substrate, the enzymatic activity, the pH, and the temperature were performed to ensure that this enzymatic hydrolysis mimics that occurs in a living system. The thermodynamic parameters, which include enthalpy change (ΔH), Gibbs free energy change (ΔG) and entropy change (ΔS) were determined. All the

enzymatic hydrolysis reactions of PC and PS in presence of PLD were thermodynamically favorable and not spontaneous.

This study has exhibited that all hydrolysis reactions of the phospholipids in the absence of the enzyme are slower than that in presence of the PLD. Consequently, all products for the hydrolysis of PC without enzyme were smoothly isolated and characterized. However, it could not isolate the products for the enzymatic hydrolysis of the PC and PS due to the reactions being very fast.

Despite the similarity in mechanisms of the hydrolysis reaction of the phospholipids (PC and PS) in different environments (acidic and alcoholic), the differences in byproducts may provide us with a good vision to predict the impact of the solvent on this process. Due to the various applications of phosphatidylcholine and phosphatidylserine, understanding of the effect of the alcoholic environment can help pharmaceutical, cosmetic, and food factories to design appropriate experiments to reduce the impact of these byproducts on the main product efficiency and yield.

List of contents

List of Tables

List of Figures

Appendixes

List of Abbreviations and symbols

Abbreviation	Terms
1,2-DAG	1,2-diacyl glycerol
1,2-DPPC	1,2-dipalmitoyl-sn-glycero-3-phosphocholine
A	Absorbance
pKa	Acid dissociation constant
pH	Acidic function
E_a	Activation energy
ATP	Adenosine triphosphate
Asp	Asparagine
b	Broad
iPLA2	Ca^{2+}-independent PLA2
BE-PSS	Calcium-dependent base exchange – phosphatidyl serine synthase
^{13}CNMR	Carbone-13 nuclear magnetic resonance
PAs	Cardiolipin
˚C	Celsius
cm	Centimeter
CoA	Coenzyme A
CoQ10	Coenzyme Q10
C	Concentration
$[S]_T$	concentration of the substrate at a certain time
$[S]_\circ$	concentration of the substrate at zero time
CD-PSS	Cytidine diphosphate diacyl glycerol-dependent phosphatidylserine synthase
CDP-ethanolamine	Cytidine diphosphate-ethanolamine
cPLA2	Cytosolic Phospholipase A2
DAG	Diacylglycerol
DGK	Diacyl glycerol kinase
DMSO-d^6	dimethyl sulfoxide–d^6
ER	Endoplasmic reticulum
EC number	Enzyme Commission number
EC	Enzyme Commission of the International Union of Biochemistry
HKD	Enzymes have HXKX4 D consensus sequence where X signifies any kind of residue
non-HKD	Enzymes not have HXKX4 D consensus sequence where X signifies any kind of residue
V̇ max	Equals half the maximum speed
E. coli	*Escherichia coli*

Abbreviation	Terms
EPs	Ether phospholipids
FAs	Fatty acids
FTIR	Fourier- Transform Infrared Radiation
CoQ10	Fully oxidized ubiquinone
CoQ10H2	Fully reduced ubiquinol
GC-mass	Gas Chromatography and Mass spectroscopy
R	Gas constant
G-3-P	Glycerol-3-phosphate
PCs	Glycerophosphocholines
PEs	Glycerophosphoethanolamines
PGs	Glycerophosphoglycerols
PIs	Glycerophosphoinositols
GPLs	Glycerophospholipids
PSs	Glycerophosphoserines
g	Gram
GEFs	Guanine nucleotide exchange factors
GPCRs	Guanine nucleotide-binding protein-coupled receptors
GTPases	Guanosine triphosphate hydrolases
GAPs	Guanosine triphosphate hydrolases-activating proteins
HDL	High density lipoprotein
His	Histidine
h	Hour
KIAA0725p	Human expressed sequence tag clone bind to p125
J	Joule
k	kelvin
Kcal	Kilocalories
LDL	Low density lipoprotein
Lys	Lysine
LPLA2	Lysosomal phospholipase A2
L-α-GPC	L-α-glycerylphosphorylcholine
p125	Mammalian Sec23p-interacting protein
M(IP)2C	Mannosyl-diinositolphospho-ceramide
λ max	Maximum wavelength
m	Medium
mPA-PLA1b	Membrane-associated phosphatidic acid - selective phospholipase A1 member b
mPA-PLA1a	Membrane-associated phosphatidic acid (PA)-selective phospholipase A1 member A
K_m	Michaels constant
mM	Mill molar
mg	Milligram

Abbreviation	Terms
ml	Milliliter
min	Minute
Ɛ	Molar absorption coefficient
nm	Nanometer
ln k	Natural logarithm of the reaction rate constant
N	Normally
NMR	Nuclear magnetic resonance
PO	Palmitoyl
PNPLA	Patatin like phospholipase
PA	Phosphatidic acid
POPC	Phosphatidyl choline
PC	Phosphatidyl choline
PC-PLCs	Phosphatidylcholine-specific phospholipases C
POPE	Phosphatidyl ethanolamine
PE	Phosphatidyl ethanolamine
PG	Phosphatidyl glycerol
POPI	Phosphatidyl inositol
PI	Phosphatidyl inositol
PI-PLCs	Phosphatidyl inositol -specific phospholipases C
PI-PLCs	Phosphatidyl inositol -specific phospholipases C
PS	Phosphatidyl serine
POPS	Phosphatidyl serine
PSS1	Phosphatidyl serine synthase 1
PSS2	Phosphatidyl serine synthase 2
PS-PLA1	Phosphatidyl serine-specific phospholipase
PLAATs	Phospholipase A/acyltransferases
PLA1	Phospholipase A1
PLA2	Phospholipase A2
PLB	Phospholipase B
PLC	Phospholipase C
PLD	Phospholipase D
PLD1	Phospholipase D 1
PLD2	Phospholipase D 2
PLs	Phospholipids
^{31}PNMR	Phosphorus-31 nuclear magnetic resonance
PSLs	Phosphosphingolipids
PAF-AH	Platelet-activating factor acetyl hydrolase
PUFAs	Polyunsaturated fatty acids
PUFAs	Polyunsaturated fatty acids
PMF	Primary myelofibrosis

Abbreviation	Terms
^{1}HNMR	Proton-1 nuclear magnetic resonance
PLP	Pyridoxal phosphate
CoQ10H	Radical semiquinone intermediate
V	Rate of the enzymatic reaction
k	Reaction rate constant
1/T	Reciprocal of temperature
RNAs	Ribonucleic acids
sPLA2	Secreted Phospholipase A2
sp	*Streptomyces*
s	Strong
PSD	The enzyme phosphatidyl serine decarboxylase
EC 7	The seventh enzyme category
SPO14	The SPO14 gene encodes phospholipase D, which catalyzes the hydrolysis of phosphatidyl choline
PSS	The synthase of phosphatidyl serine
TLC	Thin layer chromatography
Tween 20	Type of surfactant
UV-Vis.	ultra violate – visible spectroscopy
U	Unit
VLDL	Very low density lipoprotein
w	weak

Chapter one

Introduction and Literature Review

1.1 Introduction :

Phospholipids (PLs) are amphiphilic molecules, it have important roles to bull up the lipophilic moiety as well as the hydrophilic group that is phosphorylated. In addition, phospholipids are considered as the structural foundation for biological membranes in human, plant, and animal cells as well as in subcellular organelles. Along with organizing and controlling the activity of embedded proteins, PLs also control the biophysical characteristics of membrane bilayers such fluidity and permeability (1-3). Additionally, polyunsaturated fatty acids (PUFAs) at the structure of membrane PLs play significant roles as precursors of the variety of signaling molecules, including eicosanoids, leukotriene, prostaglandins, and thromboxane, which are crucial regulators of both pro-inflammatory and anti-inflammatory signals (4-6).

Based on the composition of PL backbones, phosphosphingolipids (PSLs) and glycerophospholipids (GPLs) are the two main families of PLs(3). Generally, the structure of PL involves the two fatty acids (FAs), which bind through ester bonds to the L-glycerol in the locations (*sn*-1 and *sn*-2) to create the diacyl moieties that build up the lipophilic segment of GPLs (3, 7). Commonly, the saturated fatty acids (FA) binds at the *sn*-1 position and the unsaturated FA typically binds at the *sn*-2 location in plants and animals GPLs. Furthermore, the ether phospholipids (EPs), are found in both microbial and animal organisms, in this type of PLs the lengthy O-alkyl or O-alkenyl chains bind with the backbone of glycerol instead of the FA at

the *sn*-1 and *sn*-2 positions. Moreover, the PSLs have a long-chain of the amino alcohol-sphingoid base as their main structural component. Sphingoid bases depend on their source in terms of their alkyl chain length about twelve to twenty-two atoms of carbon, the placement of the double bonds and the degree of unsaturation. For example, the sphingosine with eighteen carbons (2-amino-4-octadecene-1,3-diol) links with the FA by an amide bond which usually saturated, is the greatest widespread sphingoid base found in tissues of animals. In plants, ceramides are the amides (3, 7). (2-amino octadecano-1,3,4-triol) Phytosphingosine or its unsaturated analogues and are the most prevalent Sphingoid base (8, 9). The hydroxyl group at glycerol's sn-3 location link with the hydrophilic group's hydroxyl group and the sphingoid base's first carbon atom are substituted by phosphodiester bond as a polar moiety of GPLs, EPs, and PSLs (3, 10). The group of phosphonic, that is located in the phosphono sphingolipid and glycerolophosphonolipids structures, can take the place of the ortho-phosphate group. In this instance, the phosphorus atom in the phosphono group directly binds to the carbon atom of the hydrophilic group (11). The hydrophilic group's structure allows for the division of PLs into various categories such as glycerophosphoethanolamines (PEs), glycerophosphocholines (PCs), glycerophosphoinositols (PIs), glycerophosphoglycerols (PGs),glycerophosphoserines(PSs),glycerophosphoglycerophos phoglycerols (Likewise referred to as cardiolipin (PAs) (12, 13).

Chemical reactions are speed up and catalysed by macromolecular biological catalysts called enzymes(14, 15).

Enzymes are recognised to catalyse a variety of biological reactions, not just those in the food, increasing the rate of the reaction due to decrease of the activation energy (16). In addition, enzymes have the significant roles in the variety of industrial productions that include dyes, food, pharmaceuticals, textiles, leather, water purification, cosmetics, as well as additional biofuels (17, 18). Recently, the enzymes are used in industry to increase the yield of productions. The use of enzyme hydrolysis provides excellent specificity and efficiency in comparison to traditional processes depending on high temperatures and acid-base (19, 20). The enzymatic reactions can also be conducted in milder settings with lower levels of pollutants and waste products (21). Additionally, enzymes are altered in the different ways, and are generally nontoxic (22, 23). According to the global assessment on enzyme sales, food enzymes accounted for 31% of sales, feed enzymes for 6%, and technical enzymes for the remaining percentage. (24). On the other hand, enzymes are extremely expensive for commercial applications and have a poor degree of stability under adverse conditions. Stability, enhancing enzyme activity, enzymatic efficiency , and reuse capacity are of highly desirable in order to address these shortcomings (25) .

In 1968, Koning and McMillan conducted the hydrolysis for lecithin (phosphatidylcholine) in presence of hydraulic acid. They identified and statistically calculated the major hydrolytic products. A reaction mechanism for the acid hydrolysis of the aforementioned substances is hypothesized based on the data acquired (26)

1.2. Literature Review

1.2.1. Phospholipid

The essential lipids in the eukaryotic cell membrane are glycerophospholipids, sphingolipids, and sterols as shown in Fig. 1-1 (27). In nature, there are 180,000 different species of lipids making them numerous and distinct(28). One of the fundamental eukaryotic model species, the budding yeast *Saccharomyces cerevisiae*, is predicted to have a lipidome of roughly 300 compounds(29, 30).

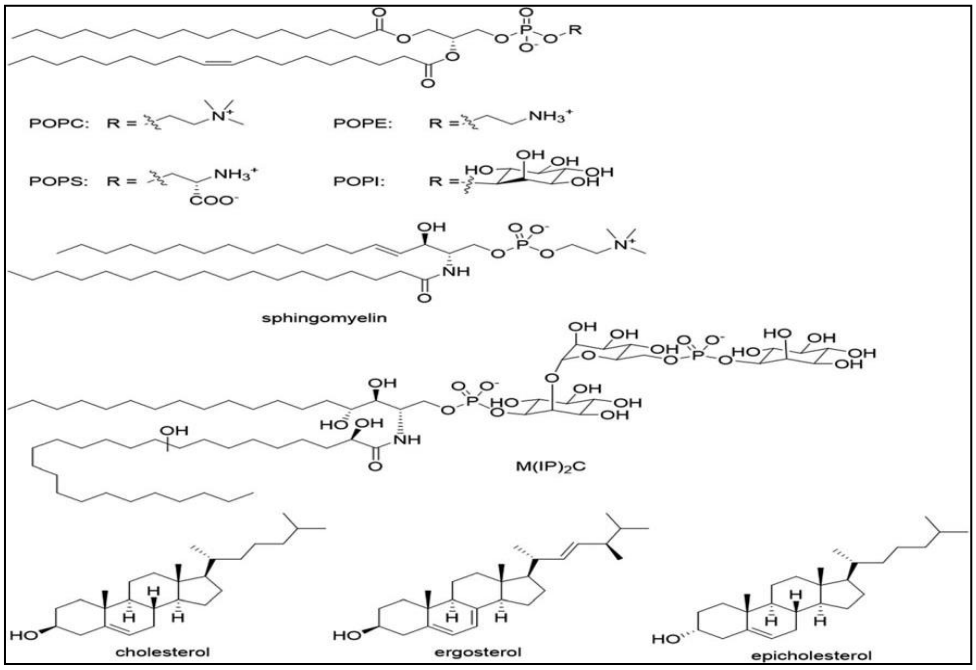

Figure (1-1): **Phospholipids', sphingolipids', and sterols' chemical structure.(31)**

Where Phosphatidylcholine (POPC), phosphatidylethanolamine (POPE), phosphatidylserine (POPS), and phosphatidylinositol (POPI) are displayed. The acyl groups are oleoyl and palmitoyl (PO). Major sphingolipids found in both humans and yeast are sphingomyelin and mannosyl-diinositolphospho-ceramide

(M(IP)2C), respectively. Three sterols are displayed: epicholesterol, which has a 3a stereochemistry and is frequently employed in sterol-binding investigations, ergo sterol, which is found in fungi, and cholesterol, which occurs in humans.(31)

All living organisms have phospholipids, which are important parts of their biological membranes. Phodpholipids are broadly divided into sphingomyelin and glycerophospholipids, including phosphatidylserine (PS), phosphatidylcholine (PC), phosphatidylethanolamine (PE), phosphatidylinositol (PI), and phosphatidylglycerol (PG) (32). In addition, the phospholipids are arranged as lipid bilayer, and have profound roles in both the composition and operation of biological membranes (32).

Phospholipids are ubiquitous amphiphilic molecules(2, 33, 34). The chemical structure of PLs involve the glycerol backbone binds to the two acyl residues obtained from fatty acids sites sn-1 and sn-2 on the carbon chain as well as the phosphodiester group in the sn-3 position as a polar head, see Fig. 1-2 for more information. Therefore, PLs have an intermediately polarized glycerol backbone, a polar hydrophilic head group, and the hydrophobic moiety made up of two fatty acid chains. The FAs chains of glycerophospholipids consist of the range of chain lengths and unsaturation states(2, 35, 36). FAs were typically discovered in the dietary supplements include linoleic acid (18:2Δ9,12), or 9-12octadecenoic acid, and oleic acid (18:1Δ9) or 9-octadecenoic acid, alpha-linolenic acid (18:3Δ9,12,15) or 9,12,15-octadecatrienoic, , and arachidonic acid (20:4 Δ5,8,11,14) is another name for 5,8,11,14-eicosatetraenoic acid (37).

The majority of the PLs have categories according to either the polar head's features Fig. 1-2, or their structural of fatty acids substituents used and the isomerism of the region in which are found(38, 39). However, numerous classification schemes exist for phospholipids, depending on factors such as their relative abundance (major lipids versus minor lipids, or less than 5% of all phospholipids), neutral vs. anionic net charges, metabolic fluxes(acute versus somewhat constant concentration) rapid turnover and production/interconversion), their place of manufacture (where something is made), their shape (conical, straight, or inverted); exported conical), and the number of unsaturated. In general, several phospholipids, including PC and PE, are generally regarded as "structural" lipids since they are required to build a barrier that deters water (40).

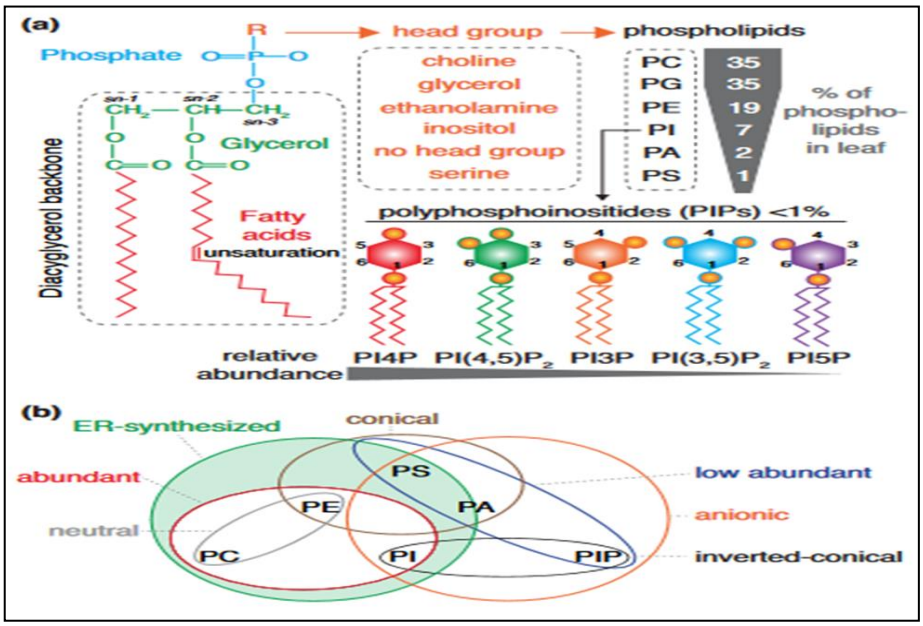

Figure (1-2): properties of phospholipids (a) A schematic of phospholipid general structure showing the relative amounts of each phospholipid species as determined in an Arabidopsis leaf. A Euler diagram showing the phospholipid characteristics is shown in (b). (40)

Most of glycerophospholipids are produced in the endoplasmic reticulum, but some of them are also formed in the inner mitochondrial membrane. Typically, the formation of PLs can be summarized as the following; (i) Glycerol-3-phosphate (G-3-P) molecule synthesis via glycolysis, (ii) FAs bind with the backbone of G-3-P in presence of FA acyl coenzyme A (CoA), (iii) addition of a hydrophilic head group, such as phosphocholine, to form PC, and (iv) dephosphorylation to 1,2-diacylglycerol(1,2-DAG).Certain glycerophospholipids are created by altering already present molecules, which are like phospholipid head groups being replaced or ethanolamine groups being methylated to produce choline. (40)

Phospholipids were inattention due to the idea that the PLs were merely inactive structural and metabolic substances with methodological issues until the 1950s, when publications elucidating their biosynthesis process started to appear. The study of phospholipids' physiological and metabolic functions is a vibrant and fascinating field right now. The extensive studies showed that the PLs are physiologically active substances (41). In addition to serving as the primary element in all biological membranes, PLs exhibit great biocompatibility as well as corresponding to the inherent characteristics of the individual molecules that offer the variety of intriguing applications .The PLs have positive benefits on human health (42, 43) and are the nourishing source of fatty acids, organic phosphate, and choline (44). The various of biomedical studies focused on the application of PLs to produce the model systems of biological membranes (45). In actuality, PLs play important roles in the

variety of biological processes (46). In addition, PLs have extremely role in molecule transportation through the cell membrane, are capable of promoting the biological activity of several membrane-bound proteins and receptors, which can be used as diagnostic biomarkers for specific diseases, and can be used as therapeutic agents (47-50). Additionally, PLs have a role in the differentiation and cellular regeneration of neural circuits (51, 52). A variety of human disorders, including coronary heart disease, cancer, and inflammation, can be prevented by dietary PLs (53). Additionally, these molecules' amphiphilic character is the primary cause of their special ability to spontaneously aggregate in watery conditions. The medicine delivery, diagnostic testing, and cosmetic industries are all highly interested in PLs ability to spontaneously self-associate to create supramolecular structures such bilayers, micelles, and liposomes (54). A wide range of PLs formulations have been used in clinical applications due to the PLs based as drug delivery system's to success in delivering medications effectively (55-57). Antioxidants, vitamins, essential oils, tastes, fatty acids, and enzymes are just a few examples for the types of substances that can be contained in liposomes(58, 59), and their gastro-resistance is a vital component in the formulation of bioactive compounds (60). The industrial use of PLs as food stabilizers, detergents, emulsifiers, surfactants, and antioxidants is also significant (44, 61). As a result, it is clearly noted that the PLs preparation approaches can apply at different fields in living system (40).

PLs are abundant in nature (62), and they can be obtained from both plants and animals sources, such as krill, peanuts, soy, milk, bovine brain, egg yolk, maize, rapeseed, sunflower linseed, and wheat germ (44, 63-65).

1.2.2. Types of Phospholipids:

1.2.2.1. Phosphatidylcholine (Lecithin):

The most prevalent phospholipid found in every mammalian cell types and subcellular organelles is phosphatidylcholine (PC) (66). Typically, the PC has important roles to build up 40–50% of all cellular phospholipids(67). The PC has a positively charged choline linked to the phosphate (68, 69). The hydrophilic part of the PC consists of choline, phosphate, and glyceride while the hydrophobic part consists of fatty acids of glycerol (70-72) (Fig. 1-3). The PC was initially identified as a phospholipid. Lecithin was firstly named, which was derived from the Greek word lekithos, which meaning egg yolk (73, 74). The expression "lecithin" describes a mixture of plant and animal based PLs with different polar head and acyl chain compositions. Lecithin is frequently produced industrially today by processing animal organs, soy beans, egg yolk, milk, biomass, and vegetable oils (2, 44). Egg yolk and soybeans are the main sources of commercial lecithin in terms of quantity. Triglycerides, carbohydrates, PLs, and other small substances make up the majority of lecithin composition (75).

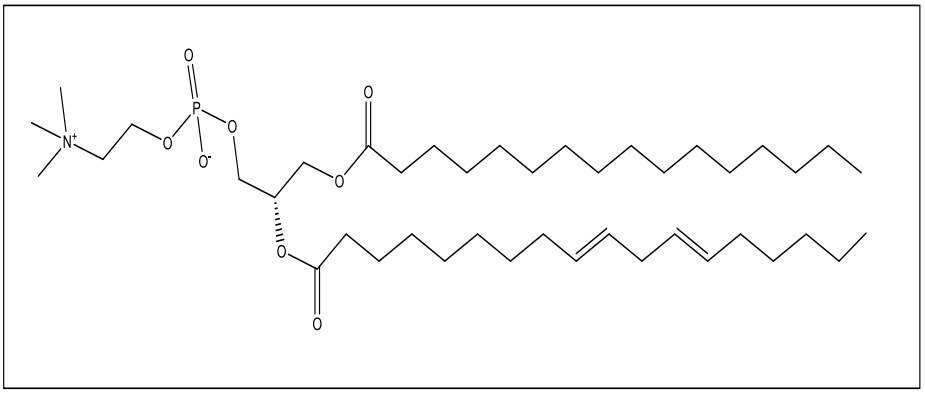

Figure (1-3): The chemical structure of phosphatidylcholine used in this study.(76)

Phospholipids have numerous biological purposes. For instance, in addition to the PLs role in cell membrane function, PLs and particularly PC, have digestive and metabolic roles in bile (as monoacyl phospholipids, or lyso-phospholipids) to solubilize cholesterol and fatty components in meals as well as lipophilic medicinal compounds(77). Furthermore, the phospholipids have the function as vital fatty acid and energy sources as well as lipoprotein components for the transportation of fat from the gut to the liver (78). In addition, lung surfactant contains a specific phospholipid called 1,2-dipalmitoyl-sn-glycero-3-phosphocholine (DPPC)(79). This reduces the surface tension at the air/water interface inside the alveoli of the lung. (80). The PC plays various roles in the regulation of blood coagulation (81) , apoptosis (82), and during the development of bone to deposite of the lipid-calcium-phosphate complex (56).

Johann (14) "shown that phosphoric acid, glycerol, and an organic base with a nitrogen atom were the byproducts of the complete hydrolysis of lecithin" . This group of phosphatides is known as the phosphoglycerolipid.

1.2.2.2. Phosphatidylethanolamine (Cephalin):

Phosphatidylethanolamine (PE), which builds up about 40% of all phospholipids in mitochondrial inner membranes, and 15–25% of all phospholipids for other organelles. Hence, the PE is considered as the second of the most common phospholipid in mammalian membranes (83). An ethanolamine group is joined to the phosphate in phosphatidylethanolamine. Both the PC and the PE have the neutral overall charge, so are found as zwitterion form (2) (Fig. 1-4).

In addition, PC and PE are sub classified as diacyl, alkyl acyl, or alkenylacyl phospholipids, respectively, depending on whether they have acyl-, ether-, or vinyl-ether linkages at the *sn*-1 location (84, 85). In rat and human liver, the great majority (95–100%) of PE and PC is diacylated (86). There are four distinct pathways exist in cellular mammalian systems for PE synthesis: the cytidine diphosphate-ethanolamine (CDP-ethanolamine) pathway, the base-exchange pathway, the phosphatidylserine decarboxylase (PSD) pathway (87), and the acylation of lyso-phosphatidylethanolamine (88),(89).

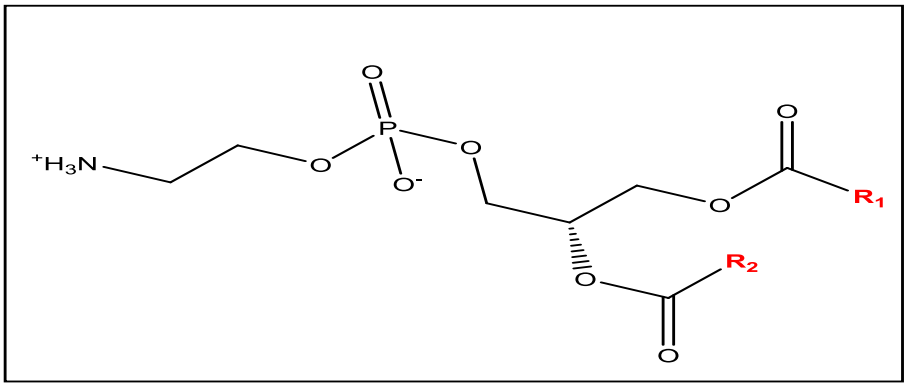

Figure (1-4): Represents the fatty acids (R_1, R_2) , the phosphate group, and the ethanolamine attached to the glycerol backbone.(76)

Many different molecular types of PE with the various acyl chains at the *sn*-1 and *sn*-2 positions are characterized in mammalian cells (90). Phospholipases and lysophospholipids acyltransferases involved in a remodelling process that results in this acyl-chain variety, at least in part (90). The head group components of membrane phospholipids as well as the acyl-chain composition determine the membrane's physical characteristics. For instance, the PE molecule's cone shape encourages membrane curvature , and PE's capacity to improve fusion of membranes is correlated with its capacity to create membranes with hexagonal II phases (91). Due to the physical characteristics of PE. It is additionally necessary for the dissolution of contractile rings near the mammalian cells' cleavage furrow at cytokinesis (92). Additionally, Dowhan's team demonstrated a number of cutting-edge investigations that " PE significantly affects the structure of membrane proteins in *E. coli*, including lactose permease, and aids in their folding by functioning as a "lipid chaperone" (93). In addition, the PE has essential role to build up the plasma lipoproteins including very low density lipoprotein (VLDL), low density lipoprotein (LDL), and high density lipoprotein (HDL). The neutral lipid core of the lipoprotein particles, principally triacylglycerols and cholesteryl esters, is surrounded by an outer monolayer of phospholipids, which is necessary for the production and stability of the particles (93, 94).

In addition to these crucial roles, PE also plays important roles in autophagy in mammalian cells (95). Moreover, the PE provides the ethanolamine moiety of the

glycerophosphatidylinositol anchors, which attach to the plasma membrane and trigger a variety of signaling proteins on the cell surface. (96). In addition, Anandamide, also known as N-arachidonoylethanolamine, is a ligand for the brain's cannabinoid receptors and the precursor of PE. (97).

1.2.2.3. Phosphatidylserine (PS):

Folch's team discovered phosphatidylserine species in whole brain lipid extracts for the first time in the 1940s (98). The PS has a polar head group, just like other phospholipids Fig. 1-5 (neutral serine group attached with the phosphate and thus has an overall negative charged) (70) linked to position *sn*-3 and two acyl chains at locations *sn*-1 and *sn*-2 of the glycerol moiety. Saturated fatty acids and have sixteen or more carbons are often connected to PS's sn-1 location, conversely, unsaturated fatty acids are typically located at the *sn*-2 site, even if different cell types and organelles have different acyl chains in PS.

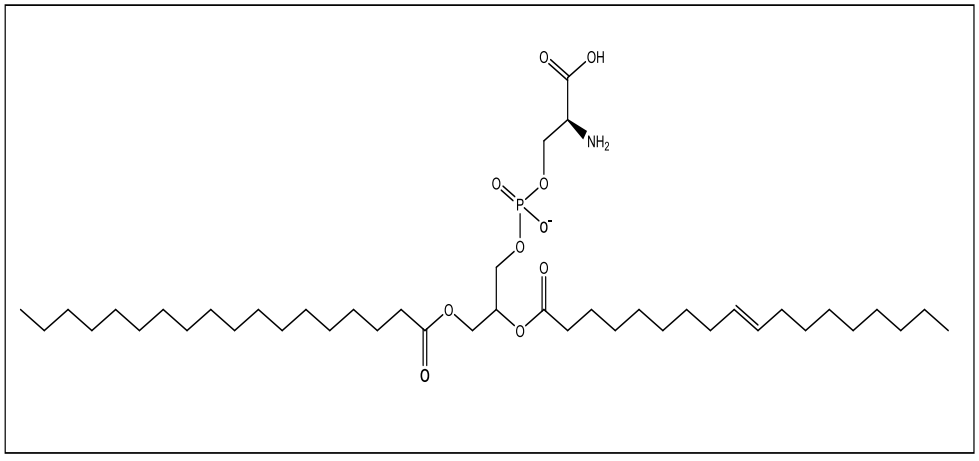

Figure (1-5): Two acyl chains, a glycerol backbone, and a phosphate head group make up the typical PS structure. (76)

The PS bulids up the small portion of the most cellular membranes. The physiological significance of PS, which is due to its special physical and biochemical features, outweighs its modest abundance, though. Important actions including the elimination of apoptotic cells and the host cells' absorption of viruses are signaled by PS, It is necessary for the induction and initiation of several enzymes and structural elements (99, 100). The PS disperses in the cell as an asymmetrical manner, probably even more so than other types of phospholipids. Finding PS's distribution within cells is a challenging issue takes on a significant dimension in light of its numerous and essential physiological activities (101). Both the calcium-dependent base exchange - phosphatidylserine synthase type (BE-PSS) and the cytidine diphosphate diacylglycerol-dependent phosphatidylserine synthase (CD-PSS) are potential pathways for PS production. The first PC was characterized in the mammals, where PS is produced from PE or PC as substrates in calcium-dependent base exchange type reactions(102). The biosynthesis of both PS and phosphatidylserine synthase (PSS) catalyzes the replacement of the polar head group of the PE or PC with L-serine, phosphatidylserine synthase 1(PSS1) and phosphatidylserine synthase2 (PSS2) to release the choline from PC and the ethanolamine from PE, respectively. While PS is produced by a different mechanism (CD-PSS) in prokaryotes and yeast at the second pathway (102).

1.2.2.4. Phosphatidylinositol (PI):

In mammalian cells, the minor anionic lipid phosphatidylinositol (PI) is present. Its components include a

backbone of glycerol, the two chains of acyl that are esterified at locations *sn*-1 and *sn*-2 , and an inositol ring that the phosphate group attaches to the position of *sn*-3 (Fig. 1-6) (103). About 5–10% of the overall lipids in mammalian cells are made up of PI, but it performs a significant function as the starting point for the production of seven PI phosphorylated derivatives (104). Lipid kinases can phosphorylate the inositol head group's to three hydroxyls, which are monophosphorylated, diphosphorylated, and triphosphorylated, that leads to form the inositol head group's negative charge. The activities of phosphorylated PIs in the cell are numerous and include membrane crossing, actin cytoskeleton control, phospholipase C (PLC), and phosphoinositide 3-kinases-mediated cell signalling, , autophagy, endocytosis protein recruitment (104).

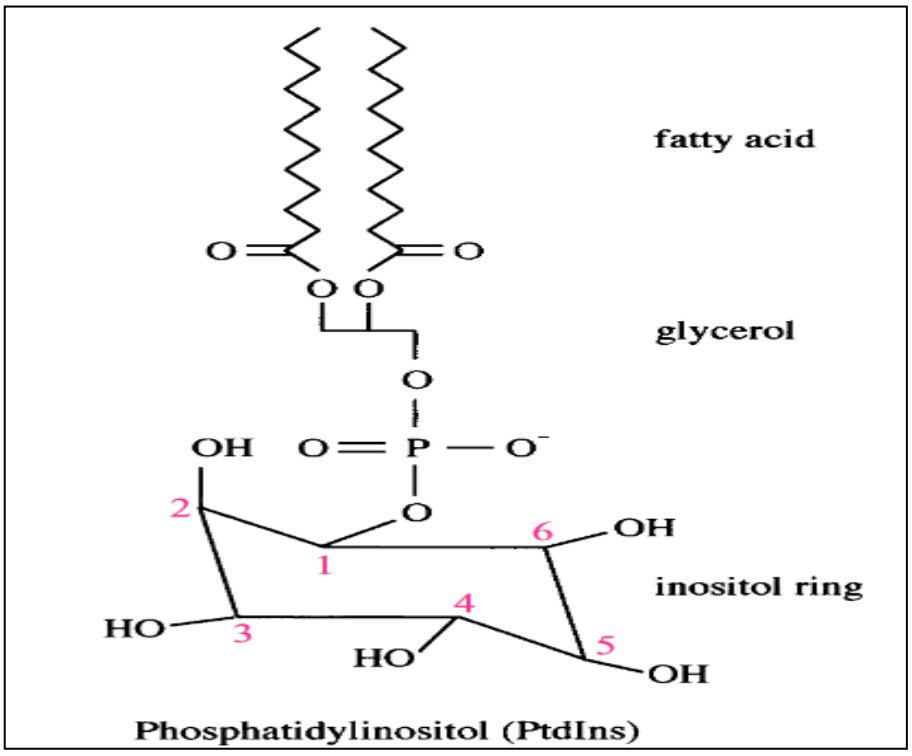

Figure (1-6): Illustration of phosphatidylinositol structure. The head group carbon atoms of phosphatidylinositol are labeled. In cerevisiae,

the major fatty acids present on the *sn*-1 and *sn*-2 positions of glycerol are oleic acid (C18:1) and palmitic acid (C16:0), or palmitic acid and palmitoleic acid (C16:1). The *sn*-3 carbon of the glycerol is connected to the inositol ring with five hydroxylated carbon atoms by a phosphate group in position 1.(105)

The biggest the cell's membrane compartment is the endoplasmic reticulum (ER),where phosphatidylcholine(PC), phosphatidylethanolamine (PE), phosphatidylserine (PS), phosphatidylinositol (PI) and triacylglycerol are synthesized (104). Other organelles' cytosolic facing surfaces frequently undergo PI phosphorylation not at the ER, but by resident kinases (104).

1.2.2.5. Phosphatidylglycerol (PG):

In natural membranes, one of the most prevalent phospholipids found is phosphatidylglycerol (PG) as shown in (Fig. 1-7). In 1985, the study showed that the PG has role as an emulsifier for drug delivery systems, and it has a great ability to form the liposomes (106). In fact, the PG have special lubricant/surfactant qualities when combined with the intact proteins. By comparison with the other mammalian membranes, as an example, it can be discovered in relatively considerable concentrations in the lungs of mammals that leads for focus the studies about the production of surfactant formulations for use in therapeutic procedures to treat a range of diseases, encompassing respiratory distress syndrome in neonates (107).

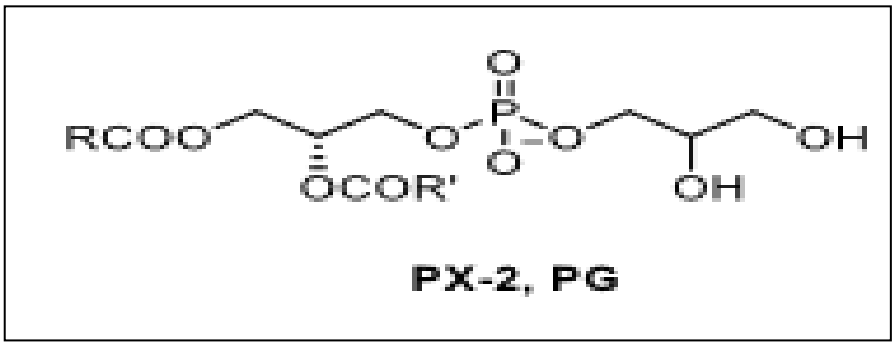

Figure (1-7): The chemical structure of phosphatidylglycerol. Where R and Ŕ represent the fatty acids attached to the glycerol backbone in the site *sn*-1 and *sn*-2 respectively. As for the glycerol moiety, it is attached to the phosphate group linked in turn to the backbone of glycerol in *sn*-3 position. (106)

Although PG is naturally found as the PL, it is only found as a little amounts in nature, as a result many researchers have successfully prepared it in presence of enzymes (108).

For instance, Piazza's team showed that the phospholipase D (PLD) from *Streptomyces (sp.)* produced PG that was almost quantifiable yields at the phospholipase D has a greater glycerol selectivity than cabbage PLD because the molar ratio of glycerol to PC is 5 to 3. (109).

1.2.2.6. Phosphatidic Acid (PA):

Phosphatidic acid is the simplest GPL (110) Fig. 1-8, and it is an effective lipid secondary messenger that leads to the variety of signaling reactions in the cell. PA has the roles in the variety of inside-the-cell activities like vesicular trafficking, membrane biogenesis and cytoskeletal rearrangements. In addition, PA effect on cellular behaviors such as growth, migration, and survival, via changing the biophysical properties of bilayer and attaching to several protein targets (111, 112). PA plays the

crucial function in maintaining dysregulation of this lipid is present in a variety of illnesses including various malignancies autoimmunity, thrombotic diseases, and Alzheimer's disease. and, cellular homeostasis. (113). Although PA is only found in trace levels in mammalian cell membranes, it is a crucial intermediary in the biosynthesis of the acylglycerols and membrane phospholipids (76). In mammalian cells the PA is produced by three distinct mechanisms, which are the diacylglycerol kinase (DGK) pathway, the phospholipase D (PLD) pathway, and the de novo process including acyltransferases (76, 114) .

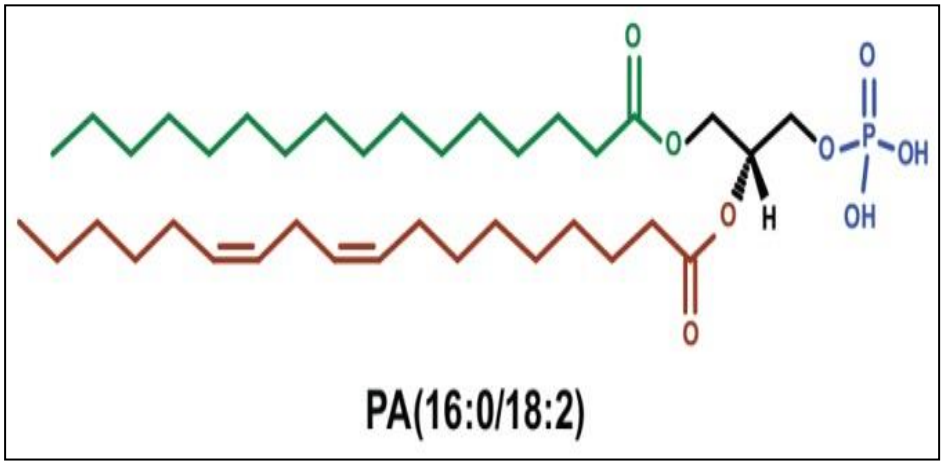

Figure (1-8): Phosphatidic acid's molecular composition. The esterified fatty acids in PA's *sn*-1 (green) and *sn*-2 (red) positions have carbon chains that are 16:0 and 18:2, respectively, on the glycerol backbone (black). Blue represents the esterified phosphate head group at *sn*-3. (115)

The various techniques were applied to viewing and disrupting the biosynthesis of the PA to cover the understanding of the specific physiological impacts of localized PA formation. However, there are a lot of challenges faced in investigation of the biology activity of the PA (116, 117).

1.2.3. Role of Enzymes in Biochemical Reactions

All living systems require enzymes, which are incredibly selective catalysts. Only a few ribonucleic acids (RNAs), primarily proteins, are capable of catalysing chemical processes. By definition, a catalyst is a substance that accelerates a chemical reaction without being consumed. Because each catalytic cycle Fig. 1-9 results in its regeneration, a single catalyst molecule can convert several substrate molecules into product. There is very little requirement for the catalyst. Though thermodynamic attributes are linked to energy balance and equilibrium, kinetic characteristics are connected to the velocity (or rate) of a reaction. Enzymes accelerate the reaction without change the equilibrium or the energy balance . However, enzymes change the kinetics of the process without impact on the thermodynamics of the reaction (118, 119) .

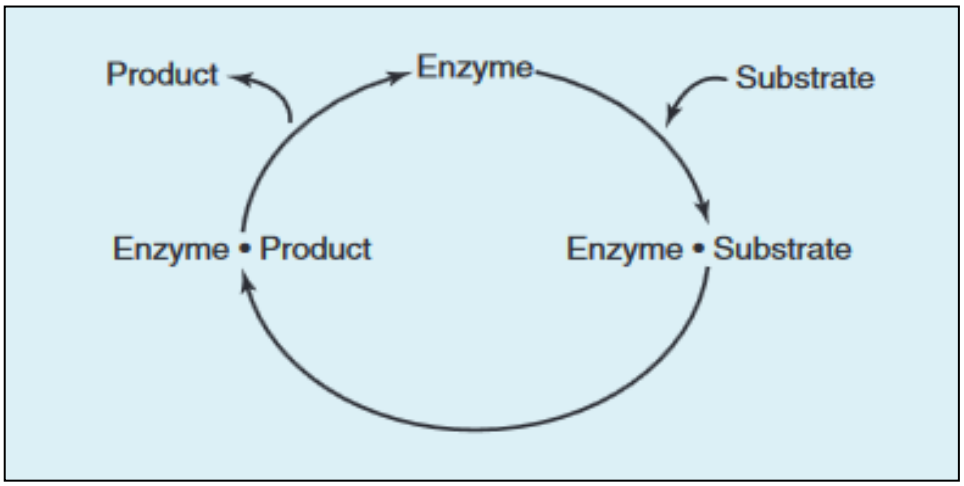

Figure (1-9): The process of catalysis. To create a noncovalent enzyme-substrate complex (enzyme-substrate), the substrate must bind to the enzyme. While the substrate is attached to the enzyme, the real reaction takes place. At the conclusion of the catalytic cycle, the enzyme is renewed (120).

The first descriptions of biological catalysts date from the late 1700s. Initial research focused on how stomach secretions break down meat. Later, during the 1800s, comparable research was done on how saliva and other plant extracts break down starch into simple sugar. Louis Pasteur proposed the theory that "ferments" catalyse the yeast-driven fermentation of sugar into alcohol in 1850. This theory suggested that the yeast cells and these structures are inextricably linked. This so-called "vitalism" viewpoint endured for many years (121).

Enzymes are recognized to catalyze a to a broad range of biological reactions furthermore to food industries (122). Similar to the total catalysts, enzymes improve the rate of the reaction by decrease of the activation energy of the reaction (123). Enzymes are employed in several industrial processes, and play significant roles in the variety of industries, including those that deal with biofuels, textiles, dyes, water treatment, pharmaceuticals, feed, and food (124). Enzymatic hydrolysis delivers excellent efficiency and specificity when compared to the classical processes that according to the high temperature and acid-base. Enzymatic reactions can also be conducted in milder environments with less pollutants and waste. Enzymes are also reasonably harmless and modifiable by the variety of techniques (22, 125, 126). According to a global study on enzyme sales, 31% of those were for enzymes of food, 6% were for feed enzymes, and the rest were for enzymes of technical (127). Enzymes, however, are expensive to utilize commercially and have a poor degree of stability in severe environments interest in improving enzyme stability, reusability, activity, and

effectiveness. Enhancing the re-use capacity, enzyme activity, efficiency, stability, are the tremendous interest in overcoming these disadvantages (128).

1.2.3.1 Active Site of Enzyme:

The enzyme's active site is where the particular substrate bind to the enzyme to catalyse the chemical reaction (129). In order to catalyse the chemical process that modifies the substrate in some way, the enzyme binds with the particular substrate. In general, the substrate is smaller than the enzyme. The active site of the enzyme ensures that the substrate is correctly positioned inside. The enzyme may have one or more substrate binding sites. The binding site is close by the catalytic site, which performs the catalysis. It is made up of two to four amino acids residues, which are involved in the catalysis of the biochemical reaction. Different sections of the enzyme's amino acid sequence contain the amino acids that consists of the active site. As a result, the fundamental design of the enzymes have pockets that, in contrast to the active site, attach to effector molecules and alter the conformation or dynamics of the enzyme. The allosteric modulation of the enzyme's reaction rate takes place at these pockets, which are referred to as allosteric sites (130).

1.2.3.2. Role of Cofactors in Enzymatic Reactions

Almost enzymes can catalyse reactions using only the groups found on their amino acids, but many need other chemical substances, often known as cofactors, to improve the enzyme function. Non-proteinogenic substances known as cofactors are

necessary for the catalytic activity of enzymes and have the ability to bind to the enzyme either covalently or non-covalently(131). A complex organic or metalloorganic molecule known as a coenzyme, and the one or more inorganic ions such as Fe^{2+}, Mg^{2+}, Mn^{2+}, or Zn^{2+} are examples of cofactors. Reversible cofactor-enzyme or substrate interactions can occur. Metal ions are the most prevalent cofactors, and enzymes that need to the cofactors are referred to as metal-activated enzymes, which are different than the metalloenzymes.

For optimal action, some enzymes need to be in the presence of both cofactors and coenzymes. For instance, the enzyme carbonic anhydrase needs the cofactor Zn^{2+} to perform its function, and glycogen phosphorylase needs the coenzyme pyridoxal phosphate (PLP) (121).

1.2.3.3. Role of Coenzyme (Q10) in Oxidative Phosphorylation Process

In 1957, coenzyme Q was discovered by Frederick Crane and others (132, 133). The molecular structure of coenzyme Q10 is a benzoquinone ring with a side chain of 10 isoprene units. This naturally occurring substance is also known as ubiquinone because it is present everywhere in nature. The coenzyme Q10 (CoQ10) can be found in three oxidation states, which are fully reduced ubiquinol (CoQ10H2), radical semiquinone intermediate (CoQ10H), and fully oxidized ubiquinone (CoQ10)

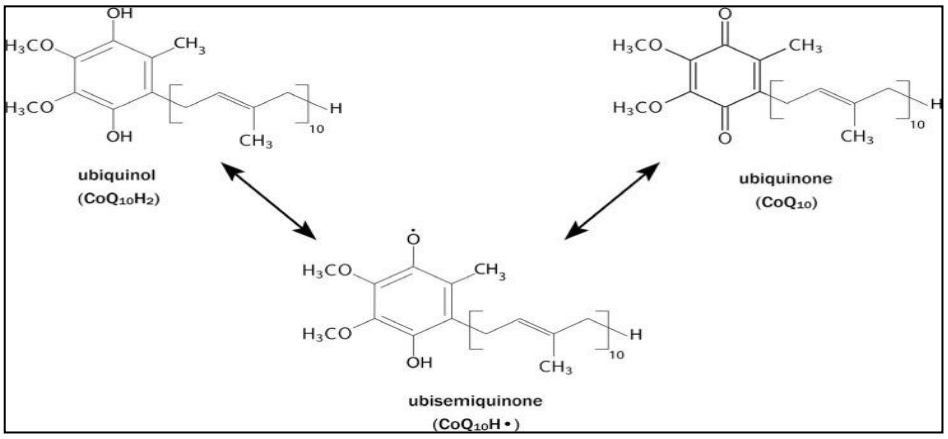

Figure (1-10): The fully reduced ubiquinol form (CoQ10H2), the radical semiquinone intermediate (CoQ10H), and the fully oxidized ubiquinone form are the three oxidative states of CoQ10 (132).

Fundamental characteristics of CoQ10 refer to the potential of the helpful in a range of therapeutic circumstances (134, 135). The CoQ10 is a cofactor for the mitochondrial enzyme complexes that are involved in oxidative phosphorylation to produce the adenosine triphosphate (ATP)(136). In addition, the CoQ10 is the crucial part in cellular bioenergetics, which has allowed for its clinical application in situations affecting tissues with high metabolic demands, such heart muscle(137). The CoQ10 also involves as antioxidant, or free radical scavenger in addition to producing ATP. The CoQ10 may recycle and renew other antioxidants in the body by its reduced form, ubiquinol, which is also a strong lipophilic antioxidant. CoQ10 is also known to affect gene expression, cell signaling, and membrane stability, among many other things (138).

1.2.3.4. Types of Enzymatic Reactions

In 1964, the International Union of Biochemistry created the Enzyme Commission number (EC number), which is a

numerical classification scheme for enzymes, depending on the chemical reactions that catalyze. As a result, enzymes are classified into main six groups comprise with the totality of the biochemical reactions as presented in Table (1-1). These categories were separated further so that an enzyme could be identified by its four-digit number beginning with the letters Enzyme Commission (EC) (121).

Table (1-1):Principal Enzyme Classes and Enzymatic Reactions (139).

Enzyme class	EC number	Selected reactions
Oxidoreductases	1	Reduction of C=O and C=C; reductive amination of C=O; oxidation of C-H, C=C, C-N, and C-O; cofactor reduction/ oxidation
Transferases	2	Transfer of functional groups such as amino, acyl, phosphoryl, methyl, glycosyl, nitro, and sulfur-containing groups
Hydrolases	3	Hydrolysis of esters, amides, lactones, lactams, epoxides, nitriles, and so on, as well as the reverse reactions to form such functionalities
Lyases (synthases)	4	Addition of small molecules to double bonds such as C=C, C=N, and C=O
Isomerases	5	Transformation of isomers (isomerizations) such as racemizations, epimerizations, and rearrangement reactions
Ligases (synthetases)	6	Formation of complex compounds (in analogy to lyases) but enzymatically active only when combined with ATP cleavage

In 2018, the seventh enzyme category (EC 7) that categorized the translocases was added to the EC (140, 141). Using evolutionary and biophysical models was possible to classify the sequences and structures of enzymes, enabling the understanding of structure and sequencing similarities (142).

1.2.4. Phospholipases

Phospholipases are enzymes that hydrolyze the ester bond of phospholipids, which are divided into five categories A–D based on the place they hydrolyze(143) see Fig.1-11. The two fatty

acid esters are hydrolyzed in the presence of type A enzyme. The phospholipases are known as A1 enzymes when they hydrolyze phospholipids at the *sn*-1 site and as A2 enzymes when they hydrolyze at the *sn*-2 site (144). In absence of lysophospholipids, the type B enzyme PLB concurrently hydrolyzes two acyl-ester bonds in phospholipids(145). The phospholipase D (PLD) cleaves the terminal phosphodiester link, releasing the head group and phosphatidic acid, whereas phospholipase C (PLC) cleaves the phosphorylated head group and diacylglyceride (146, 147) .

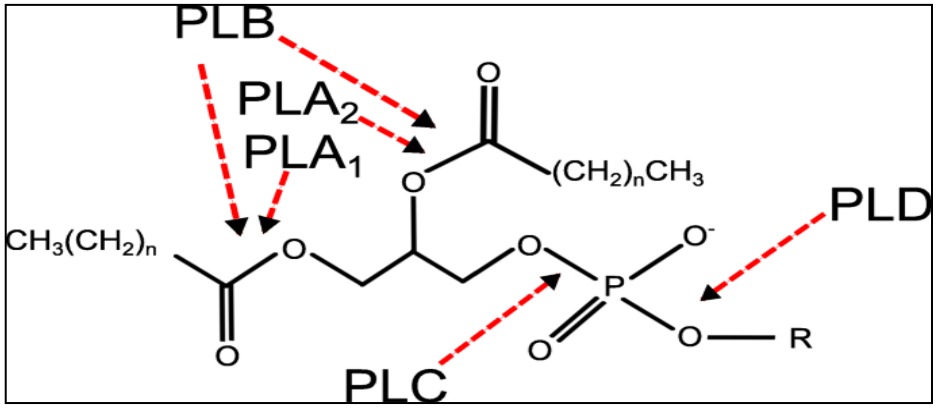

Figure (1-11) : Phospholipase A1, A2, B, C, and D-hydrolyzed sites (148).

1.2.4.1. Phospholipase A1 (PLA1)

One class of phospholipases with 1-acyl hydrolytic activity is called phospholipase A1 (PLA1). The PLA1 in particular hydrolyzes the fatty acid ester bond at the *sn*-1 position of a glycerophospholipids (149-151), so it is frequently used to alter this bond Fig.1-11. For the food and pharmaceutical industries, fatty acid esters such as polyglycerol esters of fatty acids or sugar ester work as good biocompatible emulsifiers (152). Two structurally separate groups of PLA1 isozymes, the external

PLA1 family and the intracellular PLA1 family, make up the PLA1 isozymes (153, 154).

Despite the fact that certain PLA1s are extracellular and belong to a distinct group (150), Others localize in the cytoplasm and are intracellular, mitochondria, chloroplasts, and endoplasmic reticulum (150). Phosphatidylserine specific PLA 1 is the first extracellular PLA1 that has been identified and that preferentially breaks down PS (150). These three are genuine PLA1 enzymes because membrane-associated phosphatidic acid (PA)-selective PLA1s, membrane-associated phosphatidic acid - selective phospholipase A1 member a (mPA-PLA1a) and membrane-associated phosphatidic acid - selective phospholipase A1 member b(mPA-PLA1b), only exhibit PLA 1 activity to ward PA (155).These PLA1s are believed to be engaged in signaling processes by producing 2-acyl-lysophospholipids due to their *sn*-1 regiospecificity. The mammals have three members of the intracellular PLA1 family, which are PA-preferring PLA1 (PA-PLA1), mammalian Sec23p-interacting protein (p125), and human expressed sequence tag clone bind to p125(KIAA0725p) (155). Due to the rare relationship exists between the amino acid sequences of intracellular PLA1s and external PLA1s, contrary to the external PLA1 family, the intracellular PLA1s are evolutionarily conserved genes that range from yeast to humans and generally seem to be involved in membrane transport and organelle maintenance (156).

To enhance L-α-glycerylphosphorylcholine(L-α-GPC) demonstrates promise in the treatment of dementia and

Alzheimer's disease enzymatic synthesis applying the aqueous phase of phospholipase A1 (PLA1); several surfactants (NaDC, AOT, Tween 20, Tween 60, Tween 80, Tween 85) were reviewed in 2019. According to the findings, "Tween 20 is the best surfactant for increasing L-α-GPC concentration. The ideal conditions for PC hydrolysis with 20 $g.L^{-1}$ of Tween 20 were found to be enzyme loading of 0.64 $g.L^{-1}$ and substrate concentration of 60 $g.L^{-1}$ at 45 C for 1 h. Additionally, the fed-batch catalytic process of PC was used to produce 112.56 $g.L^{-1}$ of L-a-GPC from 360.00 $g.L^{-1}$ PC with a yield of 91.36% within 3 hours, avoiding substrate inhibition and increasing product accumulation" (157) .

According to the findings of the study which was conducted in 2021 by using soybean lecithin as the substrate, the pure renatured PLA1 had a specific activity of 1380 U/mg and the ideal temperature and pH were 60 °C and 6.5. In addition, lipase activity was seen when the catalyzing temperature was below 55 °C, but the renatured PLA1 was reported to have higher activity towards phosphatidyl inositol (158).

In 2020, the study showed that "the phosphatidylserine-specific phospholipase (PS-PLA1) was a novel target in the therapy of hyperthyroidism, particularly Graves' illness, and that its assessment may be helpful as an additional diagnostic test for thyroid function. The PS-PLA1 levels were higher in individuals with Graves' illness, sub-acute thyroiditis, or silent thyroiditis, whereas they were unaffected in individuals with hypothyroidism. Particularly in the participants who had Graves' illness, there was a significant correlation between the blood PS-

PLA1 levels and the thyroid hormone levels. In addition, anti-thyroid medications reduced the blood PS-PLA1 levels in patient with Graves' illness, and the changes in PS-PLA1 were closely related to those in thyroid hormones" (159).

1.2.4.2. Phospholipase A2 (PLA2)

The PLA2 can hydrolyze glycerophospholipids at the *sn*-2 position to liberate fatty acids and lysophospholipids see Fig. 1-11. More than 50 enzymes in mammals belong to the phospholipase A2 (PLA2) superfamily, which is further split into numerous different families on the basis of biochemical and structural factors (160).

Considering its structural connections, there are different families within the PLA2 superfamily. These families include the lysosomal phospholipase A2 (LPLA2), platelet-activating factor acetyl hydrolase (PAF-AH), calcium-independent PLA2 (iPLA2), also known as patatin like phospholipase (PNPLA), secreted PLA2 (sPLA2), cytosolic PLA2 (cPLA2), and phospholipase A/acyltransferases (PLAATs), (161, 162). Through the liberation of lysophospholipids and polyunsaturated fatty acids (PUFAs) from membrane phospholipids, PLA2s stimulate the production of lipid mediators (163). The PLA2 also contribute to membrane homeostasis by changing the composition of phospholipids, providing fatty acids for oxidation to produce energy, the lipid production that forms barriers, and adjusting the micro environmental ratio of unsaturated to saturated fatty acids, between other factors. Several enzymes, including transacylase

processes, lysophospholipase, phospholipase A1, and, neutral lipid lipase, catalyse even non-phospholipase A2 activities while recognizing variations in their substrate phospholipids' fatty acyl and/or head group moieties.

Individual PLA2s' in *vivo* activities depend on a variety of pathophysiological factors, including their enzymatic, cell biological , and biochemical characteristics, or the presence of cofactors that can modulate the enzymatic function, lipid composition in target membranes, spatiotemporal availability of downstream lipid-metabolizing enzymes, tissue and cellular distributions (164).

1.2.4.3 Phospholipase B (PLB)

A specific class of enzymes that are known as phospholipase B (EC 3.1.1.5) catalyzes the hydrolysis of fatty acids esterified at the *sn*-1 and *sn*-2 positions, resulting in the formation of free fatty acids and lysophospholipids Fig.(1-11). Phospholipase B's structural details and catalytic mechanism are still unclear (165).

Animals and microorganisms are the main sources of these enzymes. The phospholipase B can play a role in virulence in animals because it can be found in mammalian tissues and venom (166). It can also be present in bacteria, fungi (both pathogenic and nonpathogenic) amoebas, and amoeba. Some plants have also been found to exhibit their enzymatic activity (167) .Several fungus, include *S. cerevisiae*, *Candida albicans*, *Candida utilus*, *P. chrysogenum*, and *Candida neoformans*, can produce the phospholipase B to perform the hydrolase and acyltransferase activity. The phospholipase B demonstrated a

strong preference for diacylphospholipids as a substrate instead of lysophospholipids and hydrolyzed diacylphospholipids without producing lysophospholipids. A portion of the phospholipase B enzyme exhibits lysophospholipase-transacylase activity, which converts free fatty acids into lysophospholipids and produces diacylphospholipid (166, 167).

Different species of phospholipase B favor phosphatidylcholine as a substrate, but PC also have a significant impact on lyso-phospholipids without any special preference (166). This substrate is crucial for industrial applications, including oil degumming using phospholipase B in the food sector. The development of synthetic phospholipids or natural phospholipids that are uncommon in nature are further factors that contribute to the high selection of phosphatidylcholine as a substrate. Phosphatidylcholine is widely present in nature and it is utilized as a building block for commercial and academic applications (56, 166).

Phospholipase B is used to modify or transform phospholipids in addition to oil degumming as an important application. Phospholipids may be altered or modified through hydrolysis, specific phospholipid synthesis, or conversion from type of phospholipid to another (167). It may be more cost-effective and ecologically beneficial to use low temperature phospholipase B enzyme compared to thermos tolerant phospholipases, the low temperature phospholipase B has not been explored as much, despite the fact that it has a wide range of potential applications. These isolates are most active at (4–37)°C and become inactive at (40–50)°C (167).

1.2.4.4. Phospholipase C (PLC)

To release phosphomonoester and diacylglycerol (DAG), phospholipases C (PLCs) catalyse the dissociation of phospholipid glycerophosphate linkages (168). PLCs are typically divided into phosphatidylinositol- and phosphatidylcholine-specific PLCs (PC- and PI-PLCs), based on the specificity of their substrates (169). Although phosphatidylinositol-containing PLCs (PI-PLCs) exclusively hydrolyze PI to liberate inositol-(1,4,5) triphosphate and diglyceride, along with other phospholipids including phosphatidylserine (PS) and phosphatidylethanolamine (PE), PC-PLCs have a preference for hydrolyzing phosphatidylcholine (PC). (170),(171).

In 1953, "it was reported that the addition of acetylcholine or carbamylcholine to pancreatic cells led to the production of phospholipids". According to investigations, when compared to control without activation, the samples treated with the medicines had levels of phospholipids that were seven times higher than the control. This was the first demonstration of phospholipase C (PLC) function in cells, though it was unknown at the time. It was demonstrated that impure PLC preparations may be used to cleave phosphatidylinositol more than 20 years later. The first pure PLC preparation was isolated in 1981 (172).

Almost all cells in the body contain phospholipases C, and the activity of these enzymes can be controlled by agonists, hormones, and neurotransmitters that act as receptors on the cell

membrane such as the guanine nucleotide-binding protein-coupled receptors (GPCRs) and receptor tyrosine kinases. In addition, small guanosine triphosphate hydrolases (GTPases) like Rac and elevations in cytosol Ca^{2+} can activate some PLCs (104). So, the PLCs are essential for controlling a range of biological reactions. Other PLCs can act as guanosine triphosphate hydrolases(GTPase)-activating proteins(GAPs) or Guanine nucleotide exchange factors (GEFs) for secondary signaling proteins, while other family members act as scaffolds for additional signaling proteins. The Ca^{2+} oscillations in the cell are amplified by other PLCs. Some members of the PLC family can go into the nucleus and regulate signalling there. PLC family members are essential for many cellular processes, hence it is crucial to understand how each PLC is controlled and the way of cellular environment impacts the length and strength of the response (173).

Due to potential use of PLCs like multipurpose biocatalysts in a variety of sectors of industry, such as food additives, nutraceuticals, ceramide manufacturing, and oil degumming. At past few decades, the PLCs have attracted growing attention (167, 174).

In 2008, the study followed the biological role of phosphatidylcholine specific phospholipase C in mammalian cells and the reached phosphocholine and diacylglycerol (DAG), which are produced as a result of the hydrolysis of PC by PC-PLC. Various substances, such as cytokines, growth hormones, mitogens, and calcium ions, involve in the phosphatidylcholine -degradation pathway in presence of PC-

PLC as catalyst. The PC degradation is connected to intracellular signal transmission that controls cell growth, differentiation, metabolism, and death (175).

1.2.4.5. Phospholipase D (PLD)

Phospholipase D (PLD, EC 3.1.4.4), a member of the PLD super family, is capable of catalyzing the PLs hydrolysis to phosphatidic acid (PA) and release free alcohol, moreover to transphosphatidylation of PC to PLs in the presence of suitable acceptor alcohols (176). When an extra alcohol is present in the reaction system, PLD preferentially catalyzes the transphosphatidylation reaction to produce a polar-head modified phosphatidylalcohol from the substrate phospholipids (177). Consequently, it would be a strong tool to inexpensively synthesis the less common phospholipids, such as phosphatidylethanolamine,phosphatidylserine,phosphatidylglycerol, and phosphatidylinositol. These phospholipids are found in nature in lower concentrations than the lecithin or phosphatidylcholine (PC), which are widely utilized in the food, cosmetic, and pharmaceutical industries (44).

PLDs are widely distributed enzymes that are found in a wide variety of microbes, plants, animals and human. The PLDs from species of *Streptomyces* were used to finding the effective of phospholipid synthesis (44, 178).

In 1947, the phospholipase D was identified from the component of carrot extracts by monitoring the capable of PLD to degrading the lipid and membranes. The PLD was described as phospholipid-specific phosphodiesterase that can create

phosphatidic acid (PA) by releasing free choline from phosphatidylcholine (PC) and using water as a nucleophilic acceptor (179-181). On the other hand, the rat brain served as the source for the much later, the PLD activity in animal tissues was discovered by Saito and Kanfer in 1975 (182) . In addition, , the PLDs in mammalian were investigated as activated quickly in response to extracellular stimuli (183).

Depending on their structure, the PLDs can be split into two main classes; the HKD group and the non-HKD group make form the basic structure (184, 185).

The PLDs from the spider *Loxosceles* and *Streptomyces chromofuscus* that are members of the superfamily of phospholipases D -like phosphodiesterases make up the non-HKD PLD group (184-187).

A standard consensus sequence for HXKX4 D, often known as the HKD concept, where X signifies any type of residue, has preserved Lysine (Lys), Histidine (His), and Asparagine (Asp), identifying it as a part of the PLD superfamily. According to reports, this pattern is mostly found in mammals, including Homo sapiens, which possesses both PLD1 and PLD2 isoforms, plants, which include the predominate PLD isoform yeast, which contains the gene SPO14 (187), and some microorganisms, which contain the crystalline PLD from Streptomyces sp. Primary myelofibrosis(PMF) strain (188). Plants' main structure replicates the HKD idea, humans, and some bacteria, and it is thought that in the tertiary structure, both motifs are located close to each other, producing a catalytic

position at the interface for the enzyme of bi-lobed (187, 189).PLDs are currently a key focus in healthcare of human (44), specifically for the treatment of cancer. (190)

In 2016 ”the direct observation of areas of PA synthesis was applied for the hydrolysis of phosphatidylcholine in the presence of PLDs as a catalyst within intact cells. It will be possible to separate the spatial requirements for the production of PA in cell signalling using chemo enzymatic synthetic technique in *vivo*. Several extracellular signals cause PLD-mediated PA synthesis on various internal membranes, which results in various signalling outputs (191). Lastly, if the technique is extended to include other functionalized alcohols, it may be possible to remodel intracellular membranes and give them unique physicochemical characteristics (191).

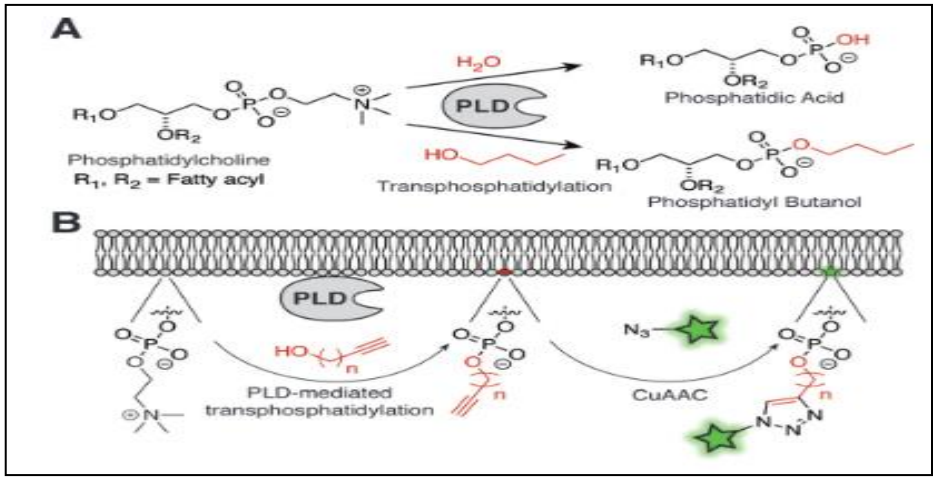

Figure (1-12): Image PA synthesis using a two-step PLD-mediated method (191). A) In cells, PLD catalyses the hydrolysis of phosphatidylcholine to create PA (top). B) It is also capable of mediating transphosphatidylation reactions with short-chain primary alcohols (such as butanol) to create phosphatidyl alcohols (192).

1.2.5. Aim and objectives of Study

This study aims to comparison between the hydrolysis of phospholipids in acidic and alcoholic environments in absence and present of the phospholipase D enzyme (PLD). Moreover due to the various applications of phosphatidylcholine, the understanding of the effect of the alcoholic environment can help pharmaceutical, cosmetic, and food factories to design appropriate experiments to reduce the impact of these byproducts on the main product efficiency and yield.

In addition, the study included the following objectives:

1- The influence of a toxic concentration of ethanol that could cause damage to the cell membrane was determined by conducting hydrolysis processes of the two PLs derivatives (phosphatidylcholine and phosphatidylserine) in water and ethanol, which were catalysed by PLD enzyme.

2- This work includes the monitoring of the kinetics of the enzymatic reaction for the hydrolysis of phosphatidyl derivatives in presence of phospholipase D as catalyst. During this study, all the conditions which may impact on the hydrolysis enzymatic reaction such as the pH, temperature, and the concentration to ensure that this enzymetic hydrolysis simulates that occurs in a living system and to suggest the appropriate mechanism for this enzymatic reaction .

Chapter Two

Materials and Methods

2.Materials and Methods

This study was conducted in the laboratory of postgraduate, University of Karbala, College of Science, Department of Chemistry.

2.1. Chemical and Materials

The materials and chemicals used in this study are shown in the following Table (2-1):

Table (2-1): Chemicals and their origin.

No.	Materials	Company
1-	Absolute Ethanol (99.9%)	Chem-Lab \ Belgium
2-	Acetonitrile	Romil \ UK
3-	Buffer solution (4,7,9)	HI Media \ India
4-	Chloroform	Gain Chemical Company \ Canada
5-	Di ethyl ether	Romil \ UK
6-	HCl acid	HI Media \ India
7-	Petroleum ether	Chem- Supply \ Australia
8-	Phosphatidyl choline (98.1 %)	Chemfish Tokyo Co.,Ltd \ Jaban
9-	Phosphatidyl serine (97.2%)	Chemfish Tokyo Co.,Ltd \ Jaban
10-	Phospholipase D	Sigma Aldrich \ USA
11-	Sodium hydroxide	Analar Trad Mark \ India
12-	TLC pleats	Cam Lab \ UK

2.1.1 Instrument and equipment:

All the instrument and equipment that used in this study are summarized in the following table:

Table (2-2): The devices and their suppliers.

No.	The device	Supplier
1-	A 7890 GC mass system	Agilent technologies \ California
2-	Avance III 400 MHz NMR spectrometer.	Bruker \ USA
3-	Electronic Balance	220-4\ KERN \UK
4-	Fourier transform infrared (FTIR)	Shimadzu (8400 S) \ Japan
5-	Hot plate stirrer	Lab Tech \ Korea
6-	Micro pipet	Drago LAB \ China
7-	Oven	Memmert \ Germany
8-	Schlink line	Newcastle University Workshop \ UK
9-	Spectrophotometer	FAIT HFUL \721\ China
10-	UV –Visible spectrophotometer	UV-1800\Shimadzu \ Japan
11-	Vacuum pump	TW -1.5 A\ China
12-	Vortex mixer 945307 /THE.U.S.	Vortex mixer 945307 \ THE.U.S.
13-	Water Distillator	Lab Tech \ Korea

2.2. Subjects and Methods

2.2.1. Hydrolysis and Nucleophilic Substitution Experiments without Phospholipase D (PLD) enzyme:

2.2.1.1. Hydrolysis of Phosphatidylcholine in Acidic Environment

The hydrolysis experiment of phosphatidyl choline was carried out without the use of the enzyme PLD and in an inert environment and completely isolated from the atmosphere using the Schlink line technique. The (0.4 g) of phosphatidyl choline was added into a strong acidic medium

(25 ml, 2 N Hydrochloric acid HCl), at 120 ˚C for a period of 168 hours. The hydrolysis reaction was followed up the reaction by ultra-violate – visible (UV-Vis) and Fourier- Transform Infrared (FTIR) measurements by withdraw a (0.5 ml) of the reaction mixture at different times after emptying the pipette and tube from the air and filling it with nitrogen gas before placing the sample drawn for the purpose of measurement. The scheme of the hydrolysis reaction for the phosphatidyl choline as shown in Fig. 2-1.

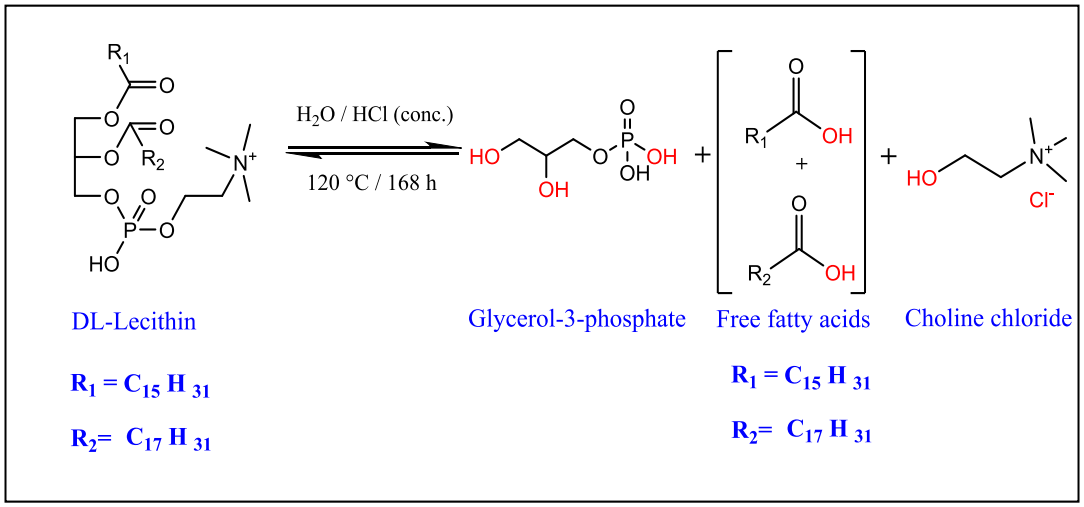

Figure (2-1): Scheme for the reaction of the hydrolysis of phosphatidyl choline with HCl.(193)

During the reaction it was noted that the color of the reaction mixture changed from light brown and gradually turned dark brown with the separation of a black fatty layer on the surface of the mixture at the first hour of the reaction and continued to increase until the first twenty-four hours of the reaction. Around the time (45-55) hours of the reaction a white oil substance appeared on the upper inner walls for the reactor and the inlet supplied with nitrogen gas, and the necessary measurements were made for it at the end of the reaction after the end of 168 hours. The reaction product was isolated from the intermediate products by the filter shown in its image below.

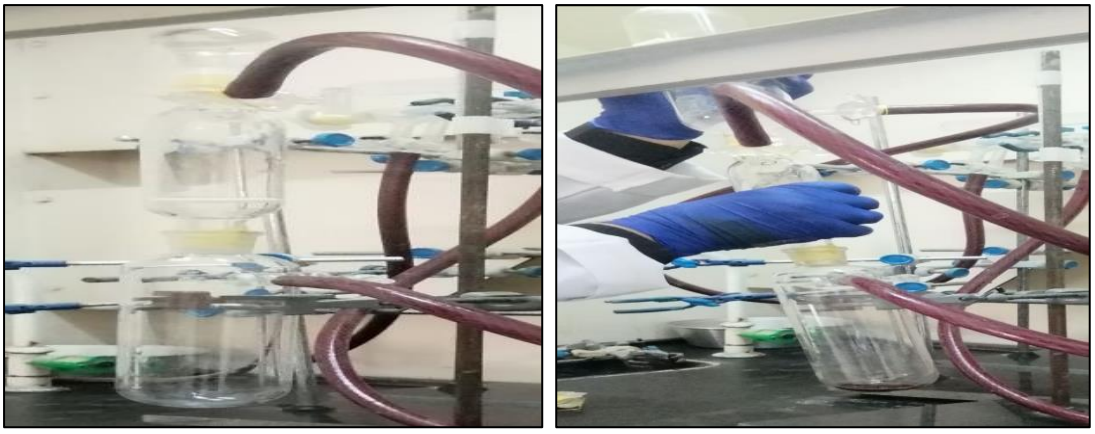

Figure (2-2): The filtration technique which was used to separate the reaction products from the side products, where the black substance on the filter surface is the byproduct. While the oil solution contains the product of the reaction with the solvent.

After isolating the product by the filter, it was placed in a nitrogen-filled reactor. the solvent was expelled by a vacuum pump for about 15 hours for the purpose of isolating the oil product. The resulting material was weighed and collected in special containers filled with nitrogen where the necessary measurements were made, and the main yield of the reaction was (67 %). All isolated products were isolated and characterized by nuclear magnetic resonance (NMR), FTIR, GC-Mass, and UV/Vis. spectrophotometer.

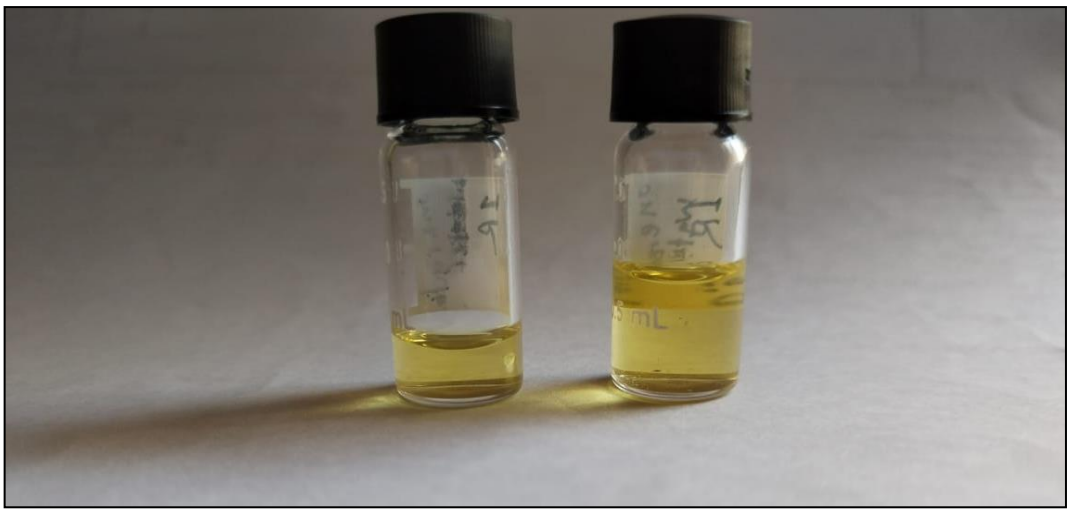

Figure (2-3): The main product (glycerol-3-phosphate) of the reaction after being placed in the nitrogen-filled atmospheric vacuum containers.

Furthermore, the solubility of the yellow oily product was tested for each of the solvents shown in the Table (2-3):

Table (2-3): The Glysrole-3-phosphate's solubility.

The solubility of the yellow oily product (Glysrole-3-phosphate)	
Acetonitrile	Dissolved
Acetone	Partially soluble
Di ethyl ether	Not soluble

2.2.1.2. The nucleophilic substitution experiment of phosphatidyl choline with ethanol:

The hydrolysis of phosphatidyl choline was performed by using the same methodology mentioned above and under the same conditions (completely isolated from atmospheric air and in absent of the PLD enzyme) using ethanol as a solvent and a strong acidic environment (pK_a = 1.2) at 85 ˚C for a period of 150 hours. The reaction was followed up by ultraviolet-visible and FTIR measurements for the purpose of comparison with the results in the case of using water in the hydrolysis process, where it was found that the ethyl group (relatively stable) was replaced instead of hydroxyl group in the nucleophilic substitution process.

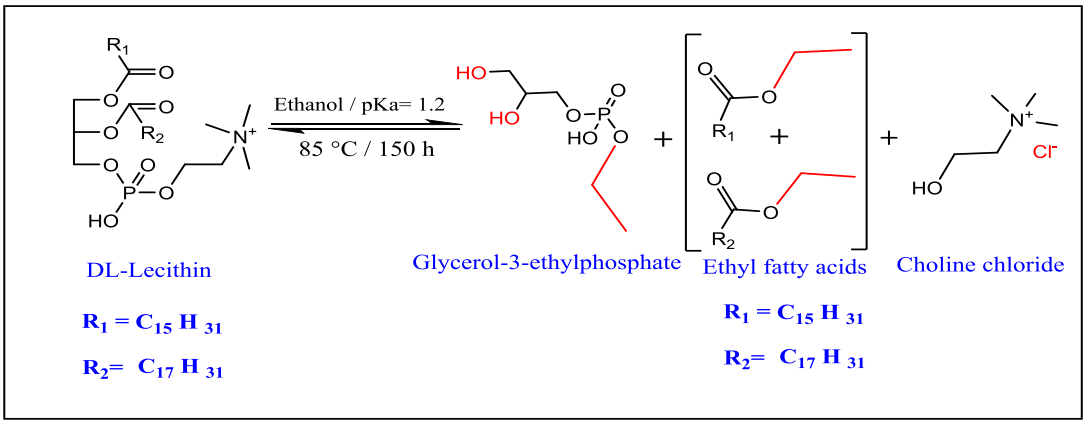

Figure (2-4): Scheme for the nucleophilic substitution reaction of phosphatidylcholine with ethanol and hydrochloric acid.(194)

The color of the mixture throughout the time of the reaction converted from light brown and gradually turned to dark brown at the end of the reaction. (Fig 2-5)

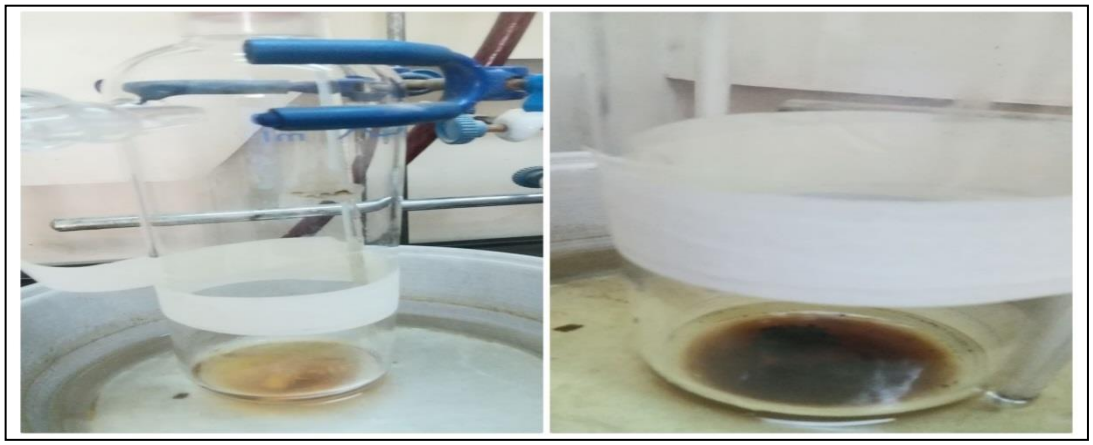

Figure (2-5): An image showing the change in the color of the reaction mixture from light brown to dark brown.

It was observed at about (45) hours after the start of the reaction The separation of a black oil side product in the form of flakes and continued to increase until the 105 hour of the reaction, where it turned in the form of an oil layer on the surface of the mixture as shown in the picture below. This side product (Fig 2-7) was isolated from the reaction mixture at the end of the reaction by a filter and appropriate measurements were made to detect it.

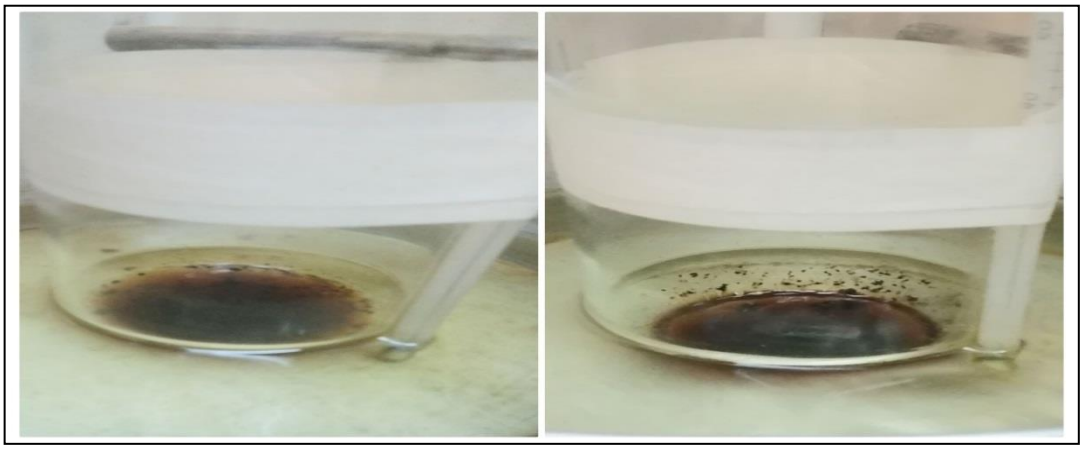

Figure (2-6): The appearance of the side product in the form of black flakes and its transformation into a black oily layer.

At the end of the reaction, the main product was isolated from the side product by an air-vacuum filter filled with nitrogen. The side product separated on the filter surface while the solvent and product separated down the filter to the reactor. Then the same previous methods that were mentioned in the hydrolysis experiment of PC were used to isolate and dry the products, where a black substance (Fig 2-7) was obtained that belongs to the by product, which was isolated from the reaction mixture after (45) hours.

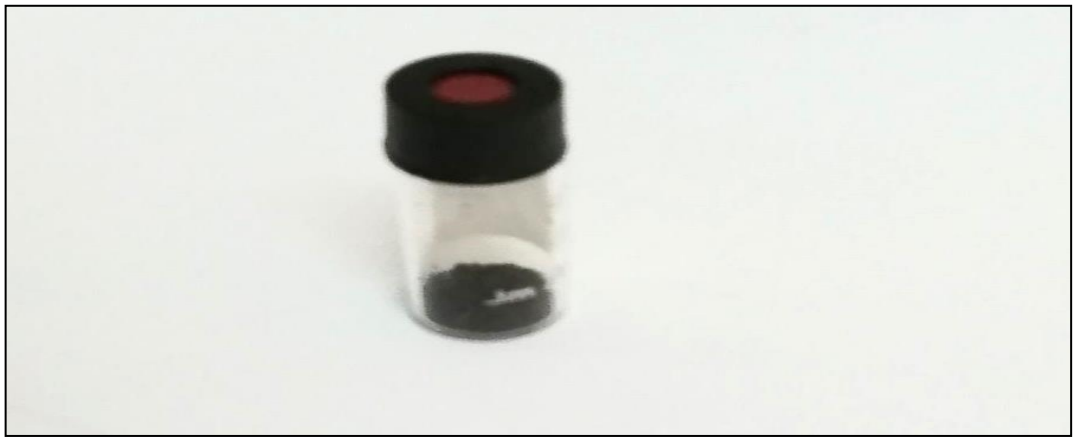

Figure (2-7): The black by product (ethyl fatty ester) which was isolated and dried.

The product for the ethyl substitution reaction of PC was a brown fatty substance and after weighing the results and calculating. The yield of the reaction was (68.8%), all products were isolated and characterized by NMR, FTIR, and UV/Vis. spectrophotometer.

2.2.2. Hydrolysis of Phospholipids Derivatives in Presence of Phospholipase D

2.2.2.1. Preparation of Phospholipase D Solutions:

The enzyme phospholipase D PLD (3.4 mg, 146 U/ mg) was dissolved in 1 ml of buffer solution (acidic function pH=8) as concentrated solution and then the stock solution was prepared from the resulting solution (0.34

mg /ml) by diluting 0.5 ml of 0.34 solution with 0.5 ml of buffer pH= 8 solution to prepare 1.7 mg/ml (73 U/mg stock solution). After that the dilute solution (50 ml, 7.3 U/mg) was prepared from stock solution by mixing 0.05 ml of 1.7 mg / ml with 4.95 ml of buffer pH= 7 solution.

2.2.2.2. Preparation of Phosphatidyl Choline Solutions

The solubility of PC was checked See Table (2-4) For more information.

Table (2-4): PC's soluble nature.

The solubility of Phosphatidyl Choline	
Buffer solution (pH=7)	Partially soluble
Water	In soluble
Acetone	In soluble
Di ethyl ether	In soluble
Petroleum ether	In soluble
Acetonitrile	In soluble

The 1mM stock PC solution was prepared by dissolving 0.037 g of PC in 50 ml of pH= 7 solution. From 1 mM solution, the set of different concentrations solutions were prepared (0.1 ,0.12, 0.14, 0.16, 0.18, 0.6, 0.8, 0.04 ,0.05 ,0.06 ,0.07 ,0.08) mM

2.2.2.3. Determination of Appropriate PC Concentration (Michaelis-Menten Equation)

The experiments on the hydrolysis of PC were performed in the presence of the PLD as a catalyst for each of the concentrations mentioned above at a temperature of (37 ± 2) °C and enzymatic activity (1.46) U/mg

of the PLD enzyme, where the color of the reaction mixture was colorless, The reaction was followed up by withdrawing 1 ml of the mixture every 10 minutes and measuring its absorbance by spectrophotometer analyzer after fixing the wavelength at 268 nm, and continue until almost constant readings of absorbance are obtained.

Figure (2-8): The reactor of the enzymatic hydrolysis of PC in presence of PLD.

Then, after observing the results, the ideal substrate concentration was reached at the concentration (0.1 mM) that provides the optimum data during work in addition for drawing the Michaelis –Menten equation to find the Michaelis constant (K_m), or the speed at which the Michaelis-Menten equation's maximum speed equals half.

2.2.2.4. Determination of Appropriate PLD Enzymatic Activity

Furthermore , the enzymatic hydrolysis experiments of PC were carried out under completely emptied conditions of atmospheric air as well and in the presence of nitrogen as an inert gas with the presence of PLD by applying different activities of phospholipase D (0.292, 0.73, 1.168, 1.46,

and 1.752) U/mg after stabilizing the concentration of the substrate at 0.1mM, The temperature at (37± 2)°C and the pH function at 7, apply the same steps in the previous enzymatic experiments and following the absorbance readings after fixing the wavelength at 268 nm. The optimal enzymatic activity using the experiment findings and creating a velocity diagram in opposition to the associated pH is (1.752) U/mg is the appropriate enzymatic activity for this reaction.

2.2.2.5. Determination of Appropriate pH for Hydrolysis of PC

A 0.1 mM solution of PC was prepared using buffer solutions of different pH values (5, 6, 7, 7.4, 8, and 9), adding (1.752) U/mg of PLD (the appropriate enzymatic activity of the reaction) and following up the reaction over time by measuring the absorbance every ten minutes until several stable readings or nearly identical were obtained. It was found from the results of the experiments and drawing a velocity diagram against the corresponding acid functions that (pH= 7) is the ideal pH for this enzymatic reaction.

2.2.2.6. Thermodynamic Study for Hydrolysis of PC

After determining the appropriate concentration of PC, the activity of PLD, and the appropriate pH, the rate of the hydrolysis reaction was monitored at different temperatures (10, 20, 30, 37, and 45) °C, by mix 0.1 mM of PC with (1.752) U/mg of PLD for each experience. When you continue to follow the absorbance readings every 10 minutes until you get stable or nearly close readings. It was found that 37°C is the best temperature suitable for the enzymatic reaction. In addition, the change in enthalpy (ΔH), the change in Gibbs free energy (ΔG), and the change in entropy (ΔS) have been measured, as item 2.8 shall explain.

2.2.3. Hydrolysis of PC in Ethanol in Presence of Phospholipase D

2.2.3.1. Following up the Effect of Change the Concentrations of PC and Enzyme Activities

After determining the maximum wavelength at 439 nm, which changed as a result of changing solvent used (ethanol instead of water). Phosphatidylcholine substitution experiments were started by preparing dilute solutions with a concentration of (1, 1.25, 1.5, and 2) mM from Stock 0.01M solution prepared by dissolving (0.19 g) of PC in (50ml) of phosphate buffer dissolved in ethanol. The activity of PLD used 1.168 U/mg at 37 ^{o}C where the color of the reaction mixture was light yellow. It was found that the concentration of (1mM) is the appropriate concentration (it provides the optimum absorbance readings when following the reaction with time) for the nucleophilic substitution reaction of PC with ethanol and to determine K_m at which the speed is equal to half maximum speed according to the Michaelis-Menten equation.

However, experiments with ethyl substitution of PC at enzymatic activities (0.292, 0.73, 1.168, 1.46, and 1.752) U/mg showed that (1.168) U/mg of enzymatic activity is the best suitable enzymatic activity for this enzymatic reaction.

2.2.3.2. Monitoring the Response of Appropriate pH and Temperature

Ethyl replacement experiments were carried out to determine the appropriate acidity of the reaction using a PC concentration of (0.001) M, enzymatic activity of (1.168) U/mg, temperature of 37 °C, and the pH values that were used in the experiments are (4, 6, 7.4, 8, and 10). After the end of the experiments, it was shown that the pH (6) is the ideal pH for this reaction.

When following up on the enzymatic ethyl substitution of PC with ethanol at different temperatures (10, 20, 30, 37, and 45) °C with time after determining the pH used at (6), it was noted that the optimum reaction temperature is 37 °C which gave the most regular absorbance readings with time and having drawn the relationship between temperature and velocity.

2.2.4. Hydrolysis of Phosphatidylserine (PS) in Presence of PLD

2.2.4.1. Determination of Appropriate PS Concentration and PLD Activity

In the beginning, the solubility of phosphatidylserine was tested for the purpose of fixing the maximum wavelength, as follows in Table (2-5).

Table (2-5): The Phosphatidylserine Solubility.

The solubility of PS	
Buffer solution (pH= 7.4)	Not dissolved
Buffer solution (pH= 9.5)	Partially soluble
Methanol	Partially soluble
Acetone	Partially soluble
Di ethyl ether	Not dissolved
Petroleum ether	Completely soluble
Chloroform	Completely soluble

In order to ensure that there are no interferences during the measurement of the ultraviolet-visible rays, it was relied on buffer solution pH (9.5) in the dissolution. Stock's solution (0.01) M was prepared from phosphatidylserine (0.397 g in 50 ml of pH= 9.5 solution). Its λ max was = 365 nm.

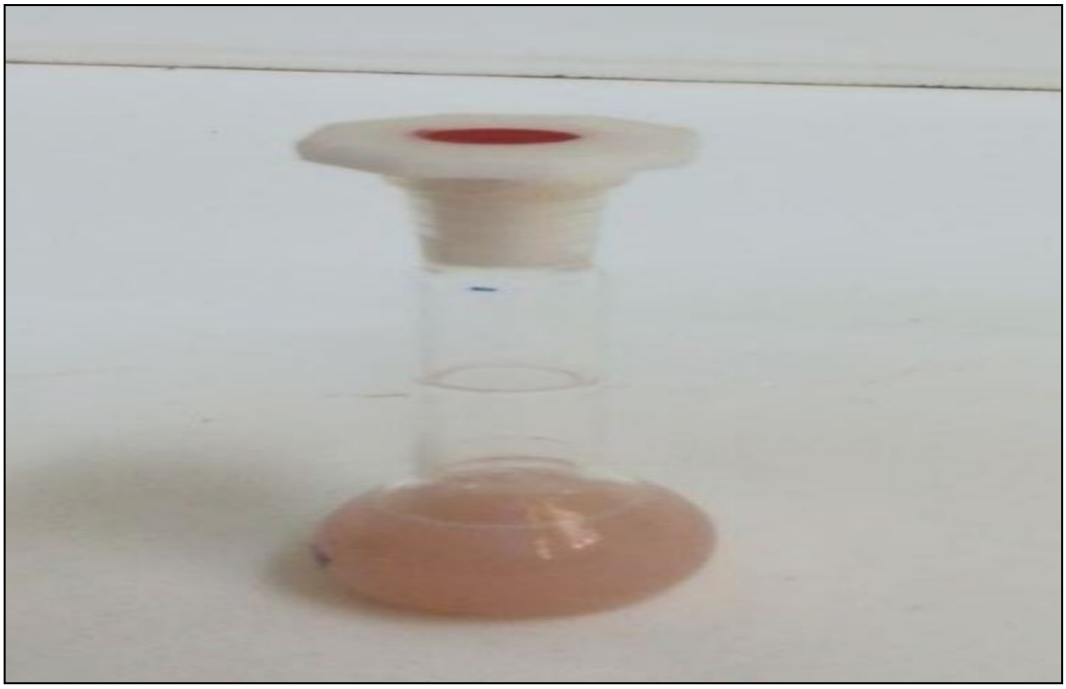

Figure (2-9): (0.01) M stock solution of phosphatidylserine.

After that, diluted solutions with concentrations (2, 4, 5, and 6,8 mM) were prepared from a 0.01 M solution of PS, and ethyl substitution experiments were conducted in the presence of the enzyme PLD 1.46 U/mg as a catalyst at 37 ^{o}C. When following up the hydrolysis reaction with time, it was observed that the concentration of (4 mM) is the appropriate concentration of PS, which gave the most regular absorbance readings and to calculate the K_m at which the Michaelis-Menten equation's maximum velocity equals half.

While the hydrolysis experiments of PS in the presence of PLD enzyme showed the best enzymatic activity at (1.752 U/mg) among the different activities used (0.584, 0.73, 0.876, 1.022, 1.168, 1.46, and 1.752 U/mg) after being determined by drawing the relationship between enzymatic velocity and activity.

2.2.4.2. Determination of Appropriate pH for Hydrolysis of PS

To conducting the experiments for the hydrolysis of PS in different pHs (4, 5, 6, 7.4, 8, 9, and 10). It was found that pH=9 is the best pH for

this enzymatic reaction, as a consequence of graphing the relation between speed and the associated pH.

2.2.4.3. Thermodynamic Study for Hydrolysis of PS

To finding the thermodynamic parameters ΔH, ΔG, and ΔS as stated in Section 2.8, for the hydrolysis reaction of PS in presence of PLD as catalyst. The enzymatic reaction hydrolysis experiments for PS at different temperatures (10, 15, 20, 25, 30, 37, 40, and 45) °C were observed. When plotting velocity versus temperature, it was found that 35 °C is the ideal temperature for the hydrolysis of PS reaction.

2.2.5. Hydrolysis of PS in Ethanol in Presence of PLD

After dissolving 0.379 g in 50 ml of pH= 7.4 (the phosphate buffer solution was dissolved in ethanol) to prepare a 0.01M stock solution, and after examining its ultraviolet spectrum and determining the maximum wavelength at 365 nm, the reaction kinetics was followed up.

2.2.5.1. Follow up the reaction with time to determine the optimal (enzymatic activity and concentration of PS) for this reaction.

When conducting ethyl substitution experiments with ethanol for PS at different concentrations (1, 1.25, 1.5, 2, and 2.5 mM), enzyme activity 1.46 U/mg and temperature 37 °C and then monitoring the reaction with time by measuring the absorbance of a sample withdrawn from the reaction mixture every ten minutes until obtaining constant or close readings of the absorbance observed. It found that the concentration of (2.5) mM is the optimal concentration to give it the most regular readings with time and to calculate the km at which the speed, as calculated by the Michaelis-Menten equation, equals half the maximum speed (V max).

After fixing the concentration at the optimal concentration of (2.5) mM for PS and conducting ethyl substitution experiments at different enzymatic activities (0.292, 0.73, 1.168, 1.46, and 1.752 U/mg) and following up the reaction with time, then drawing the relationship between the activity and the enzymatic reaction rate, it appeared that (1.46) U/mg is optimum enzymatic activity of the reaction.

2.2.5.2. Determine the reaction's optimal pH and temperature by studying the ethanol substitution reaction over time.

After fixing the concentration of PS at 2.5 mM and the enzymatic activity at (1.46) U/mg. The experiments to monitor the reaction with time at different pHs (4, 6, 7.4, 8, and 10). From the velocity vs. pH chart it is found that pH (6) is the optimal pH for the ethyl substitution reaction of PS with ethanol.

In addition, the temperature of (37 °C) was the optimum temperature for the reaction, after following up the reaction with time at different temperatures (10, 20, 30, 37, and 45 °C) and with the conditions (2.5 mM of PS, enzymatic activity (1.46) U/mg and pH 6) for the purpose of obtaining the most regular absorption results over time.

2.6. Experiments of preparation of phospholipid derivatives

After identifying the appropriate pH, temperature, substrate concentration, and enzymatic activity for the enzymatic reaction, experiments were performed to prepare the phosphatidyl derivative for both phospholipids (PC and PS) at each solvent (water and ethanol).

The thin-layer chromatography method was used to monitor the product's production in each of these experiments. Aluminum plates were covered with thin layer plates made of alumina (Fixed phase), While three different solvents made up the mobile phase: (6mL of water ,2 mL of

ethanol, and 2 mL of n-hexane). Every ten minutes, a reaction mixture sample was taken and the spot was coloured with iodine. One spot appeared in the first ten minutes, with an (RF = 2cm) and remained constant throughout the reaction time as a result of the product forming in the first ten minutes of the reaction.

2.6.1 Preparation of phosphatidic acid (PA)

Phosphatidic acid was prepared by the hydrolysis of PC in present of PLD enzyme after multiplying and reacting under ideal conditions, the concentration of PC and the enzymatic activity of PLD increased to 15 times (1.5 mM of PC at the enzymatic activity of the enzyme PLD 26.28 U/mg, pH 7, and a temperature of 37 ^{o}C) where the reaction was followed by thin layer chromatography (TLC), where one spot was appeared for the product, the reaction continued until we got a fixed spot.

An hour after the reaction. Then, for the purpose of separating the fatty derivative, the reaction mixture was transferred to the separation funnel and an amount of petroleum ether was added to it. Then, for an hour, the mixture was mixed by mixing every ten minutes, then the mixture was left for half an hour, and after an hour had passed, the mixture was left in the separating funnel for half an hour, after which the aqueous mixture was separated from the etheric layer, and then the mixture was left to evaporate the petroleum ether, we obtained a liquid crystalline substance, and when n-hexane was added to it and left to dry, it was observed that a yellow precipitate appeared.

2.6.2. Creating the Phosphatidyl derivative from PC by substituting ethyl

After defining the previously mentioned ideal conditions for the ethyl substitution reaction of phosphatidylcholine, substitution experiments

were conducted by doubling the concentration of the substrate and the enzymatic activity tenfold (10 mM) of PC and 11.68 U/mg respectively, 6 pH and temperature 37 °C. The reaction mixing color was light yellow, and the reaction was followed up by TLC until the appearance of a fixed-height spot an hour after the start of the reaction, then the reaction mixture was separated in the same way mentioned above by using a separation funnel, where we obtained two layers after adding petroleum ether, one etheric and the other ethanolic, then after mixing and separation and adding n-hexane to the ether layer after its evaporation and letting it dry A beige precipitate (0.1) g appeared, while the ethanolic part was obtained after letting it dry light yellow flakes (0.01) g, the yield of the reaction was 62%.

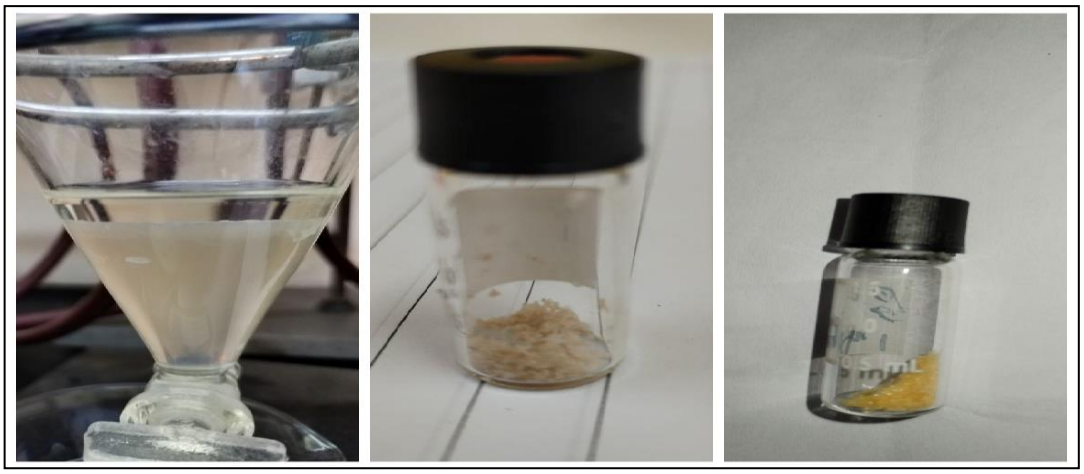

Figure (2-10): The separation funnel during the separation of the two layers, as well as the products of the etheric and ethanolic layers, respectively.

2.6.3. Hydrolysis of PS and preparation of the lipid derivative

The hydrolysis experiment for PS took an hour also when reacting (8 mM) of PS with (3.504 U/mg) of the enzymatic activity of PLD (two times the ideal conditions) at the conditions (pH= 6, and 37 °C) and following the same method mentioned above in a hydrolysis experiment for PC by following up the reaction and separating the product, we got (0.001) g a white substance from the fatty derivative in the petroleum portion of the mix. While the aqueous part did not appear to precipitate.

2.6.4. Ethyl substitution of PS results in the creation of a phosphatidylserine derivative

With a pink reaction mixture, and with five times, the ideal conditions for PS and PLD activity (12.5 mM, 7.3 U/mg, pH= 6, 37 ^{o}C), an experiment was conducted to prepare the fatty derivative to replace phosphatidylserine with ethanol and continued for 45 minutes after following up the reaction with the TLC technique, then following the same steps. The previously mentioned method separated the reaction products, where a precipitate (light pink flakes) weighing (0.058) g was observed. The ethanol part showed (0.052) g of white residue, while the yield of the reaction was 65%.

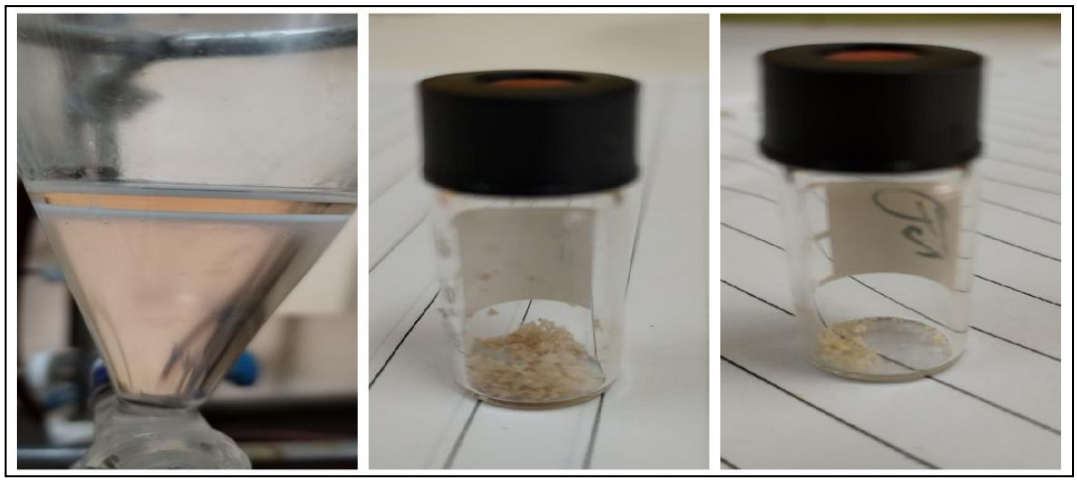

Figure (2-11): A figure showing the separation of the two layers in the separation funnel, where the ethanolic layer (at the top) and the etheric layer (at the bottom), and the products of the primary and side reaction, respectively.

2.7. Monitoring of Kinetic Parameters

2.7.1. Michaelis-Menten Equation

Following the Michaelis - Menten equation, the substrate concentration (for each derivative on its own) appropriate for the reaction was determined by monitoring changes in derivative concentrations (PC, PS) in water and ethanol as a solvent at a particular (enzymatic activity

1.46, 1.168, 1.46, 1.46 U/mg ,7.4,7,6,9 acidity functions) respectively and a constant temperature of 37 °C. The concentrations of each derivative separately were then plotted against the velocity. Determine the derivative's concentration at which the reaction velocity is half based on the information provided which known as the Michaelis constant (K_m).

2.7.2. Determine the product's concentration

Using Lambert-Beer's law (equation (Eq) (1)), the concentration of the substrate was determined for each experiment at every time, where (C) is the concentration of the substrate, (b) is the thickness of the cells (1 cm), (A) is the measured absorbance of the reaction mixture while following enzymatic experiments, and (Ɛ) is the molar absorption coefficient from the slope of calibration curve for each reaction see appendix 1,6,12 and 15 for more information.

$$C = A \setminus b\, \varepsilon \qquad \text{Eq}\ldots\ldots\ldots(1)$$

The product concentration was then measured using the following equation each time:

$$[P] = [S]_T - [S]_\circ \qquad \text{Eq}\ldots\ldots\ldots(2)$$

Where $[S]_T$ represents the concentration of the substrate at a certain time. Whereas $[S]_\circ$ represents the concentration of the substrate at time zero for each experiment.

2.7.3. Find the values of the reaction rate constant and enzymatic reaction rate

It was noted that there is a linear relationship when drawing between the natural logarithm of the product concentration (ln p) and time (t) in

minute, so the first-order equation Eq.(3) for the reaction can be applied to find the reaction rate constant and the enzymatic reaction rate.

$$\textbf{Slope = k (min}^{-1}\textbf{) = Velocity (}_{V}\textbf{)} \qquad \text{Eq}\ldots\ldots\ldots(3)$$

2.7.4 Calculating the values of K_m and V-Max for each reaction

By applying the Michaelis-Menten equation Eq.(4) and establishing the relationship between the substrate concentration [S] and the rate of the enzymatic reaction (V) as well as the line weaver Burk equation Eq.(5) is the relationship between reciprocal of velocity (1/ V) and reciprocal of substrate concentration (1/[S]). The values of the maximum velocity (V max) of the enzymatic reaction and a velocity constant were established. As shown in appendix 3,8,13, and 17.

$$v = \frac{V_{max}[S]}{K_m + [S]} \qquad \text{Eq}\ldots\ldots\ldots(4)$$

Michaelis-Menten equation

$$\frac{1}{v} = \frac{K_m}{V_{max}[S]} + \frac{1}{V_{max}} \qquad \text{Eq}\ldots\ldots\ldots(5)$$

Line Weaver Burk equation

2.7.5. Achieving the optimal activity for enzyme reaction

The optimal enzyme activity of an enzymatic reaction after which the speed becomes constant was calculated due to binding all substrates to the enzyme by drawing the linear relationship between the enzymatic activity and the related velocity, as in the appendixes 3,8,13, and 17.

2.7.6 Determine the optimal temperature and pH for enzymatic action

The optimum acidity function was identified by plotting the relationship between each velocity and the matching pH function (appendixes 5,10,15, and 19), which displayed a bell-shaped curve. As for the optimum temperature, it was determined through the bell curve resulting from plotting the speed values against the temperatures.

2.8. Calculate the Thermodynamic Parameters Δ H, Δ S and Δ G.

The slope of the straight line equation for Arrhenius Eq.(6) between the natural logarithm of the reaction rate constant (ln k) and reciprocal of temperature (1/T) was used to calculate the activation energy(E_a) necessary for the reaction to occur. For more information, see appendixes 4,9,14, and 18.

$$\ln k = \ln A - E_a / RT \qquad \text{Eq}\ldots\ldots\ldots(6)$$

Arrhenius equation

The value of (ΔS) and (ΔH) of the reaction can be found through the scheme of Van 't Hoff equation Eq.(7) between (ln k) and (1/T), where the slope is represented (-ΔH/R), but the intercept is represented cutting with the y- axis (ΔS/R).

$$\ln k_{eq} = -\Delta H/TR + \Delta S/R \qquad \text{Eq}\ldots\ldots\ldots(7)$$

R = The gas constant (8.314 Joule/mole)

Van 't Hoff equation

The Gibbs equation Eq.(8) can be used to compute the change in Gibbs free energy (ΔG) by using the ΔH and ΔS values:

$$\Delta G = \Delta H - T\,\Delta S \qquad \text{Eq}\ldots\ldots\ldots(8)$$

Where $\Delta H = E_a$ for liquid

Gibbs equation

Chapter Three

Results and Discussion

3. Results and Discussion:

3.1 Hydrolysis of Phosphatidylcholine

3.1.1. Phosphatidylcholine hydrolysis in an environment of strong hydrochloric acid:

The experiments for the hydrolysis of PC in presence of HCl were monitored by UV-Vis. and FTIR. A distinct peak at λ_{max} = 214nm, attributable to the n-π* transition of C=O for the fatty acid ester, can be seen in the UV-Vis. spectra of PC prior to the hydrolysis. The n-π* transition of (C=O) for free fatty acid and the ester of PC, respectively, are represented by two peaks at λ_{max} =200 nm and 212 nm after 1 hour of hydrolysis. The signal at 214 nm vanished over the course of the reaction period, and only the peak at 200 nm was recorded, showing that the two groups of free fatty acids from the PC were separated, as shown in Fig. 3-1, and Table 3-1.

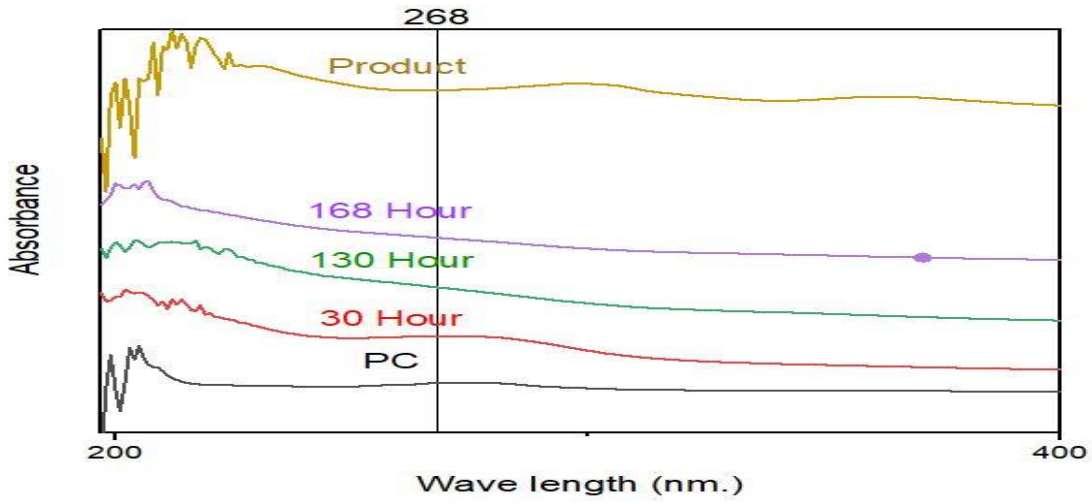

Figure (3-1): UV-Vis Spectra for the Hydrolysis of PC with HCl. A spectrum of PC before to the reaction is shown by the black curve. The red curve represents the PC spectrum at 30 hours into the reaction. At 130 hours into the reaction, the PC spectrum is shown as a green curve. At 168 hours into the reaction, the PC spectrum is shown as a purple curve. The end product, glycerol 3-phosphate, has a spectrum that is brownish yellow.

Table (3-1): PC undergoes changes in wavelengths and energy while being hydrolyzed in the presence of HCl.

Time (h)	λ_{max} (nm)	Transition	Energy (Kcal/mole)
0	214	n-π* (C=O, ester)	133.6
1	212	n-π* (C=O, ester)	134.87
	200	n-π* (C=O, fatty acid)	142.96
5	210	n-π* (C=O, ester)	136.15
	198	n-π* (C=O, fatty acid)	144.4
10	210	n-π* (C=O, ester)	136.15
	200	n-π* (C=O, fatty acid)	142.96
30	214	n-π* (C=O, ester)	133.6
	202	n-π* (C=O, fatty acid)	141.54
45	210	n-π* (C=O, ester)	136.15
	199	n-π* (C=O, fatty acid)	143.68
75	198	n-π* (C=O, fatty acid)	144.4
130	200	n-π* (C=O, fatty acid)	142.96
145	200	n-π* (C=O, fatty acid)	142.96
168	201	n-π* (C=O, fatty acid)	142.25

The investigation of FTIR spectra showed that at zero time of reaction, the strong peak at 1735 cm^{-1} was due to stretching of the C=O ester group, along with additional medium peaks at 2854 cm^{-1} and 2924 cm^{-1} that peaks are related to the two associated fatty acids for PC, and another medium peak at 3363 cm^{-1} that refers to stretching of N-H for aliphatic amine for choline.

After one hour of the hydrolysis reaction, a new and strong peak for the OH group at 3430 cm^{-1} emerged, which indicating to the dissociation of one fatty acid from the PC and the formation of an aliphatic alcohol as a result of substituting hydroxyl groups instead of fatty acids on the backbone of glycerol and this is supported by the separation of a black fatty layer belonging to the fatty acids attached to the backbone of glycerol on the surface of the reaction mixture since the first hour and continued increasing within 24 of the reaction, which was separated at the end of the reaction. The reaction continued, and it was observed that the peak at 1735 cm^{-1} progressively vanished, see Table 3-2 and Fig. 3-2. At the conclusion of the hydrolysis reaction, the FTIR spectra revealed an increase in the intensity of OH for aliphatic alcohols due to the substitution of two hydroxyl groups for two fatty acids on the backbone of glycerol to form the glycerol-3-phosphate as a final product of the hydrolysis reaction for the PC.

Table (3-2): The FTIR peaks for the PC functional groups during the hydrolysis of PC in 2M of HCl.

Time (h)	Position of peak (cm^{-1})	Intensity	Group	Notes
0	3363	m	N-H (ν)	Choline (195)
	3009-2924	m	C-H (ν)	Alkene of FA (196)
	2854	m	C-H (ν)	Alkane of FA (196, 197)
	1735	s	C=O (ν)	Ester (196, 197)
	1647	w	C=C (ν)	Alkene of FA (196)
	1230	m	C-N (ν)	Choline (195)
	597	w	P-O (ν)	Phosphate (198)

1	3430 1739 1651 1211 605	s s w m w	O-H (ν) C=O (ν) C=C (ν) C-N (ν) P-O (ν)	Alcohol (198) Ester (196, 197) Alkene of FA at *sn*-2 (196) Choline (195) Phosphate (198)
5	3380 1643 1226 602	br, s w m w	O-H (ν) C=C (ν) C-N (ν) P-O (ν)	Alcohol (198) Alkene of FA at *sn*-2 (196) Choline (195) Phosphate (198)
10	3364 1709 1640 1230 598	br, s m w m w	O-H (ν) C=O (ν) C=C (ν) C-N (ν) P-O (ν)	Alcohol (198) Carboxylic of free FA (196) Alkene of free FA (196) Choline (195) Phosphate (198)
30	3364 1196 602	br, s w w	O-H (ν) C-N (ν) P-O (ν)	Alcohol (198) Choline (195) Phosphate (198)
45	3379 1709 1640 1227 602	br, s m w w w	O-H (ν) C=O (ν) C=C (ν) C-N (ν) P-O (ν)	Alcohol (198) Carboxylic of free FA(196) Alkene of free FA (196) Choline (195) Phosphate (198)
75	3364	br, s	O-H (ν)	Alcohol (198)

	1712 1647 1223 598	w w w w	C=O (ν) C=C (ν) C-N (ν) P-O (ν)	Carboxylic of free FA (196) Alkene of free FA (196) Choline (195) Phosphate (198)
130	3364 1651 1210 602	br, s w w w	O-H (ν) C=C (ν) O-H (ν) C=C (ν) C-N (ν) P-O (ν)	Alcohol (198) Alkene of free FA (196) Choline (195) Phosphate (198)
145	3368 602	br, s w	O-H (ν) P-O (ν)	Alcohol (198) Phosphate (198)
168	3360 602	br, s w	O-H (ν) P-O (ν)	Alcohol (198) Phosphate (198)

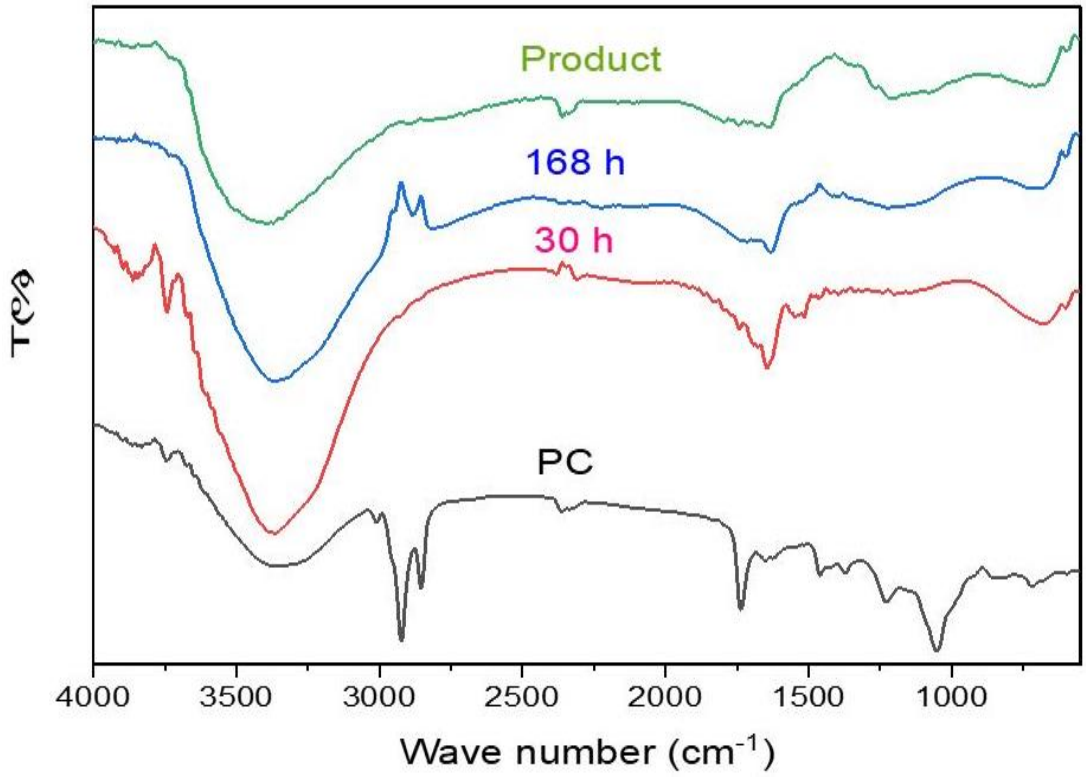

Figure (3-2): The spectra of FTIR for PC hydrolysis with HCl present. The PC spectrum before the reaction is shown by the black curve. At 30 hours into the reaction, a PC spectrum is shown in red. The blue curve represents a PC spectrum at 168 hours into the reaction. A spectrum of the finished product, glycerol 3-phosphate, is shown by the green curve.

The major three final products of the PC hydrolysis reaction, glycerol-3-phosphate, free fatty acid, and choline chloride were isolated and characterized using NMR, GC-Mass and FTIR spectroscopy.

3.1.2. Characterization of Products for hydrolysis of PC in HCl

3.1.2.1 Characterization of glycerol-3-phosphate

The ^{1}HNMR spectrum for glycerol-3-phosphate in dimethyl sulfoxide–d^6 (DMSO-d^6) (Fig.3-3) displays a doublet-doublet peak at δ 1.23 - 1.16 belonging to the two hydrogen atoms attached to carbon atom of CH_2 group which attached to glycerol-3-phosphate at position *sn*-1,

while the proton of the hydroxyl group attached to it in addition proton of the hydroxyl group attached to the carbon atom of the methylene group at position *sn*-3 showed a singlet peak at δ 3.31, due to they have the same environment. In addition to singlet peak at δ 2.73 belonging to the hydrogen atom of the middle group CH at position *sn*-2 of the glycerol backbone, while the proton of the OH group associated with it showed a singlet peak at δ 5.32. On the other hand, the two

protons of the other terminal CH_2 group at position *sn*-3 show a doublet-doublet peak at δ 4.02 - 4.04.

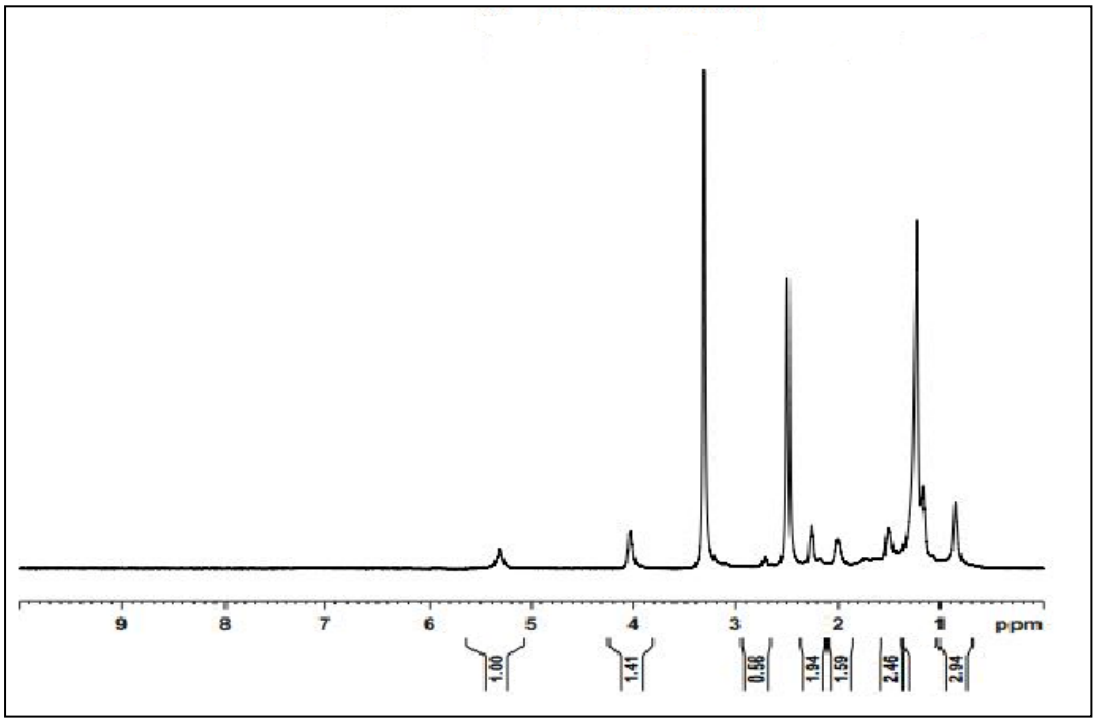

Figure (3-3): Glycerol-3-phosphate's ^{1}H NMR spectrum in DMSO-d^{6}.

The ^{13}C NMR spectrum showed that the carbon atom of the methylene group at position *sn*-1 of the glycerol backbone showed a peak at δ 63.2 in the spectrum of ^{13}C NMR for glycerol-3-phosphate in DMSO-d^{6}.The carbon atom of the other terminal CH_2 group at position *sn*-3 of glycerol-3-phosphate showed a peak at δ 73.9. In addition to peak at δ 72.7 belonging to the carbon of the CH group at position *sn*-2, see Fig. 3-4.

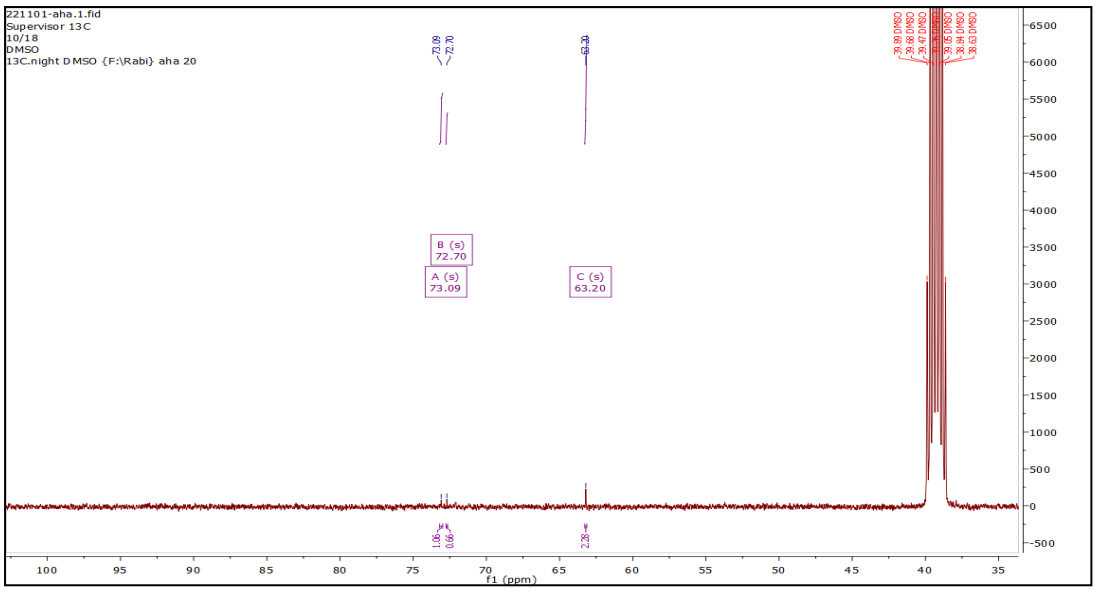

Figure (3-4): The ^{13}C NMR spectrum of glycerol-3-phosphate's in DMSO-d^{6}.

The ^{31}P NMR spectrum of glycerol-3-phosphate in DMSO-d^{6}: spectrum shows a singlet peak δ 1.48 that belongs to the 1 P of phosphate group ($PO4^{2-}$) arranged on the glycerol backbone at position *sn*-3.

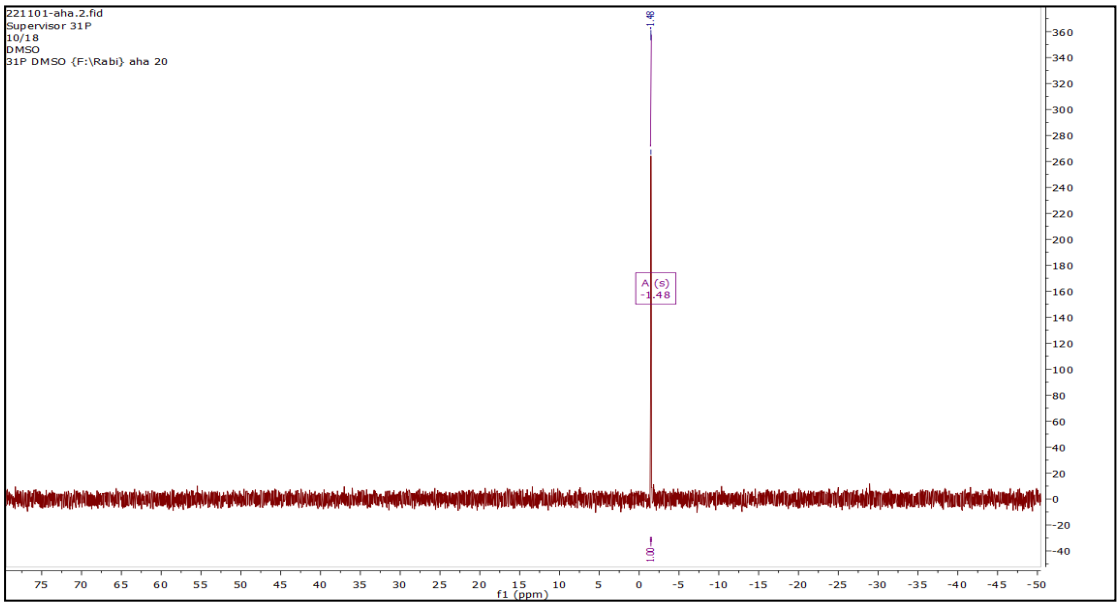

Figure (3-5): The ^{31}P NMR spectrum of glycerol-3-phosphate in DMSO-d^{6}.

The FTIR spectrum of glycerol-3-phosphate showed that the strong broad peak at 3371 cm^{-1} associated with stretching of the *sn*-1 OH and *sn*-2 OH groups as a result of the breakdown of fatty acids associated with the

backbone of glycerol and their replacement with a hydroxyl group, the medium peak at 2897 cm^{-1} related to stretching of the C-H alkane at the *sn*-1, *sn*-2, and *sn*-3 positions, and the weak peak at 598 cm^{-1} associated with the P-O of the $PO4^{2-}$ group were all visible in the FTIR spectrum of glycerol-3-phosphate, as shown in Fig. 3-6.

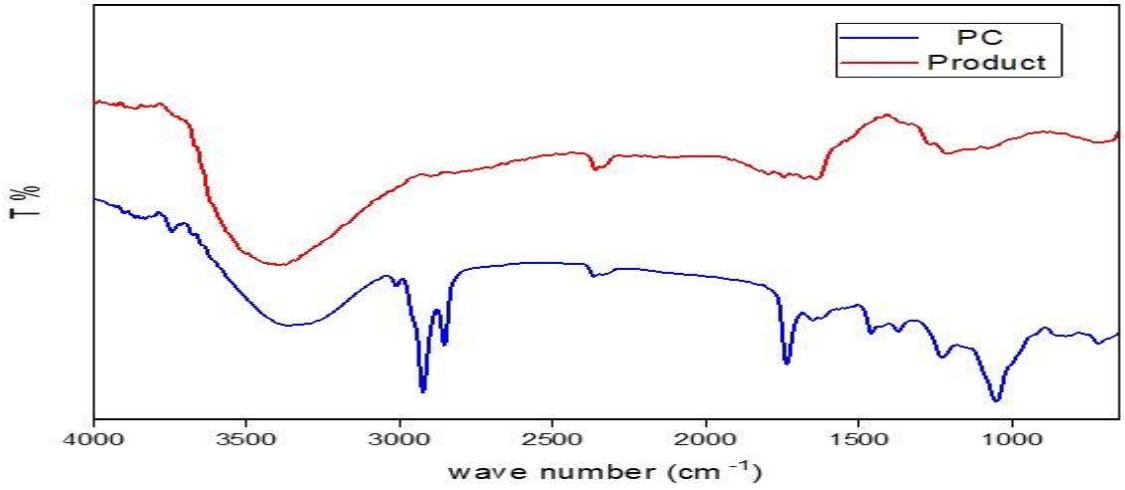

Figure (3-6): The FTIR spectra for the hydrolysis of PC in HCl. The FTIR spectrum of PC is shown by the blue curve, while a spectrum glecerol-3-phosphate, is shown by the red curve.

The mass spectrum of glycerol-3-phosphate appears in the signal at (168.9 m/z) relative to the molecular ion, corresponding with the calculated molecular weight (170 g/mole), as shown in Fig. 3-7.

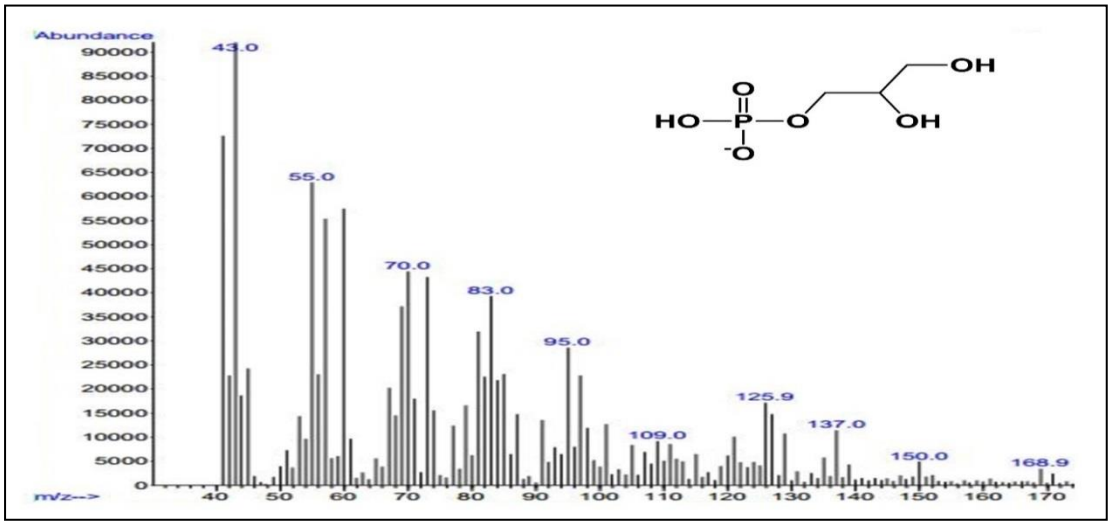

.

Figure (3-7): The GC- mass spectra of glycerol-3-phosphate.

3.1.2.2. Characterization of Dissociative free fatty acids

Figure 3-8 illustrates the ^{1}H NMR spectrum of free fatty acids in DMSO-d^{6} contains a triple peak at δ 1.07 back to the protons of the terminal methyl group, in addition to the presence of a δ 2.32–2.45 multiplet peak return to 20 protons for the CH_2 groups present in the structure of fatty acids. For the other CH_2 groups, their eight protons show a multiplet peak at δ 3.11–3.72, the doublet-doublet peak at δ 5.22–5.63 which they belong to the four protons of the methylene group adjacent to the double bond carbon atom in the compound. They added a final singlet peak δ 8.52 to the proton of the terminal hydroxyl group of the carboxylic acid.

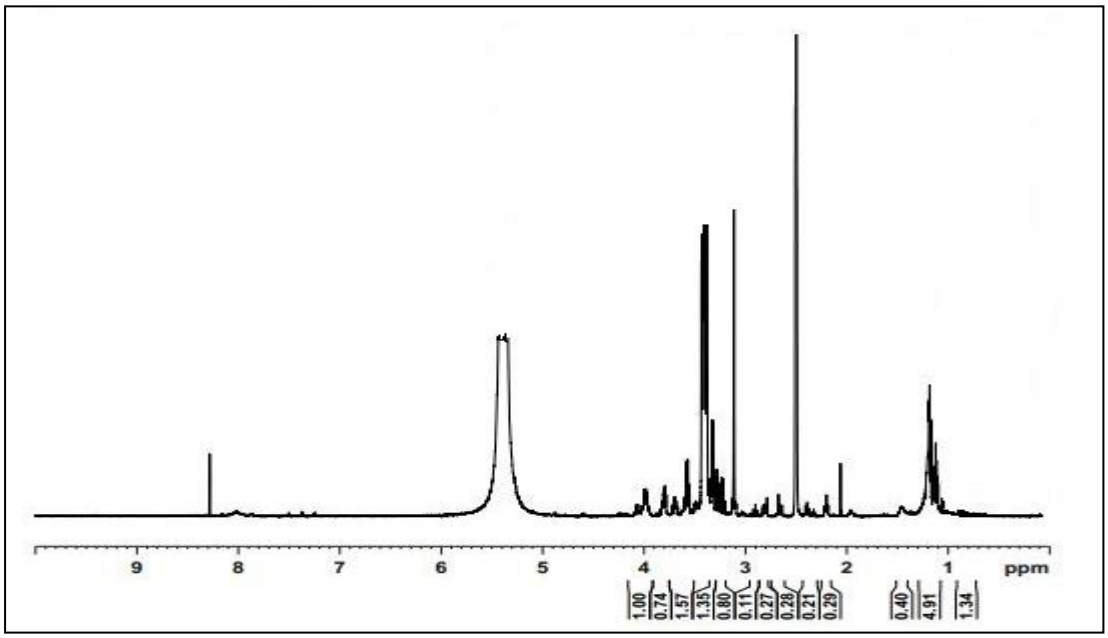

Figure (3-8): The ^{1}H NMR spectrum of free fatty acid in DMSO-d^{6}.

As seen in Fig. 3-9, the free fatty acid ^{13}C NMR spectrum in DMSO-d^{6} has 18 C peaks, including: δ 14.42, δ 14.59, δ 28.18, δ 30.08, δ 37.98, δ 53.58, δ 53.62, δ 53.65, δ 55.55, δ 57.89, δ 62.91, δ 63.49, δ 71.03, δ 72.34, δ 72.96, δ 73.06, δ 73.22, and δ 75.70

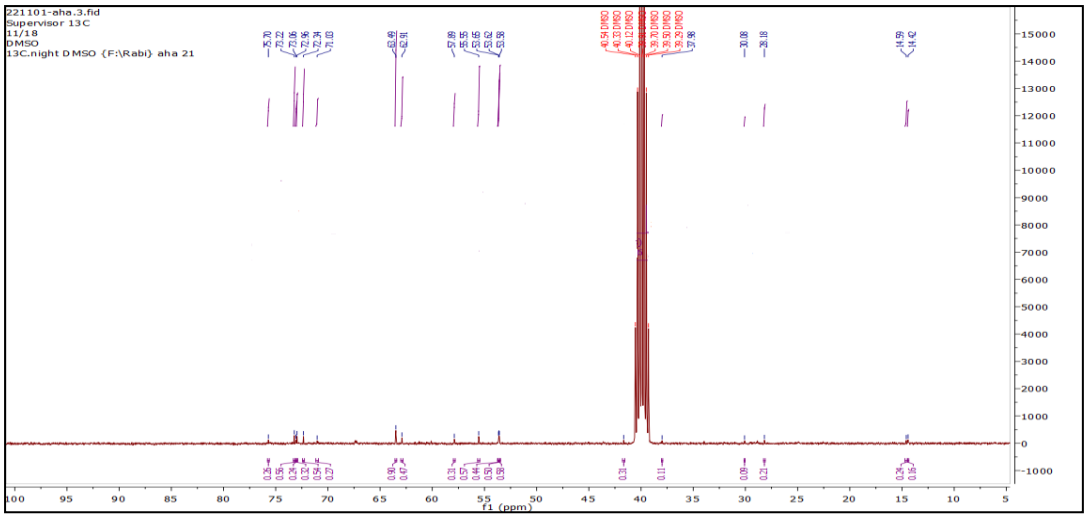

Figure (3-9): The ^{13}C NMR spectrum of free fatty acid in DMSO-d^{6}.

The Fourier transform infrared (FTIR) spectrum of free fatty acids revealed a strong peak at 1709 cm^{-1} that refers to stretching of C=O fatty acid, as well as other peaks at 3359 cm^{-1} return to free O–H of carboxylic acid. In addition to weak peak at 1095 cm^{-1} for the (C–O) bond. 2924 cm^{-1} and 2854 cm^{-1} that are attributed to stretching of C-H alkane. The stretching of C–H alkene showed a weak peak at 3009 cm^{-1} due to the present of double bond in the structure of fatty acid. two another peaks at 1373 cm^{-1} belong to the bending of methyl groups and 1462 cm^{-1} belong to the bending of methylene groups and a weak peak at 721 cm^{-1} belongs to the rocking of methylene groups (> 4C), which indicates that we have a series hydrocarbons are more than four carbon atoms. See Fig.3-10.

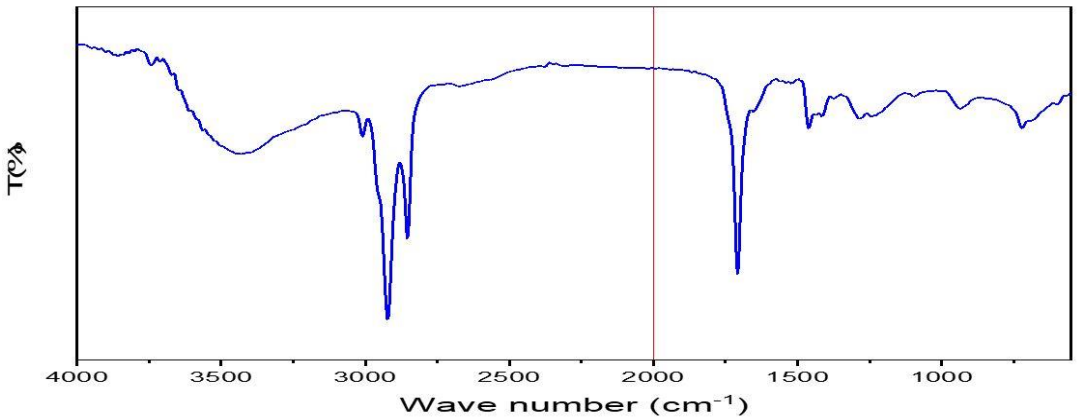

Figure (3-10): The FTIR spectrum of fatty acid.

The mass spectrum of palmitic acid appears in the signal at (256.1 m/z) relative to the molecular ion, the value close to the calculated molecular weight (255 g/mole), as shown in Fig. 3-11.

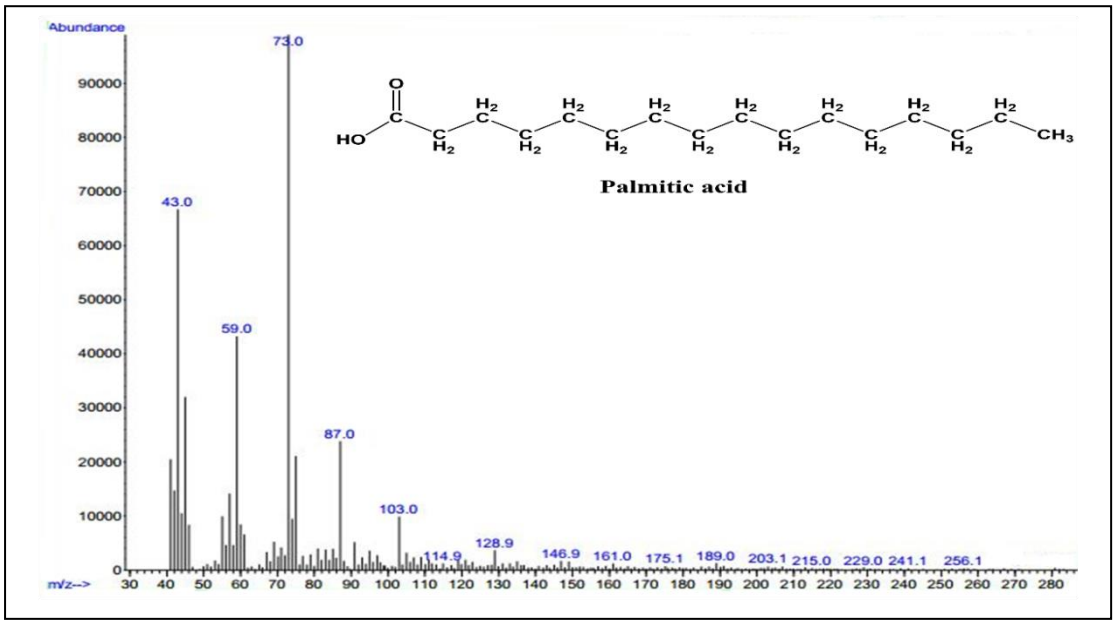

Figure (3-11): The GC-mass spectra of palmitic acid.

The mass spectrum of octadeca-9,12-dienoic acid appears in the signal at (281.0 m/z) relative to the molecular ion, the value close to the calculated molecular weight (279 g/mole), as shown in Fig. 3-12.

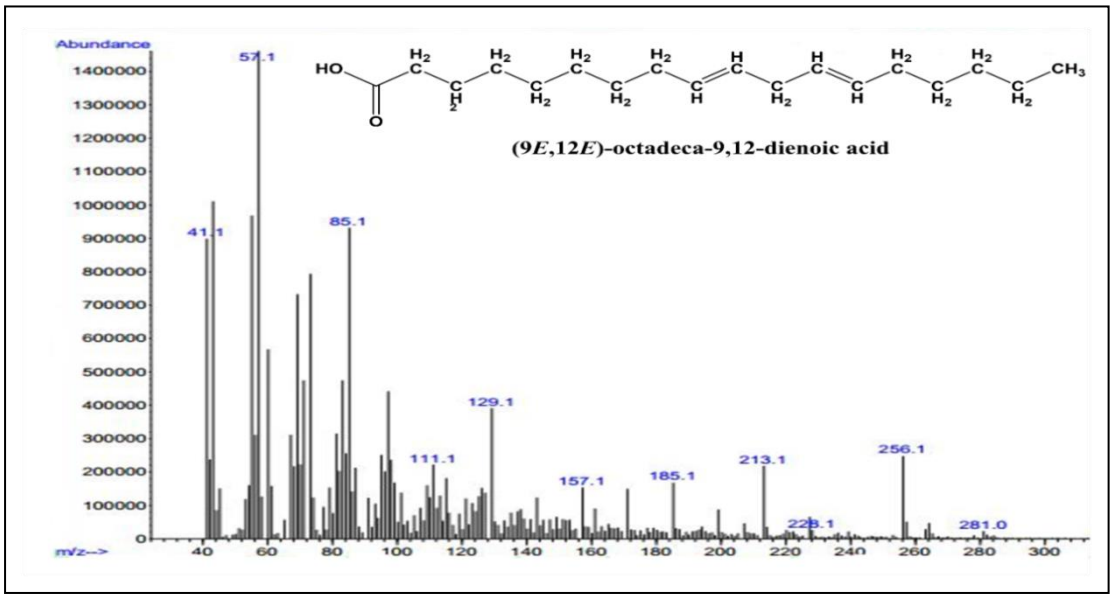

Figure (3-12): The GC-mass spectra of octadeca-9,12-dienoic acid.

3.1.2.3. Characterization of Choline Chloride:

The ^{1}H NMR spectrum of choline chloride in DMSO-d^{6} shows a triplet peak at δ 3.34 that belongs to the protons of the nine methyl groups, in addition to a doublet-doublet peak that belongs to the proton of CH_2 group adjacent to the nitrogen atom at δ 3.65, another doublet-doublet peak at δ 3.86 return to two proton of methylene group attached to the oxygen atom of the hydroxyl group, and a single peak at δ 5.17 that belongs to the proton of the hydroxyl group. See Fig. 3-13.

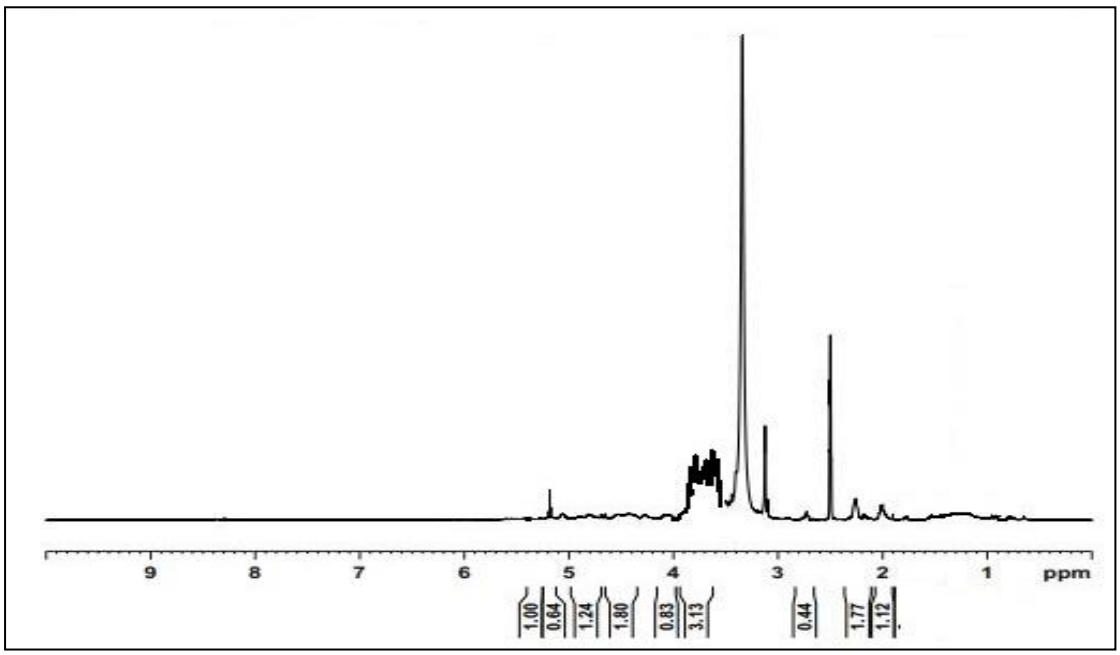

Figure (3-13): The ^{1}H NMR spectrum of choline chloride in DMSO-d^{6}.

As for the ^{13}C NMR spectrum of choline chloride in DMSO-d^{6}, it contains a peak at δ 22.44 that belongs to the carbon atom of the methylene group attached to the hydroxyl group. The carbon atom of the methyl group appears as a peak at δ 29.19 in addition to a peak at δ 29.5 belonging to two carbon atoms of the other methyl group. The peak at δ 31.37 belongs to the carbon atom of the group attached to the nitrogen atom, as shown in Fig. 3-14.

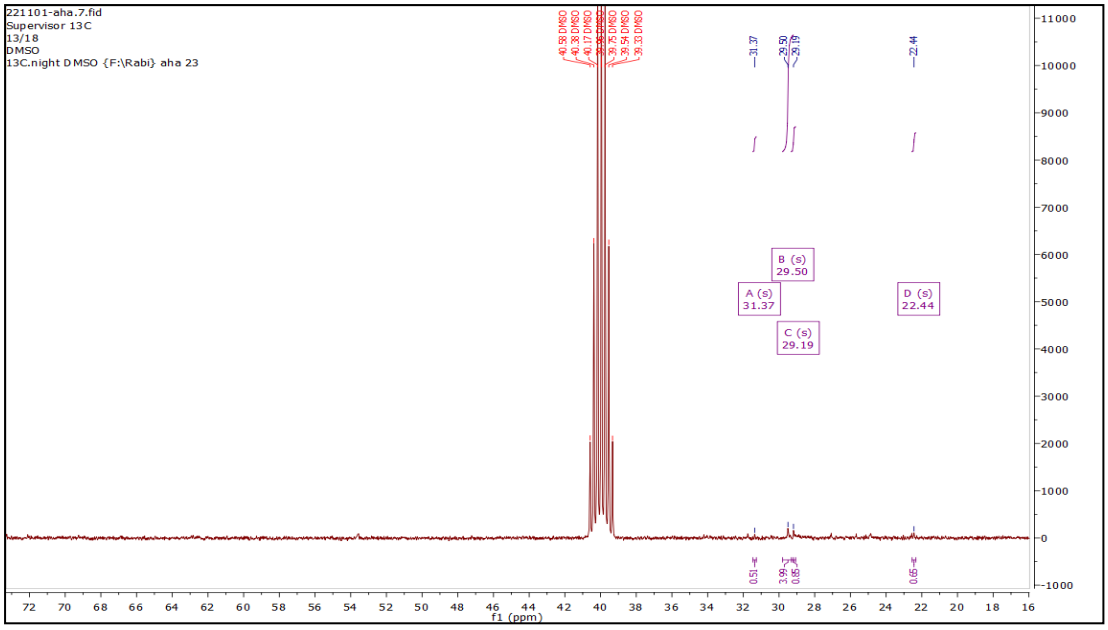

Figure (3-14): The ^{13}C NMR spectrum of choline chloride in DMSO-d^{6}.

As illustrated in Fig.3-15, the Fourier transform infrared spectrum of choline chloride showed three peaks: a weak peak at 1259 cm^{-1} ascribed to stretching C-N aliphatic amine, a medium broad peak at 3472 cm^{-1} attributed to stretching O-H bond, and a strong peak at 2940 cm^{-1} referring to stretching C-H alkane.

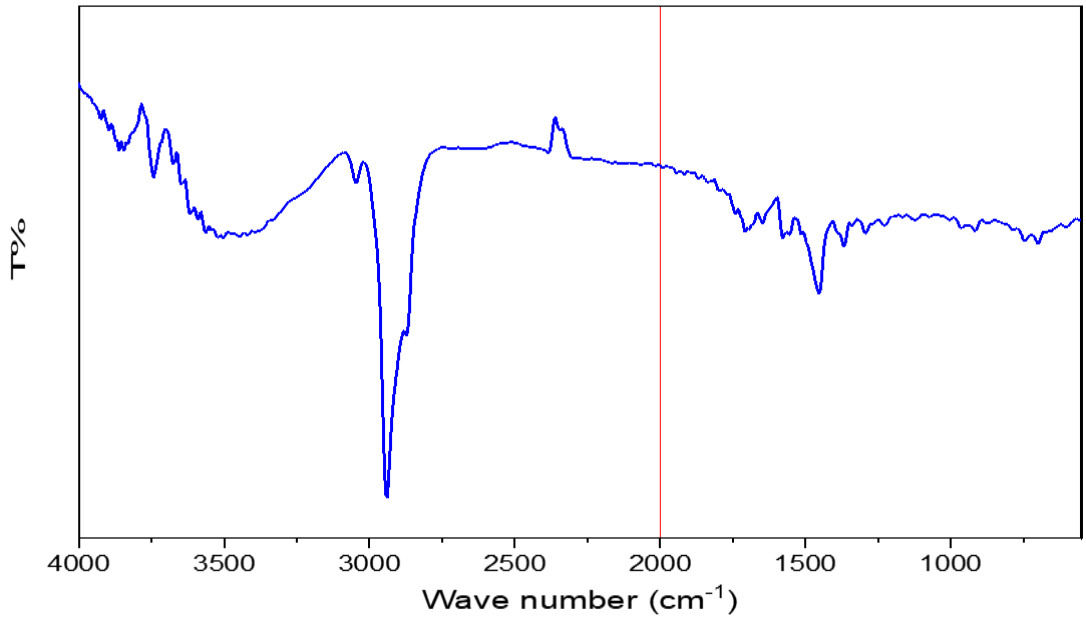

Figure (3-15): The FTIR spectrum of the choline chloride produced as a byproduct of PC hydrolysis.

The mass spectrum of choline chloride appears in the signal at (137.0 m/z) relative to the molecular ion, the value close to the calculated molecular weight (139.5 g/mole), as shown in Fig. 3-16.

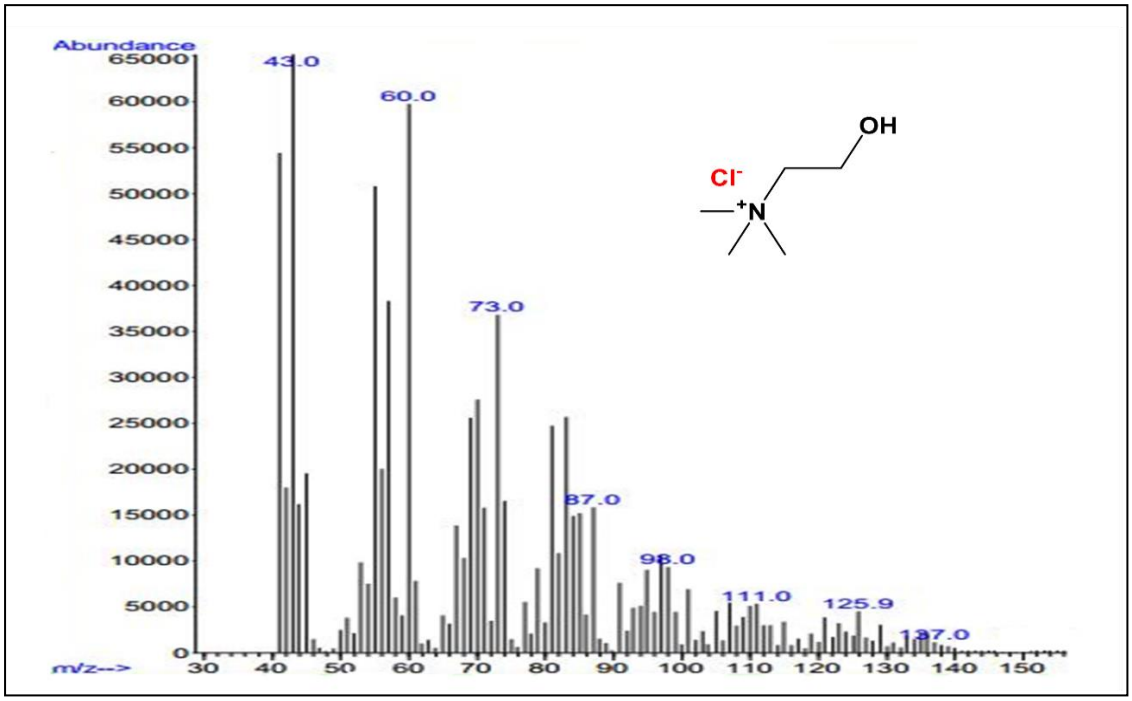

Figure (3-16): The GC-mass spectra of choline chloride.

Based on the findings, it appears that there are three primary steps involved in the hydrolysis of PC. First step, the carbonyl groups at positions *sn*-1 and *sn*-2 and phosphate at position *sn*-3 are protonated. Next step, the water molecule attacked as a nucleophilic agent. The second phase of the procedure involves the proton moving into the ester bond's oxygen, which is followed by the liberation of free fatty acid groups from the *sn*-1 and *sn*-2 positions. As indicated in Fig. 3-17, the subsequent step entails creating an intra-hydrogen bond between the oxygen of phosphate and the hydrogen of *sn*-2 OH, which is followed by protonation of the oxygen for choline, which results in dissociation as choline chloride.

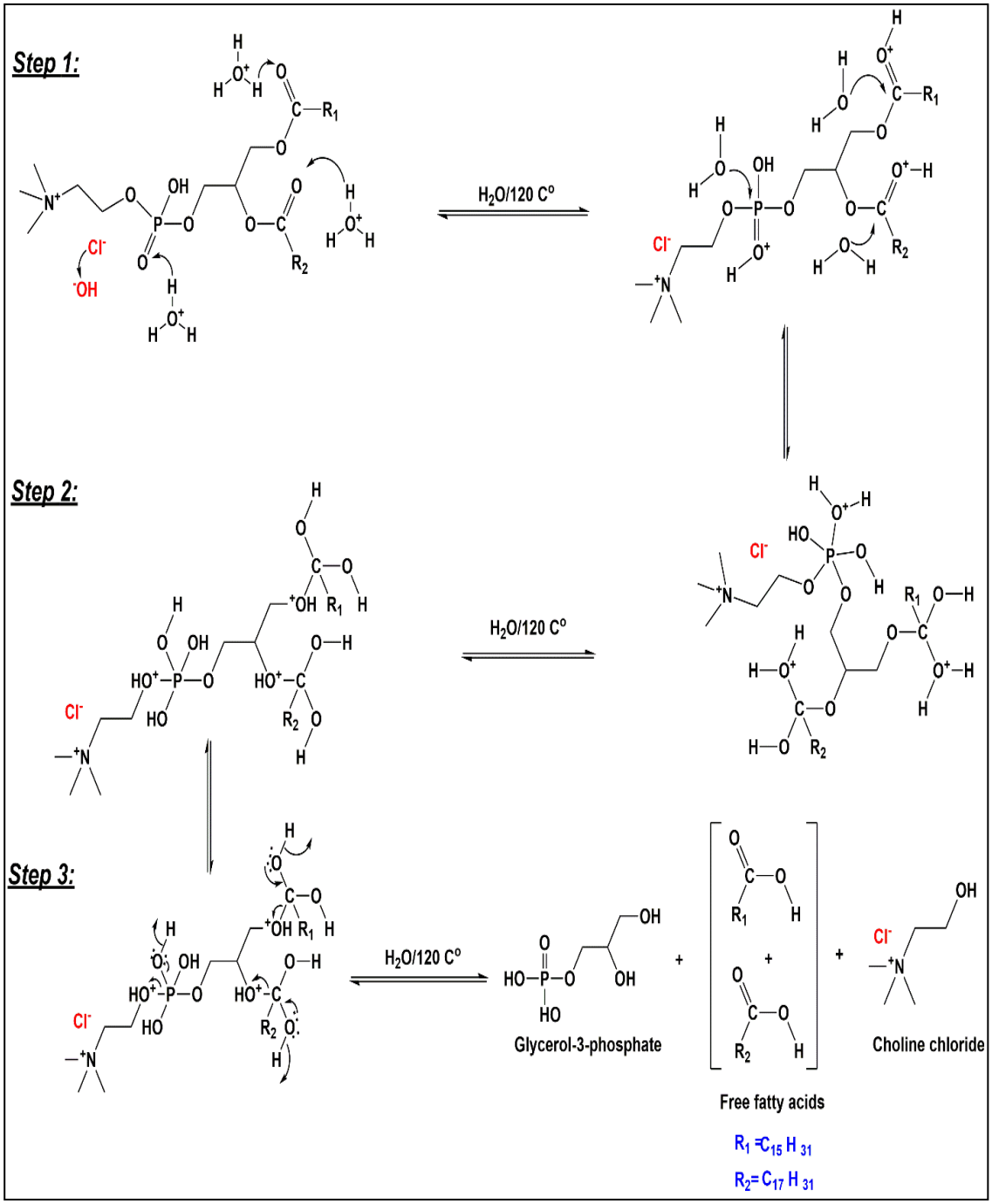

Figure (3-17): The suggested mechanism for the PC hydrolysis reaction in presence of the HCl.

3.2.2. Hydrolysis of Phosphatidylcholine in Ethanol

The UV/Vis. and FTIR spectroscopy were also used to observe the response of PC hydrolysis in the presence of ethanol in an acidic environment.

3.2.2.1. Spectral observations in the UV-visible range:

As demonstrated in Table 3-3, utilizing ethanol as a solvent has a minor impact on the UV/Vis. spectra of PC during the hydrolysis procedure. Additionally, it should be highlighted that ethanol is crucial to the hydrolysis reaction of PC. The UV/Vis. spectra of PC displayed a peak at λ_{max} = 279 nm at the beginning of the process, which is attributed to the carbonyl's n-π* transition for the PC ester group. The spectrum showed two peaks at λ_{max} =281 nm refer to n-π* transition of C=O for the PC ester group and another peak at λ_{max} =212 nm refer to produce new ethyl ester with the fatty acid residue at PC after the PC hydrolysis reaction had been going on for an hour.

Table (3-3): The variations in PC's wavelengths and energy caused by the presence of ethanol during hydrolysis.

Time (h)	λ_{max} (nm)	Transition	Energy (Kcal/mole)
0	279	n-π* (C=O, PC ester)	102.48
1	281	n-π* (C=O, PC ester)	101.75
	212	n-π* (C=O, ethyl fatty ester)	134.87
5	283	n-π* (C=O, PC ester)	101.03
	215	n-π* (C=O, ethyl fatty ester)	132.98
24	275	n-π* (C=O, PC ester)	103.97
	212	n-π* (C=O, ethyl fatty ester)	134.87
45	279	n-π* (C=O, PC ester)	102.48
	213	n-π* (C=O, ethyl fatty ester)	134.23
85	268	n-π* (C=O, PC ester)	106.68
	211	n-π* (C=O, ethyl fatty ester)	135.5

100	258	n-π* (C=O, PC ester)	110.82
	210	n-π* (C=O, ethyl fatty ester)	136.15
150	268	n-π* (C=O, PC ester)	106.68
	212	n-π* (C=O, ethyl fatty ester)	134.87

Monitoring the shift in UV/Vis. spectra while PC was being hydrolyzed in the presence of ethanol gave solid proof that the fatty acid was being dissociated as an ethyl fatty ester rather than remaining in the PC as a free fatty acid. The formation of high concentrations of ethyl fatty ester during the hydrolysis of PC in the presence of ethanol may explain why the absorbance at the $\lambda_{max} \approx 212$ nm increased and the absorbance at the $\lambda \approx 280$ nm reduced at the conclusion of the reaction, as shown in Fig. 3-18.

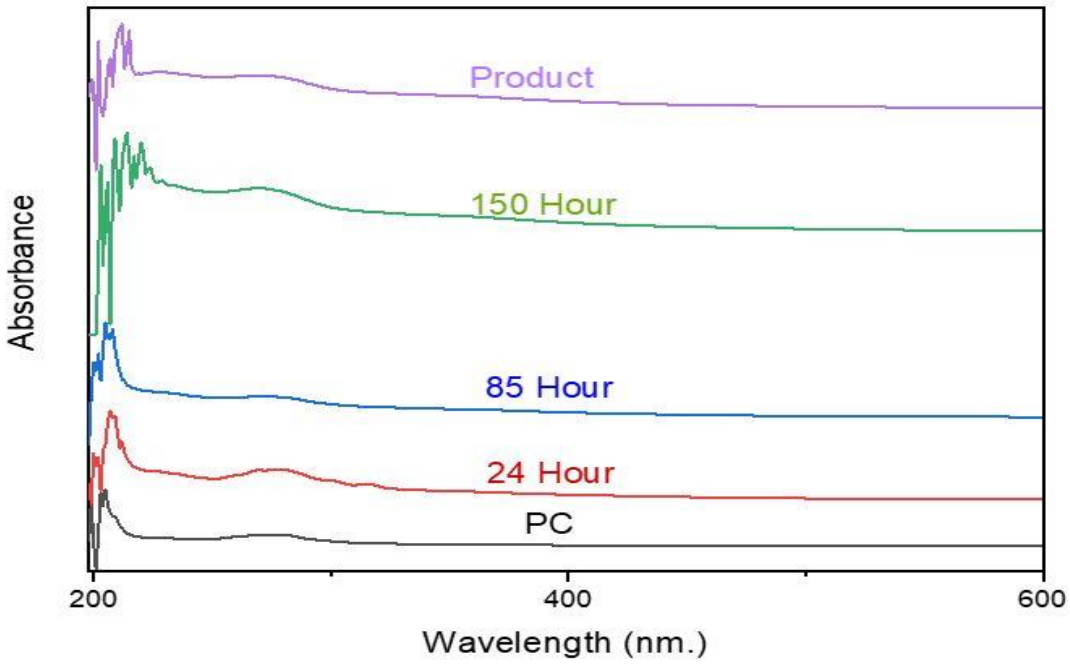

Figure (3-18): UV-Vis. spectra for the ethanol-induced hydrolysis of PC. The PC spectrum before the reaction is shown by the black curve. Spectrum of PC at 24 hours into the reaction is shown by the red curve. Spectrum of PC at 85 hours into the reaction is shown by the blue curve. A PC spectrum at 150 hours into the reaction is shown by the green curve. A spectrum of PC for the finished product (Ethyl fatty ester) is shown by the purple curve.

3.2.2.2. Monitoring FTIR Spectra for Phosphatidylcholine Hydrolysis in Presence of Ethanol:

The observation of the infrared spectra of the nucleophilic substitution reaction with the ethyl group of ethyl alcohol decrease in the intensity of the peak belonging to the ester carbonyl group(C=O) and a shift of it towards a lower wave number 1681 cm^{-1} since the first hour of the reaction, this indicates the separation of fatty acids at the *sn*-1 and *sn*-2 sites attached to the glycerol backbone. However, it is worth noting that upon the gradual separation of fatty acids, it disappears in the form of a fatty layer on the surface of the reaction mixture as in the hydrolysis reaction of phosphatidylcholine, but it was mixed with the reaction mixture causing the gradually change in the color of the reaction mixture from light yellow to brown color. After that, monitoring the interaction at 40 h from the start of the reaction black oily flakes appeared on the surface of the mixture and continued to increase until the time 105 h of the reaction and gradually became in the form of a black oily layer on the surface of the reaction mixture. A sharp peak appeared in the infrared spectrum during this time (at 40 h) at 1739 cm^{-1}, its intensity continued to increase until it became medium in intensity and remained visible in the spectrum until the end of the reaction at 150 h because the same active C=O ester group as the PC is produced in ethyl fatty ester. From the foregoing, it is clear that this is the black compound that appeared and was separated at the end of the reaction is the by-product (ester compound). However, after one hour of the reaction, a new strong broad peak at 3330 cm^{-1} emerged. This peak is attributable to stretching of the O-H bond for the primary product of the hydrolysis reaction of the PC, glycerol-3-phosphate, as indicated in Table 3-4 and Fig.3-19.

After PC was hydrolyzed in ethanol, the various end products were isolated and analysed using NMR and FTIR spectroscopy.

Table (3-4): Features of PC functional group FTIR peak during ethanol-induced hydrolysis.

Time (h)	Position of peak (cm^{-1})	Intensity	Group	Notes
0	3290	br, w	N-H (ν)	Choline (195)
	2978	m	C-H (ν)	Alkene of FA (196)
	2890	m	C-H (ν)	Alkane of FA (196, 197)
	1735	s	C=O (ν)	Ester (196, 197)
	1647	w	C=C (ν)	Alkene of FA (196)
	1260	m	C-N (ν)	Choline (195)
	601	w	P-O (ν)	Phosphate (198)
1	3330	s	O-H (ν)	Alcohol (198)
	1740	m	C=O (ν)	Ester (196, 197)
	1662	w	C=C (ν)	Alkene of FA at *sn*-2 (196)
	1273	w	C-N (ν)	Choline (195)
	602	w	P-O (ν)	Phosphate (198)
5	3306	br, s	O-H (ν)	Alcohol (198)
	2974	m	C-H (ν)	Alkene of FA (196)
	2893	w	C-H (ν)	Alkane of FA (196, 197)
	1651	w	C=C (ν)	Alkene of FA at *sn*-2 (196)
	1273	w	C-N (ν)	Choline (195)
	602	w	P-O (ν)	Phosphate (198)
24	3329	br, s	O-H (ν)	Alcohol (198)

	2974	s	C-H (ν)	Alkene of FA (196)
	1674	w	C=C (ν)	Alkene of FA at *sn*-2 (196)
	1381	m	O-H (δ)	Alcohol (198)
	1273	w	C-N (ν)	Choline (195)
	601	w	P-O (ν)	Phosphate (198)
45	3340	br, s	O-H (ν)	Alcohol (198)
	2978-2928	m	C-H (ν)	Alkene of FA (196)
	1739	m	C=O (ν)	Ester of Ethyl FA ester (196)
	1651	w	C=C (ν)	Alkene of free FA (196)
	1381	m	O-H (δ)	Alcohol (198)
	1250	w	C-N (ν)	Choline (195)
	606	w	P-O (ν)	Phosphate (198)
85	3352	br, s	O-H (ν)	Alcohol (198)
	2987	m	C-H (ν)	Alkene of FA (196)
	2897	m	C-H (ν)	Alkane of FA (196, 197)
	1739	m	C=O (ν)	Ester of Ethyl FA ester (196)
	1678	w	C=C (ν)	Alkene of FA (196)
	1381	m	O-H (δ)	Alcohol (198)
	1223	w	C-N (ν)	Choline (195) Phosphate (198)
	601	w	P-O (ν)	

100	3321	br, s	O-H (ν)	Alcohol (198)
	2979	m	C-H (ν)	Alkene of FA (196)
	2901	m	C-H (ν)	Alkane of FA (196, 197)
	1739	w	C=O (ν)	Ester of Ethyl FA ester (196)
	1675	w	C=C (ν)	Alkene of free FA (196)
	1377	m	O-H (δ)	Alcohol (198)
	1226	w	C-N (ν)	Choline (195)
	601	w	P-O (ν)	Phosphate (198)
150	3365	br, s	O-H (ν)	Alcohol (198)
	3009	m	C-H (ν)	Alkene of FA (196)
	2875	m	C-H (ν)	Alkane of FA (196, 197)
	1739	w	C=O (ν)	Ester of Ethyl FA ester (196)
	1645	w	C=C (ν)	Alkene of free FA (196)
	1376	m	O-H (δ)	Alcohol (198)
	1223	w	C-N (ν)	Choline (195)
	602	w	P-O (ν)	Phosphate (198)

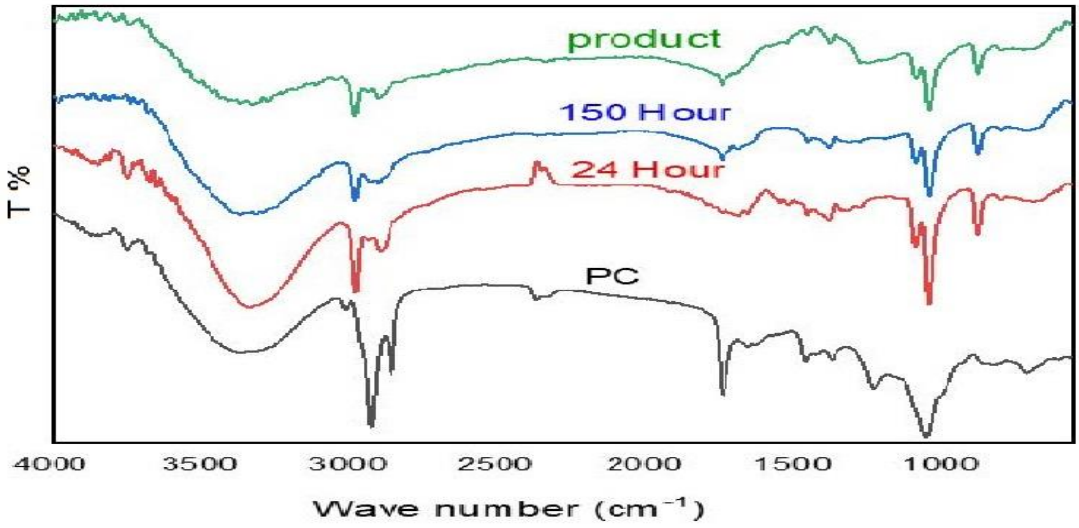

Figure (3-19): The FTIR spectra for the hydrolysis of PC in ethanol. PC's pre-reaction spectrum is shown by the black curve. The red curve represents the PC spectrum after 24 hours of the response. A PC spectrum at 150 hours into the reaction is shown by the blue curve. The end product's (Ethyl fatty ester) spectrum is represented by the green curve.

3.3. The Characterization of Products for the Hydrolysis of PC in Presence of Ethanol

3.3.1. Characterization of Glycerol-3-ethylphosphate.

The observations of glycerol-3-phosphate, the primary product of PC hydrolysis, yielded identical results for ^{1}H NMR, ^{13}C NMR, ^{31}P NMR, FTIR, and Mass spectra as shown in Figs. 3-3, 3-4, 3-5,3-6 and 3-7.

3.3.2. Characterization of Choline Chloride

Referring to the characterization that mentioned above the ^{1}H NMR, ^{13}C NMR, FTIR, and Mass spectra results for the choline chloride were identical as shown in Figs 3-13, 3-14, and 3-15.

3.3.3. Characterization of Ethyl Fatty Esters

The second product which is ethyl fatty ester was characterized and the ^{1}H NMR spectra in DMSO-d^{6} showed the triplet peak belonging to the

protons of the three methyl groups at δ 0.89 and another triplet peak at δ 1.08 belonging to the protons of the terminal methyl group close to the ester group. In addition to a singlet peak, the methyl group returns to δ 2.1. A multiplet peak at δ 3.32 – 3.8 belongs to ten protons of the methylene group, and another doublet – doublet peak belongs to the protons of the twenty CH_2 groups at δ 4.8 - 5.1, as shown in Fig. 3-20.

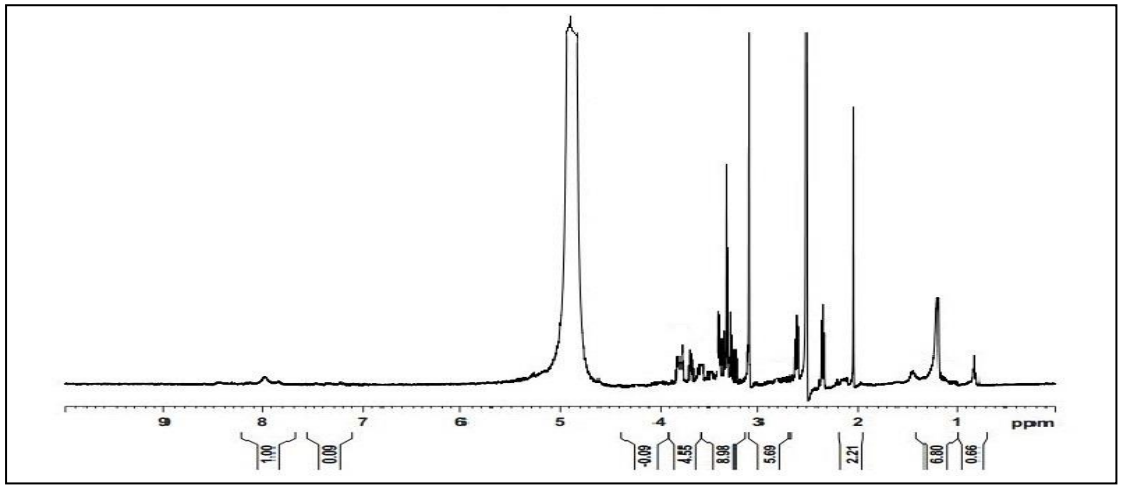

Figure (3-20): The ^{1}H NMR spectrum of Ethyl fatty ester in DMSO-d^{6}.

Figure 3-21 illustrates the 20 C peaks seen in the 13C NMR spectra of ethyl fatty ester in DMSO-d^{6}: 14.33, 14.7, 28.3, 31.1, 41.44, 41.66, 53.56, 53.60, 53.64, 55.73, 58.88, 63.01, 63.51, 71.11, 72.64, 72.77, 73.09, 73.32, and 75.8.

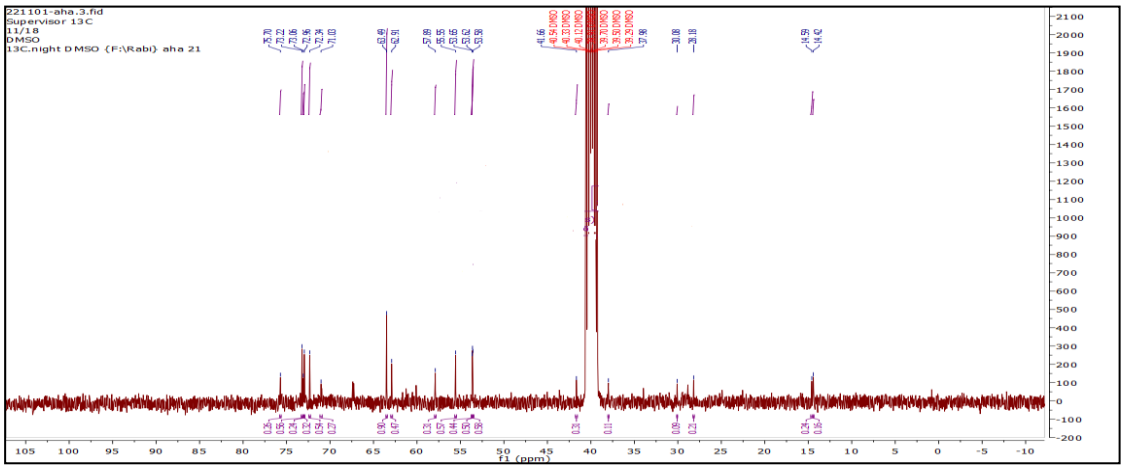

Figure (3-21): The ^{13}C NMR spectrum of ethyl fatty ester in DMSO-d^{6}.

The FTIR spectrum showed that the strong sharp peak at 1737 cm^{-1} indicates to stretching the active carbonyl ester groups for the presence fatty acid in different composition.

Two sharp and medium peaks at (2926,2854) cm^{-1} belong to the (CH_2) symmetric and asymmetric groups, respectively, which indicates the presence of hydrocarbon groups (CH_2) within the composition of the compound. The C-H alkane is responsible for the medium peak at 1620 cm^{-1}. There are two peaks at 1178 cm^{-1} and 1095 cm^{-1} return to (C–O) bonds in the compound in addition to the presence of two weak peaks at 721 cm^{-1}, 667 cm^{-1} belonging to rocking of methylene groups (> 4C) which indicate the presence of long hydrocarbon chains of more than four carbons in the compound. Three peaks at (1462,1456 and 1371) cm^{-1} are due to the bending C-H of CH_3 groups. From the foregoing, it is clear that this compound is an ester that contains long hydrocarbon chains of more than four carbon atoms in its structure, see Fig. 3-22.

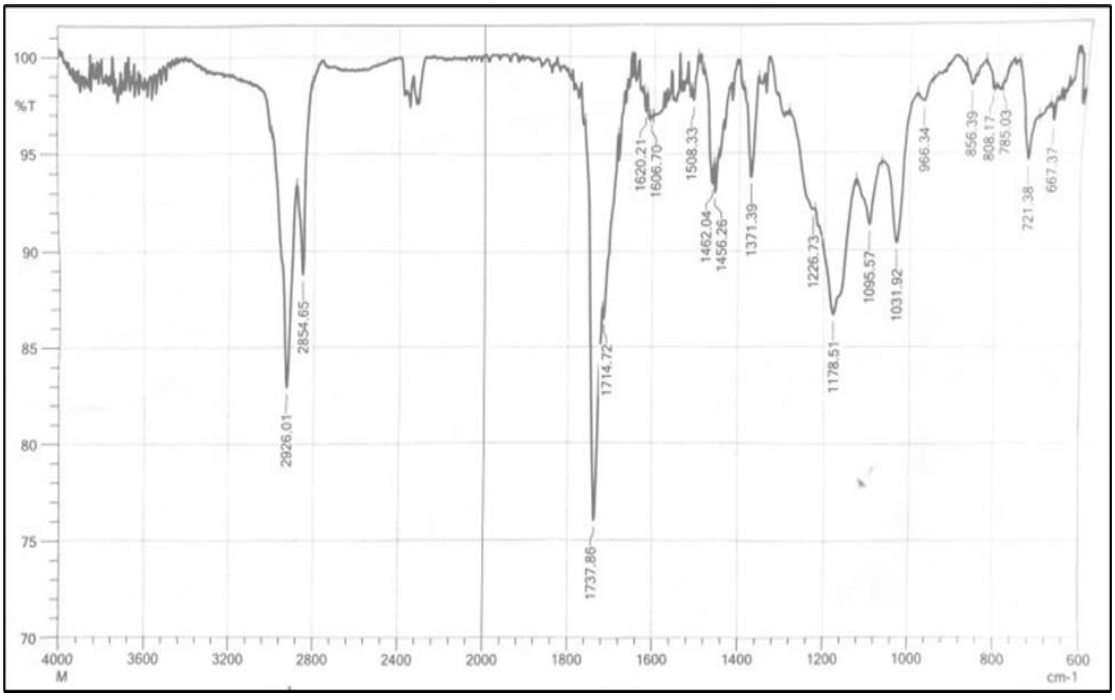

Figure (3-22): The FTIR spectrum for ethyl fatty ester as product for the hydrolysis of PC in presence of ethanol as solvent.

The mass spectrum of ethyl palmitate appears in the signal at (299.1 m/z) relative to the molecular ion, the value close to the calculated molecular weight (300 g/mole), as shown in Fig. 3-23.

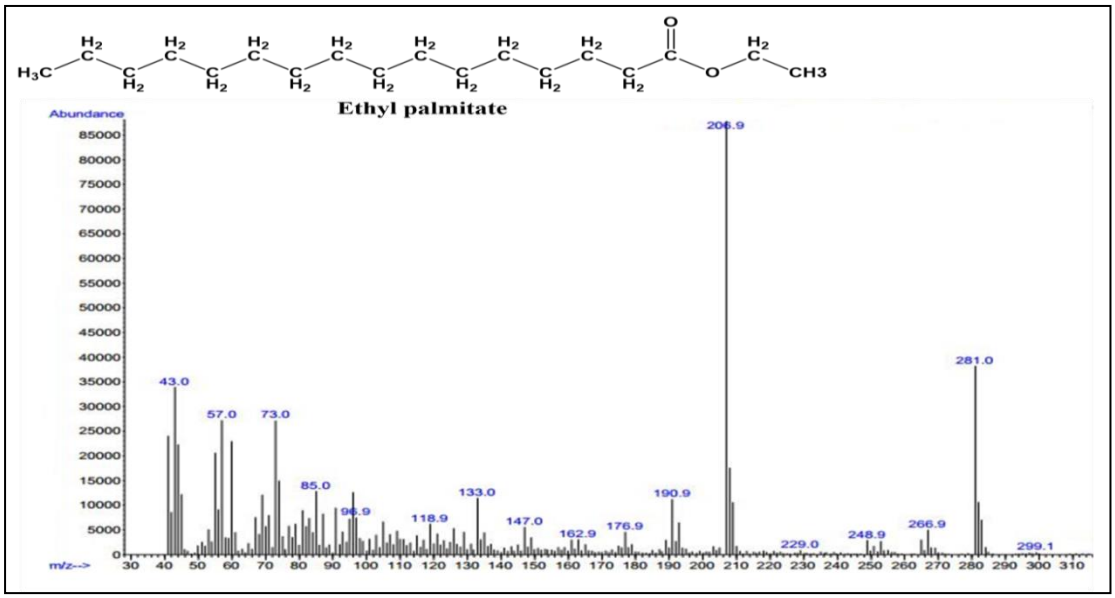

Figure (3-23): The GC-mass spectra of ethyl palmitate.

The mass spectrum of ethyl octadeca-9,12-dienoate appears in the signal at (326.9 m/z) relative to the molecular ion, the value close to the calculated molecular weight (324 g/mole), as shown in Fig. 3-24.

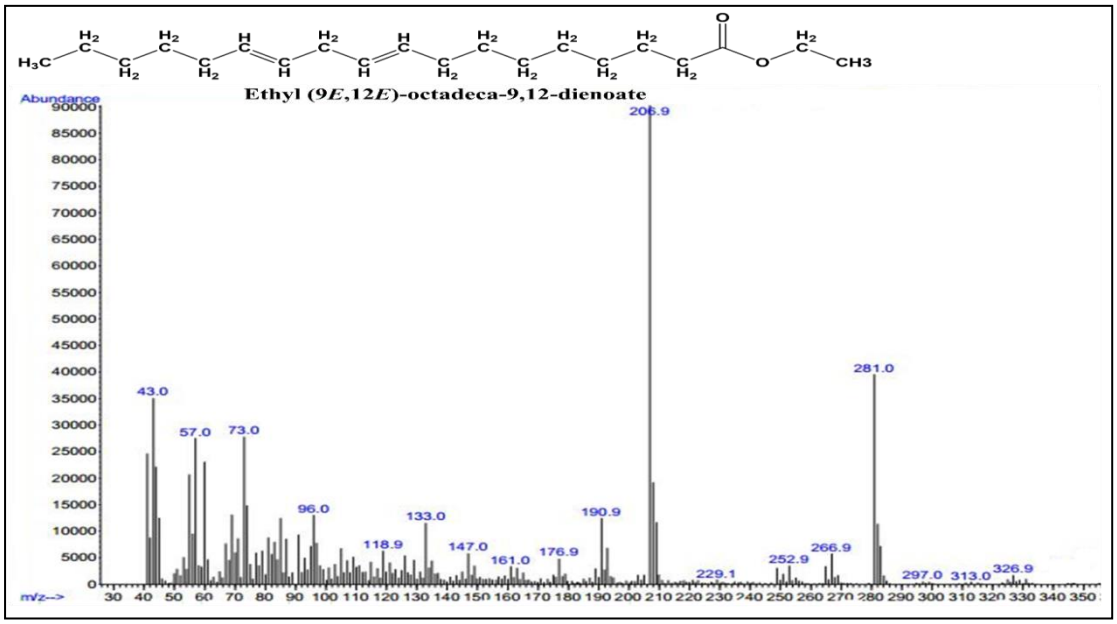

Figure (3-24): The GC-mass spectra of ethyl octadeca-9,12-dienoate.

The mechanism of PC's hydrolysis reaction in the presence of ethanol at p*K*a = 1.2 can be hypothesized as shown in Fig. 3-25.

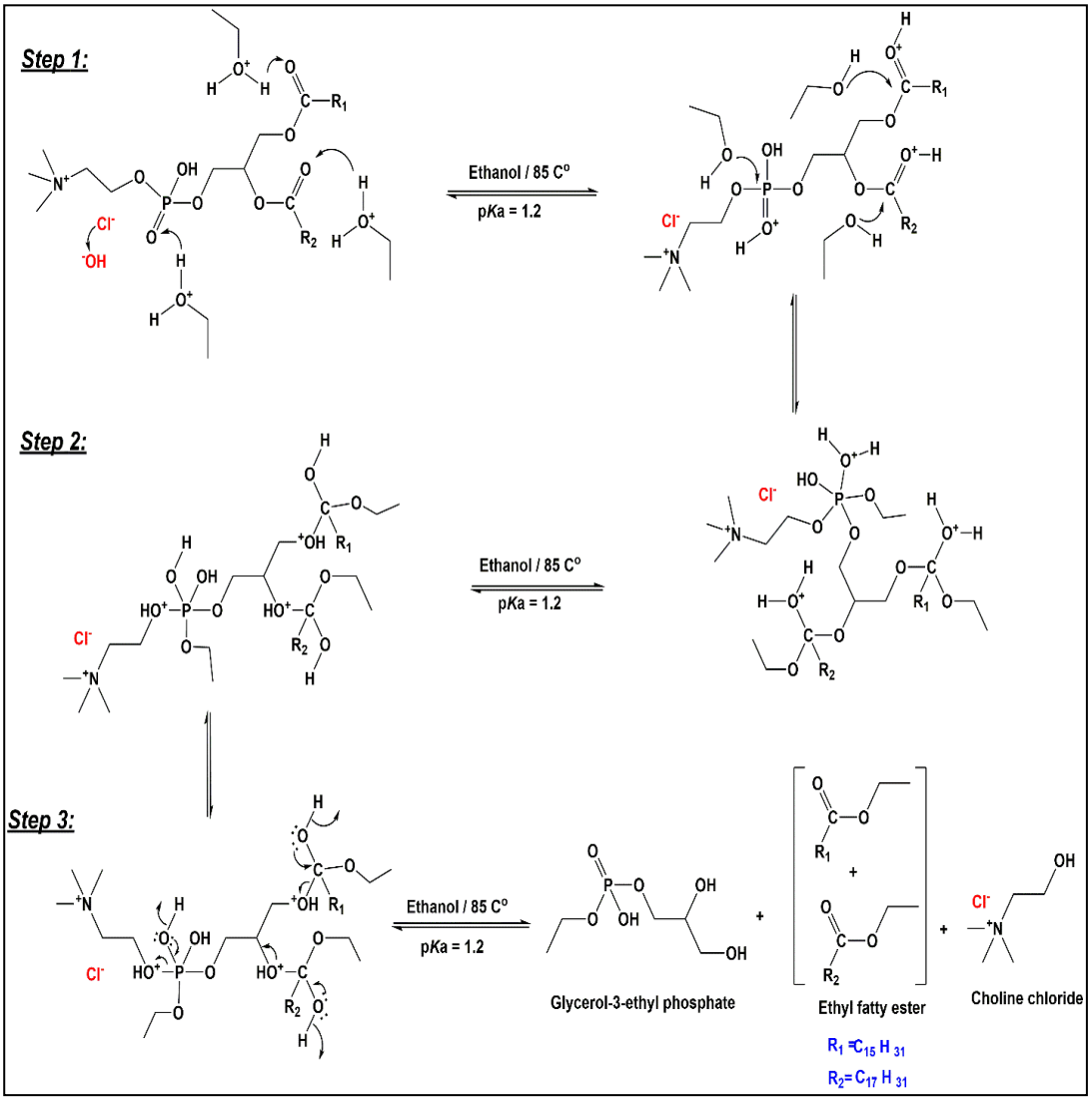

Figure (3-25): The suggested mechanism for PC hydrolysis reaction with ethanol present at p*Ka*=1.2.

3.4. Kinetic Study of Hydrolysis of PC in Presence of PLD as Catalyst

3.4.1 Determine the values of the reaction rate constant (Michaelis-Menten constant) and the maximum velocity of the enzymatic reaction:

From the absorbance readings against the PC concentrations, the corresponding reaction rate was found. After that, the Michaelis-Menten

equation was applied (Fig. 3-26) by drawing the relationship between the velocity of hydrolysis enzymatic reaction and the concentration of the PC as substrate, as well as the line Weaver-Burk equation was applied by plot the relationship between the reciprocal of the velocity (1/V) versus the reciprocal of the concentration (1/[S]) to reach the value of the enzymatic reaction rate constant (K_m) and the maximum velocity of the enzymatic reaction (V_{max}).

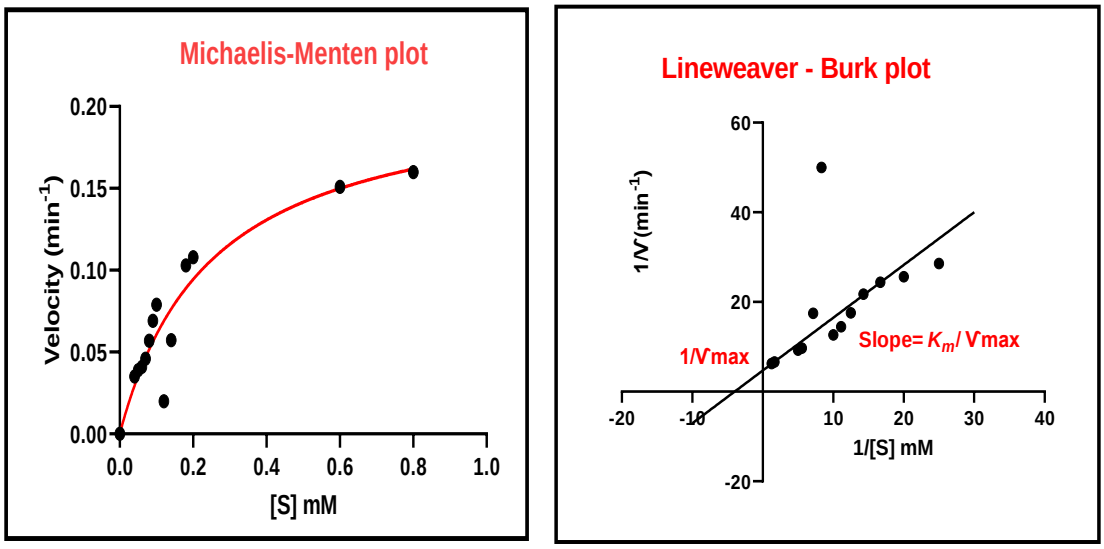

Figure (3-26): Michaelis-Menten diagram and line weaver - Burk diagram of the hydrolysis reaction of PC.

Table (3-5): The Values of K_m and V_{max} for hydrolysis of PC in presence of PLD

kinetic Parameters	Michaels Menten plot	line weaver Burk plot
V_{max} (min^{-1})	0.2124	0.2124
K_m	0.2502	0.2502

3.4.2. Finding of Enzymatic Activity of PLD for Hydrolysis Reaction of PC

The ideal enzymatic activity was determined by drawing the relationship between the enzymatic reaction speed and the activity, where a bell-like shape was obtained (Fig. 3-27).

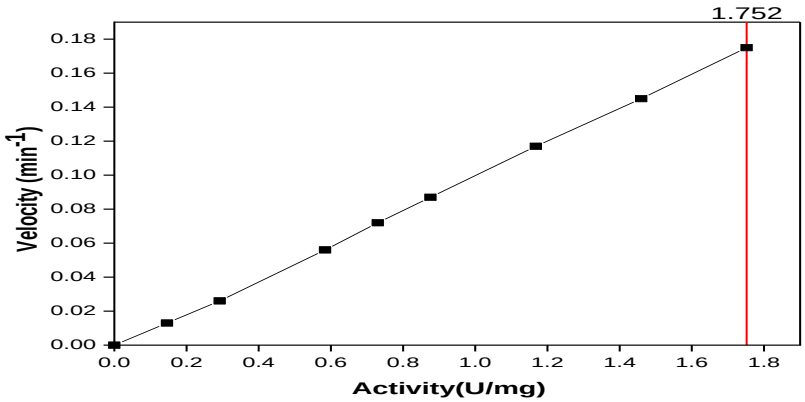

Figure (3-27): Finding of the enzymatic activity for the hydrolysis reaction of PC.

From the foregoing, the ideal enzymatic activity for this reaction is 1.752 U/mg.

3.4.3. Determination of pH Value for the Enzymatic Hydrolysis of PC in Presence of PLD

The appropriate pH value for the enzymatic hydrolysis of PC in presence of PLD was measured by applying the velocity chart to the appropriate acidity functions employed in the enzymatic reactions produced a bell-like shape, and it was discovered that (pH = **7**) is the suitable acidity function for this enzymatic reaction (Fig. 3-28).

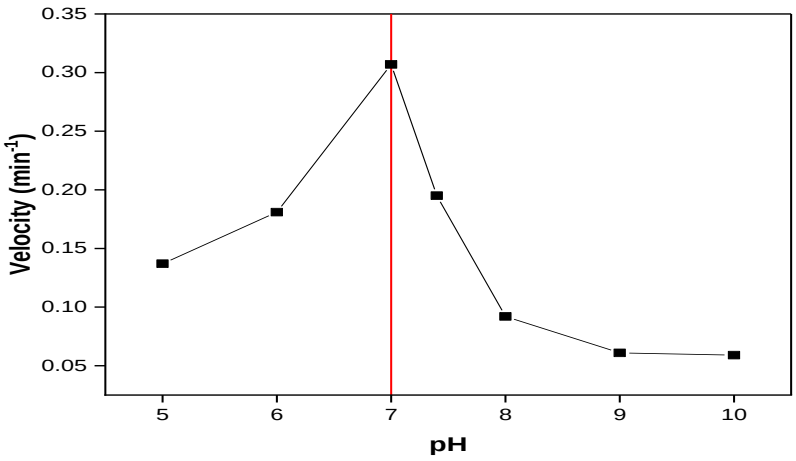

Figure (3-28): Figure showing the ideal pH for this reaction.

3.4.4. Finding Optimum Temperature for hydrolysis of PC in Presence of PLD:

The optimum temperature for the enzymatic hydrolysis of PC in presence of PLD was determined by plot the velocity of the reaction against the different temperatures (10-45 °C). The 35℃ is the ideal temperature (Fig.3-29) for the hydrolysis reaction of phosphatidylcholine determined by drawing the relationship between the speed values and their corresponding temperatures.

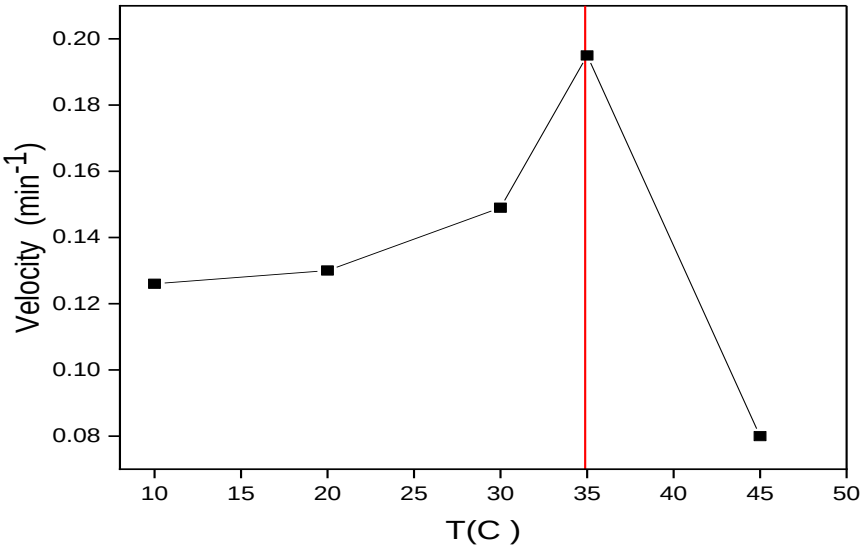

Figure (3-29): Image showing the ideal temperature for the reaction.

3.4.4.1. Finding the Thermodynamic Parameters for Enzymatic Hydrolysis of PC:

By applying the Van't Hoff equation, drawing the relationship between ln*K* against the reciprocal of temperature. The value of (ΔH) was calculated from the slope and the value of the activation energy (ΔE_a) is equal to the (ΔH) value of the liquids, while a (ΔS) value was calculated from the intersection with the y-axis. As for the Gibbs free energy, it was found by applying the free Gibbs equation.

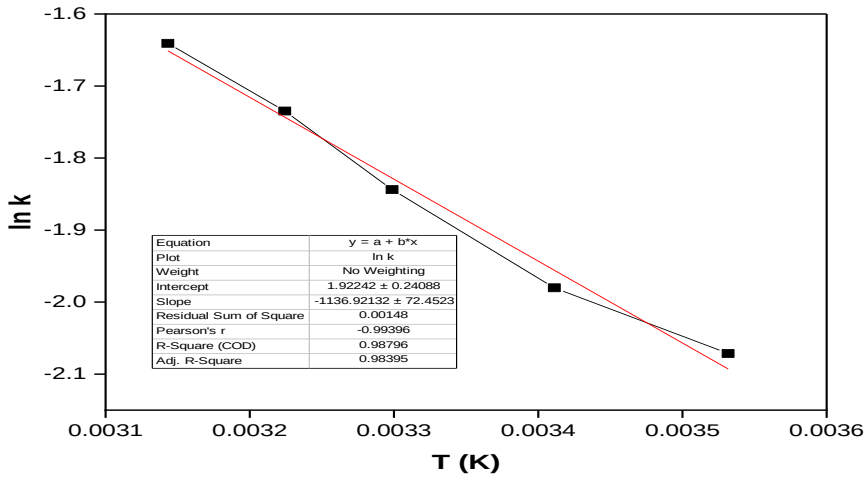

Figure (3-30): Van't Hoff equation for the Hydrolysis of PC in present of PLD

Table (3-6): The values of (ΔH), (ΔS) and (ΔG).

ΔH (kJ/mole)	ΔS (J/K)	ΔG (J)
136.747	0.231	65.102

The positive value of the Gibbs free energy indicates that the enzyme reaction is nonspontaneous. It also has a positive entropy value, making it random.

3.5. Characteristics of phosphatidic acid (PA) as Product for Enzymatic Hydrolysis of PC in Presence of PLD

3.5.1. Infrared spectrum of the aqueous layer product

The infrared chart (Fig. 3-31) showed a strong and broad peak at 3213 cm^{-1} refer to the hydroxyl group. There are also two sharp peaks of medium and strong intensity at 2854 cm^{-1} and 2924 cm^{-1}, which indicate to (CH_2) group symmetric and asymmetric, respectively. In addition to the absence of two ester bonds at 1725 cm^{-1}. The presence of a (C-O) bond at 1195 cm^{-1}, as well as a (C-N) bond at 1195 cm^{-1}, indicates that this

compound is the product lateral and that the expected structure is the following :

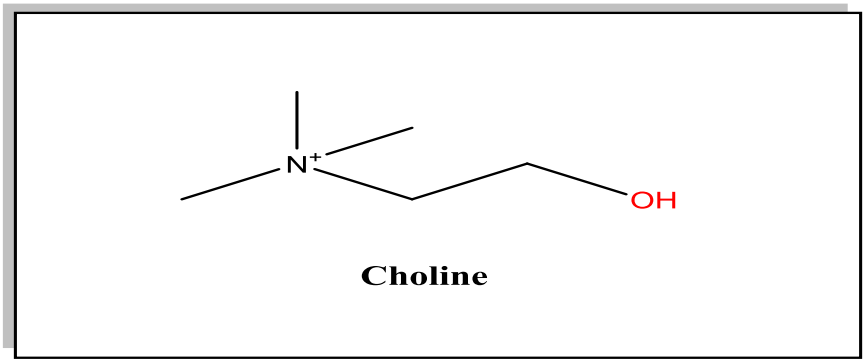

Figure (3-31): The expected chemical structure of the side product.

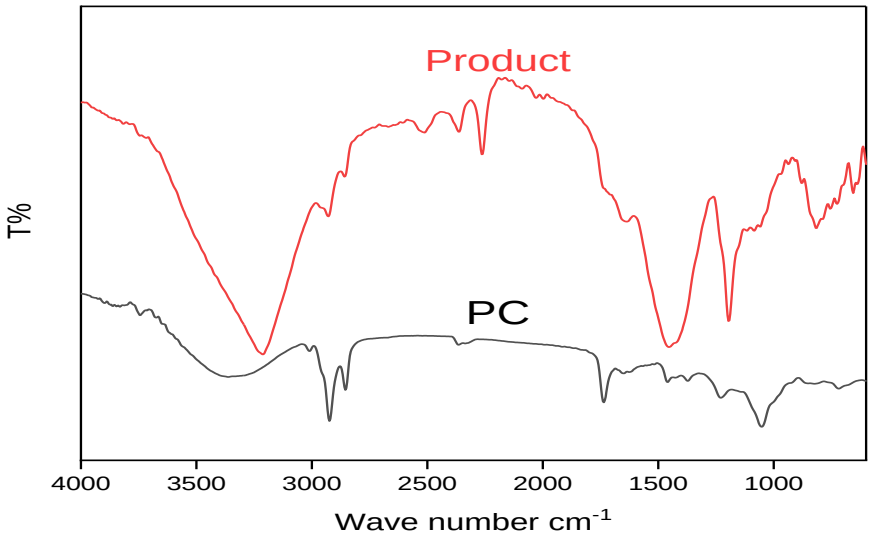

Figure (3-32): PC and side product infrared spectra.

3.5.2. The infrared spectrum of the etheric layer

It was observed (Fig. 3-34) that there was a broad and strong peak at 3336 cm^{-1} belonging to the alcoholic (OH) group, in addition to the presence of a peak at 1739 cm^{-1}. Belonging to the ester bonds associated with the backbone of the glycerol, in addition to the presence of two peaks at (1060 and 1176) cm^{-1} belonging to the different (C-O) bonds present in

the compound, which provided this supports the occurrence of hydrolysis of the PC at the D site with the effect of PLD enzyme.

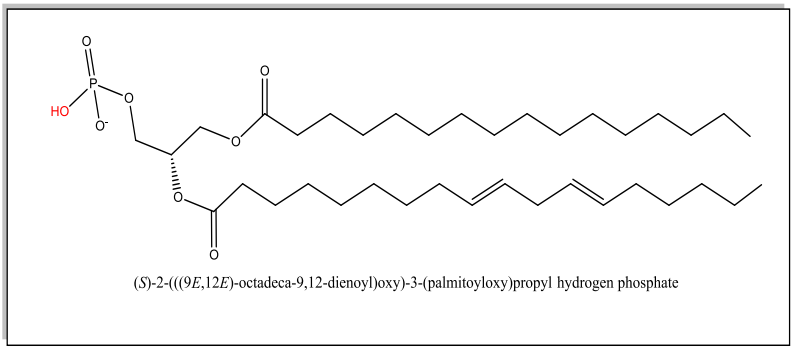

Figure (3-33): The chemical formula for PA as final product for the enzymatic hydrolysis of PC in presence of PLD.

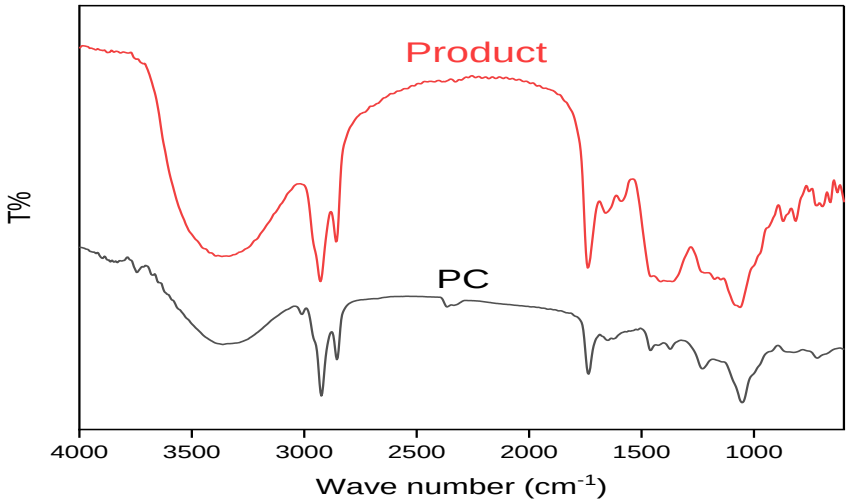

Figure (3-34): FTIR spectra for both PC (black curve) and PA (red curve).

3.6. Enzymatic Hydrolysis of PC in Ethanol

3.6.1. Finding the Michaelis-Menten Parameters for the Enzymatic Hydrolysis of PC in Ethanol

The Michaels-Menten and Line Weaver-Burk equations were applied to monitor the enzymatic hydrolysis of PC in ethanol. In addition, the impact of the concentration of PC on the ethyl substitution reaction were observed to find, the values of the maximum velocity of the enzymatic

reaction and the reaction rate constant were as shown in the Fig. 3-35, and in Table (3-6).

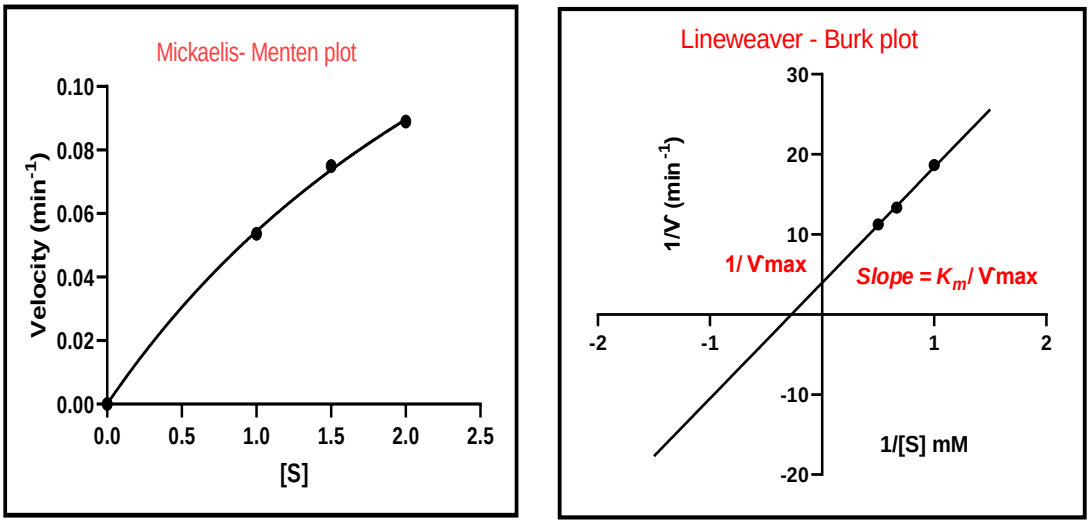

Figure (3-35): The line weaver - Burk diagram and a Michaelis-Menten diagram for the enzymatic hydrolysis of PC in ethanol in presence of PLD as catalyst.

Table (3-7): Values of K_m and V_{max} for hydrolysis of PC in ethanol as a solvent.

kinetic Parameters	Michaels Menten plot	line weaver Burk plot
V_{max} (min^{-1})	0.253	0.253
K_m	3.664	3.664

From the aforementioned and depending on the value of the Michaelis-Menten constant (K_m), the affinity between the substrate (PC) and the enzyme (PLD) in this reaction is the least value among the four interactions mentioned.

3.6.2 Determination of Enzymatic Activity for the Hydrolysis of PC in Ethanol in Presence of PLD

The activity of PLD enzyme was determined by plotting of velocity of the enzymatic hydrolysis of PC in ethanol against the activity of PLD enzyme as shown in figure 3-36. It is clear that 1.168 U/mg is the enzyme activity suitable for the ethyl substitution reaction of PC.

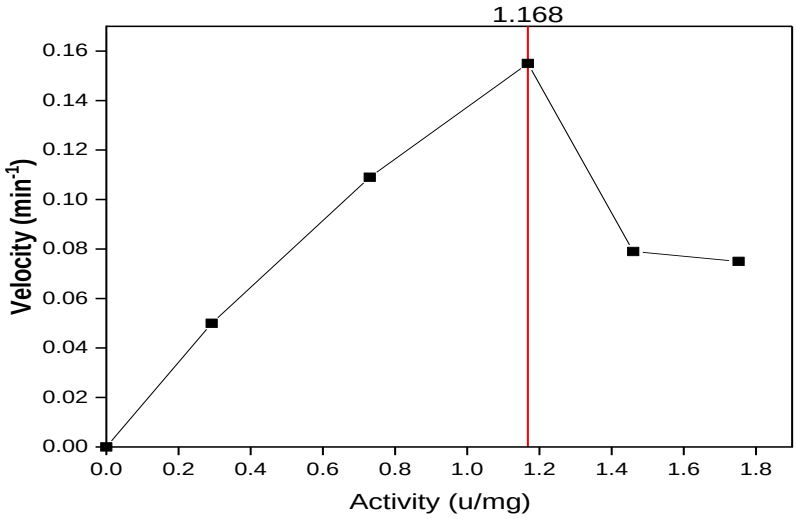

Figure (3-36): Plot of velocity against PLD enzyme activity for the enzymatic hydrolysis of PC in ethanol.

3.6.3. Finding the Appropriate pH Value for Enzymatic Hydrolysis Reaction of PC in Ethanol

By plotting the chart for the velocity against the corresponding acidity functions (pHs) that were used in the enzymatic reactions, it was found that (pH = **6**) is the appropriate acidity function for this enzymatic reaction, see (Fig.3-37).

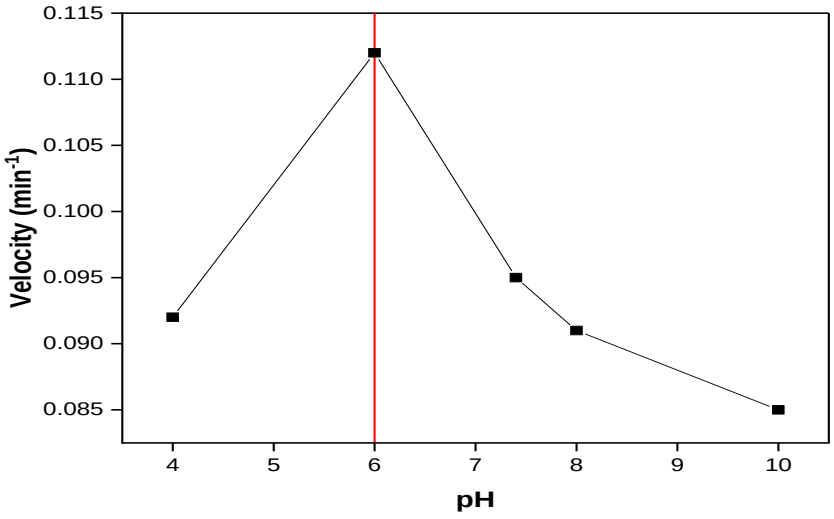

Figure (3-37): Figure showing the ideal pH for this reaction.

3.6.4. Determination of the Ideal Temperature for the Enzymatic Hydrolysis of PC in Ethanol in Presence of PLD.

By drawing the relationship between the change of velocity against the corresponding temperature, the appropriate temperature was limited at 37 °C for the enzymatic hydrolysis action of PLD.

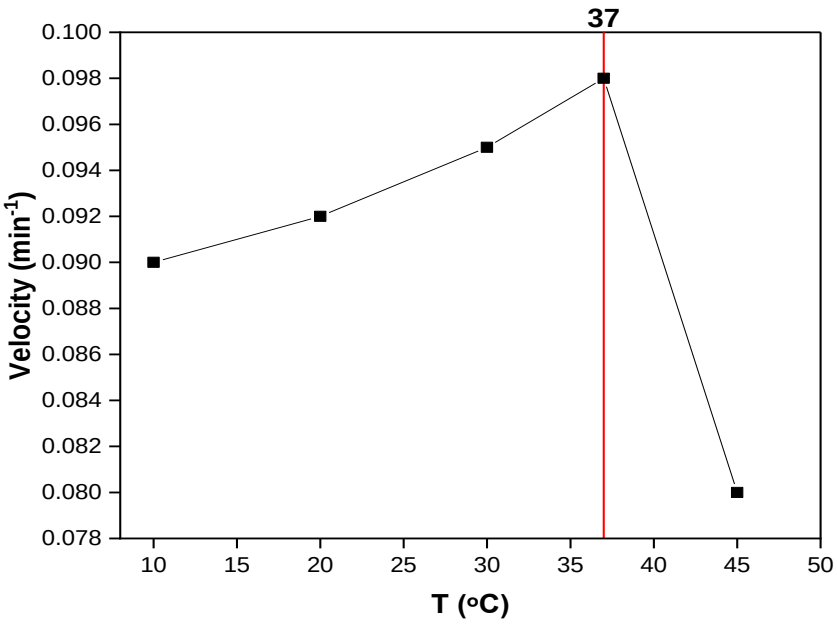

Figure (3-38): Diagram showing the ideal temperature for an enzymatic hydrolysis of PC in ethanol in presence of PLD as catalyst.

3.6.5. Determination of Thermodynamic Parameters for Enzymatic of Hydrolysis of PC in Ethanol values

The values of thermodynamic parameters, which include the (ΔH), (ΔS), (ΔEa), and (ΔG) were determined by drawing a Van't Hoff diagram, which plots the values of (ln*K*) against the inverse of the temperature, and by adhering to the previously specified procedures.

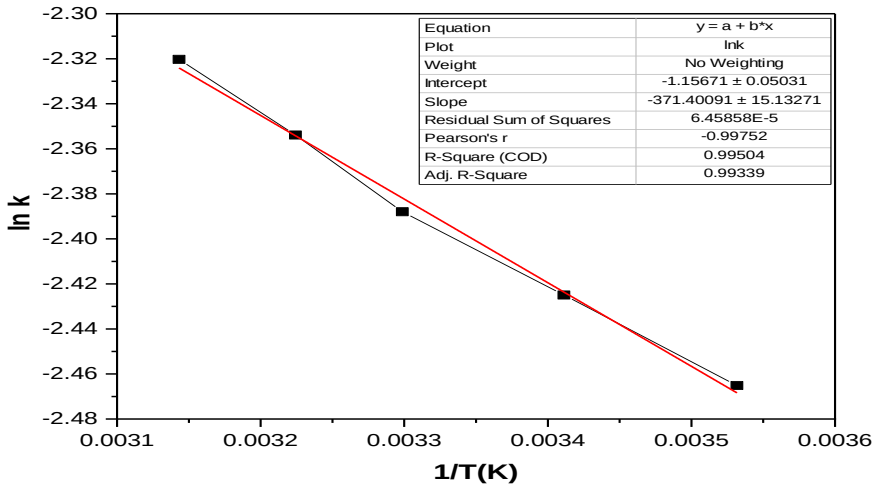

Figure (3-39): Van't Hoff plot for the enzymatic hydrolysis of PC in ethanol in presence of PLD as catalyst.

Table (3-8): The values of (ΔH), (ΔS) and (ΔG) for the enzymatic ethyl substitution reaction of PC.

ΔH(kJ/mole)	ΔS (J/K)	ΔG (J)
44.671	- 0.139	87.781

It can be noted the enzymatic reaction occurs non-spontaneously due to the positive value for the free Gibbs energy. It is the only non-random reaction because it has a negative entropy value. In addition, it has the lowest activation energy among the mentioned reactions.

3.7. Characteristics of the Derivative of PC as Product for Enzymatic Substitution Reaction between PC and Ethanol

3.7.1. FTIR Spectrum for Choline as Product for Enzymatic Hydrolysis of PC in Ethanol in Presence of PLD:

The FTIR spectrum for the first dissociative part for the reaction between the PC and the ethanol in presence of PLD showed the following peaks for the main grope; the peak at 1057 cm^{-1} refer to C-O group of

alcohol, a high and sharp peak at 1195 cm^{-1} indicate to the C–N for the quarterly amine, and a strong peak at 3213 cm^{-1} refer to the of the hydroxyl group OH. In addition to C-H bending of CH_3 and CH_2 groups is responsible for two weak peaks at (1462 and 1371) cm^{-1} and C-H stretching of alkane at (2956 and 2860) cm^{-1} .This demonstrates that this compound (Fig. 3-41) is the product created by the dissociative of the bond between the phosphate group and the choline in PC due to presence of PLD as catalyst. As a result, the separation of the choline group from the compound by the action of the enzyme.

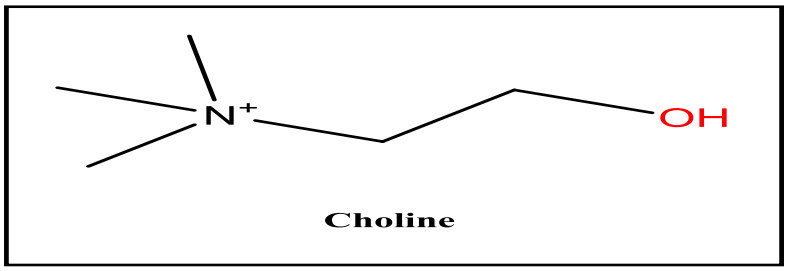

Figure (3-40): The ethanol fractions anticipated chemical structure.

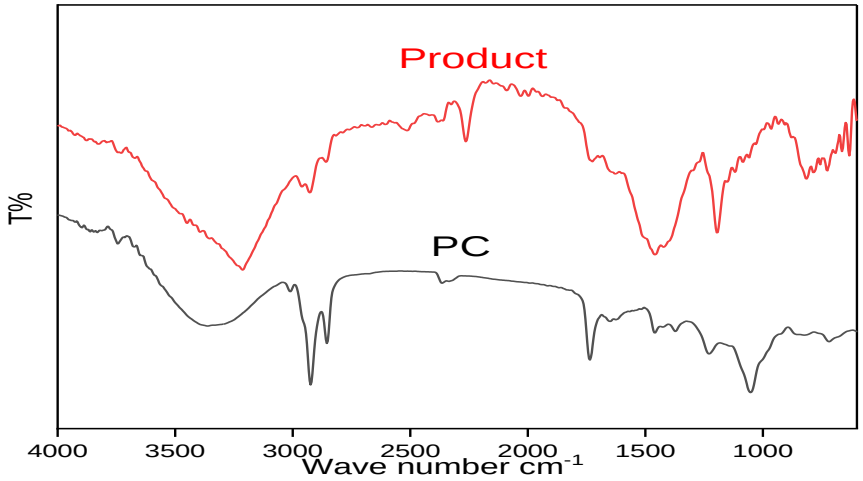

Figure (3-41): FTIR spectra of the choline (red curve) and PC (black curve).

3.7.2. FTIR Spectrum for Phosphatidyl Derivative:

The infrared spectrum (Fig.3-43) shows a sharp peak of moderate intensity at 1739 cm^{-1}, which belongs to the ester bonds present in the

compound. There is a broad, medium-intensity peak at 3290 cm^{-1} belonging to the hydroxyl group attached to the phosphate atom attached to the glycerol backbone. Additionally, there are two distinct peaks of medium and strong intensity at 2854 cm^{-1} and 2924 cm^{-1} belonging to the symmetric and asymmetric (CH_2) group at, respectively. In addition to the presence of two medium-intensity peaks at 1080 cm^{-1} and 1053 cm^{-1} that belong to the different (C-O) bonds associated with the ester groups of the glycerol backbone. Also, the presence of a weak peak at 1157 cm^{-1} belongs to for the (C-O) etheric bond formed. As a result, it can be predicted that the ethyl group bind with PC instead of the choline by the action of the PLD enzyme. From the foregoing, it is clear that this product is the main product and the expected chemical composition for it:

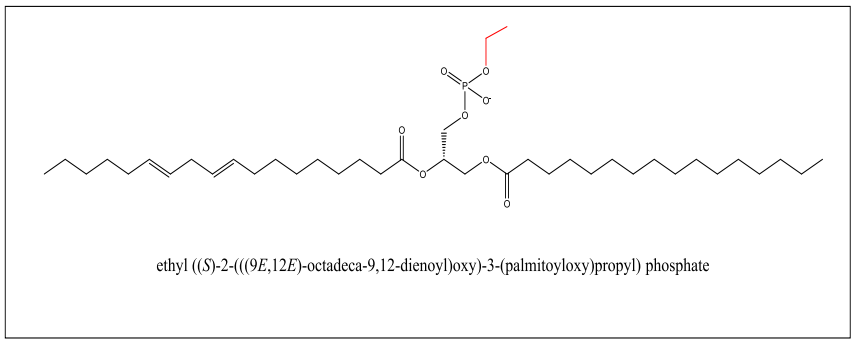

Figure (3-42): The predicted chemical structure of the etheric part.

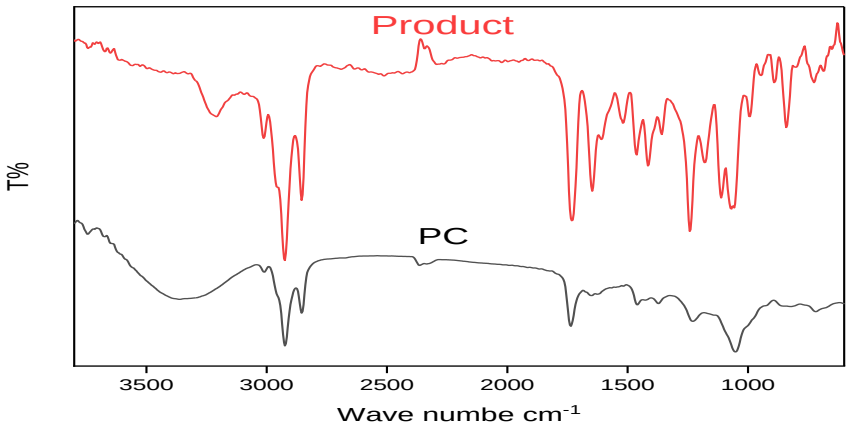

Figure (3-43): FTIR spectra of the Phosphatidyl derivative (red curve) and PC (black curve).

3.8. Hydrolysis of Phosphatidylserine (PS) in Presence of PLD

3.8.1. Determination of Michaelis-Menten Parameters for Hydrolysis of PS in Presence of PLD

The results of the enzymatic hydrolysis reaction of PS when using various concentrations of it can be determined by applying the Michaels-Menten plot by drawing the relationship between the enzymatic reaction velocity and the concentration of the substrate, and Line Weaver-Burk scheme by drawing the relationship between the reciprocal of the velocity versus the reciprocal of the concentration, as shown in Fig.3.44. The values of the reaction constant (K_m) and the maximal speed of the enzymatic reaction (V_{max}) are displayed in Tables (3-8).

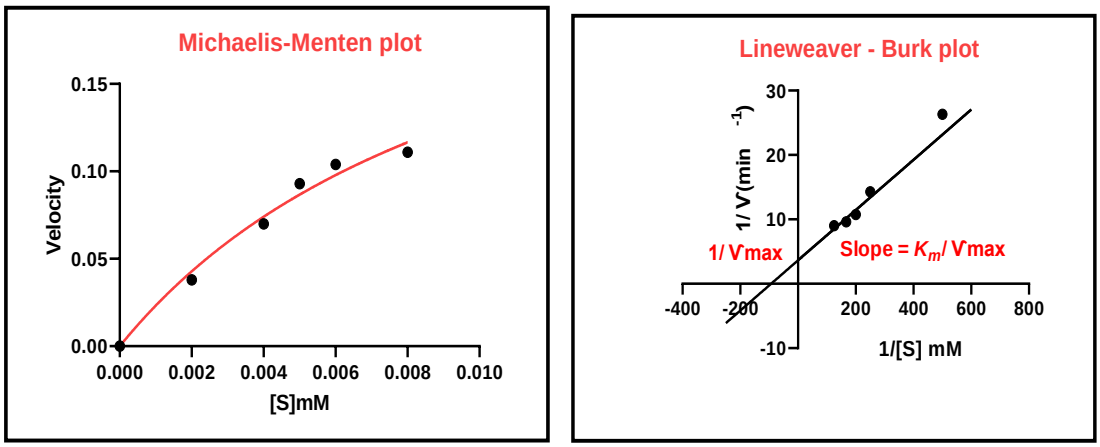

Figure (3-44): PS is hydrolyzed in water as seen in the line Weaver-Burk and Michaelis-Menten diagrams.

Table (3-9): Values of Km and V max for hydrolysis of PS.

kinetic Parameters	Michaels Menten plot	line weaver Burk plot
V_{max} (min^{-1})	0.274	0.274
K_m	0.010	0.010

From the values of the table above, It was noted that K_m value of this reaction is the lowest among the four reactions, and this means that this reaction has the highest affinity between the substrate (PS) and the PLD enzyme.

3.8.2. Finding the Appropriate PLD Enzymatic Activity for Hydrolysis of PS

A bell-like shape was generated by plotting the association between the enzyme reaction velocity Y-axis *via* PLD enzymatic activity. It is obvious that the enzyme activity necessary for the hydrolysis reaction of PS is 1.752 U/mg (Fig. 3-45).

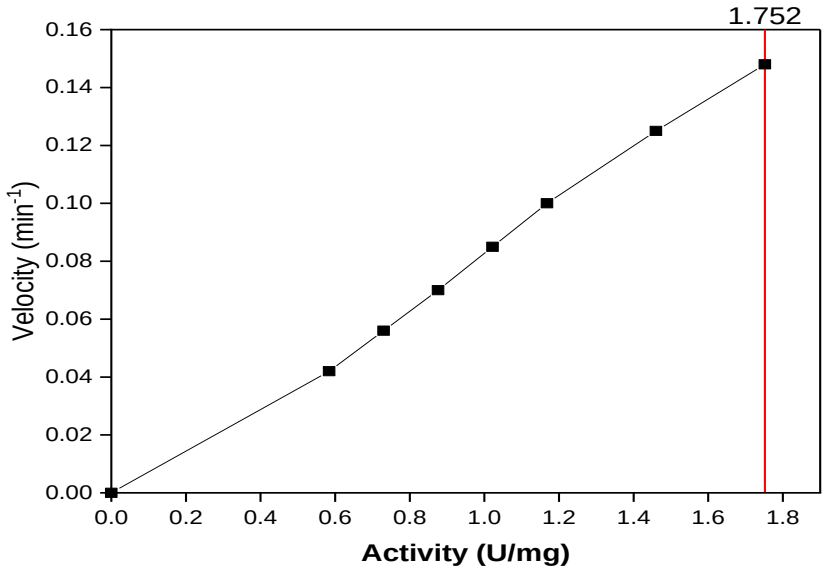

Figure (3-45): The appropriate enzyme activity for PS hydrolysis.

3.8.3. Determination of pH for Enzymatic Hydrolysis of PS

The best acceptable acidity function for this enzymatic reaction (pH= **9**) that was determined by using the graph for the velocity of enzymatic hydrolysis against the relevant acidity functions utilised in the enzymatic reactions (Fig. 3-46).

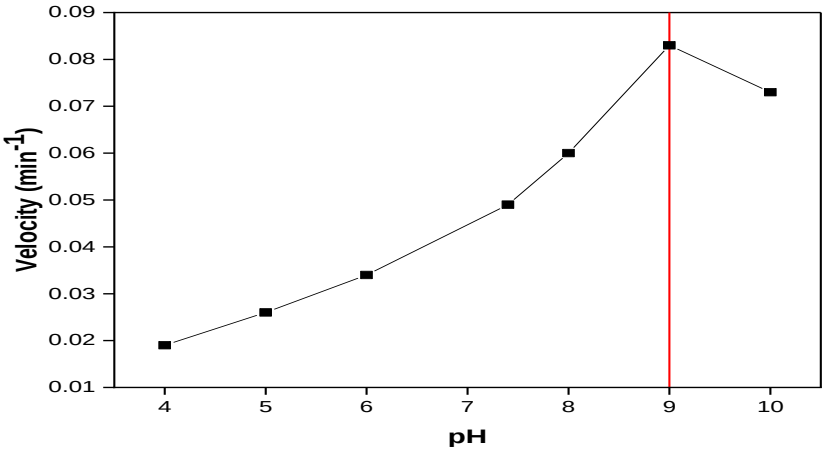

Figure (3-46): Figure illustrating the reaction's optimal pH.

3.8.4. Finding the Optimum Temperature for Hydrolysis of PS

A bell-like curve (Fig. 3-47) showing 35 °C is the ideal temperature when plotting velocity values vs. temperatures.

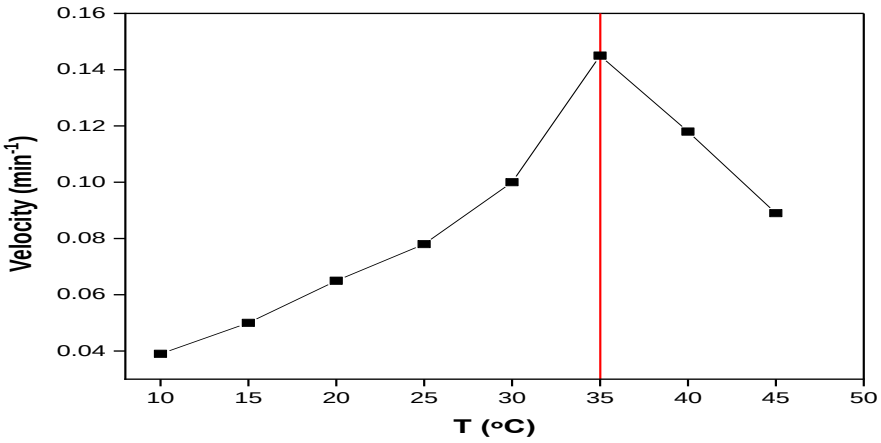

Figure (3-47): The optimum temperature for the hydrolysis of PS in presence of PLD.

3.8.4.1. Identify the Thermodynamic Parameters for Enzymatic Hydrolysis of PS

By creating a Van't Hoff diagram (Fig. 3-48), which graphs the values of (ln *K*) against the inverse of the temperature, and by following the

previously mentioned processes, the values of the change in ΔH, ΔS, , and ΔG are presented in Table (3-9).

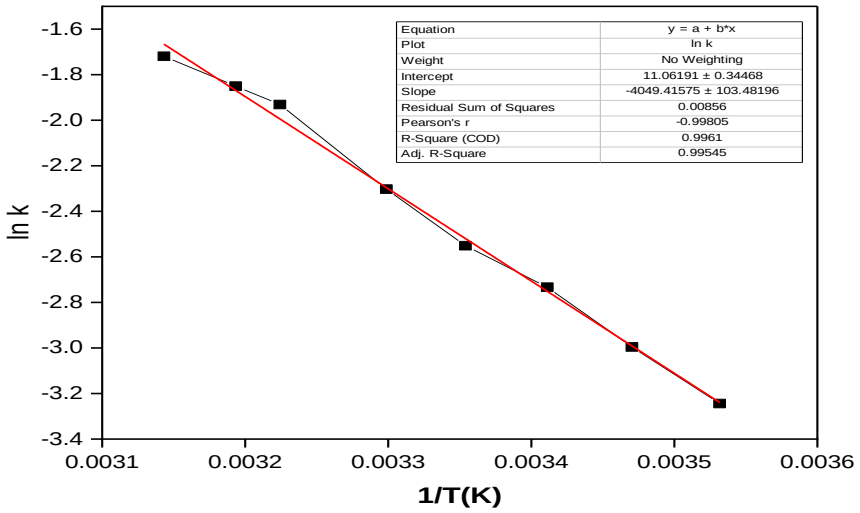

Figure (3-48): Van't Hoff diagram for the enzymatic hydrolysis of PS.

Table (3-10): The thermodynamic parameters for enzymatic hydrolysis of PS in presence of PLD

ΔH(kJ/mole)	ΔS(J/K)	ΔG (J)
487.059	1.330	74.559

The values mentioned above indicate that a high activation energy (487.059J/mole) is needed for this reaction to take place. It is highly random value (1.330 J/K). Given that it has a positive Gibbs free energy value; it does not occur spontaneously.

3.9. The phosphatidylserine ethanol substitution reaction

3.9.1. Determination of the Michaelis-Menten Parameters for Substitution of PS with Ethanol in Presence of PLD

The K_m and V_{max} values for the enzymatic substitution reaction between PS and ethanol in presence of PLD were determined by applying

the Michaels-Menten and Line Weaver-Burk equations (Fig. 3-49) and the V_{max} and K_m values were presented in Tables (3-10).

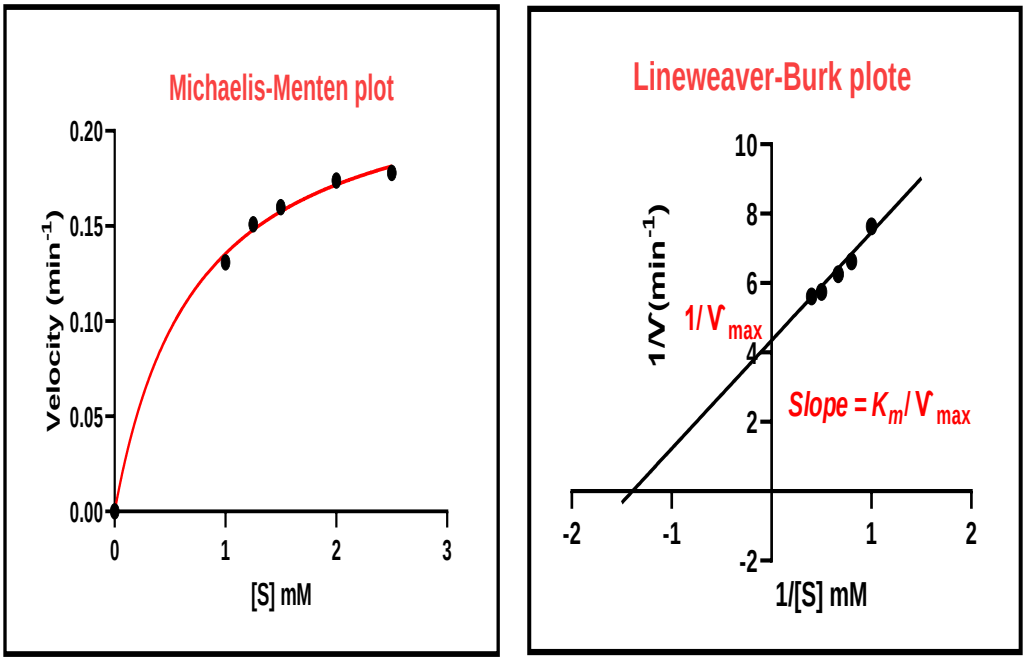

Figure (3-49): Michaelis-Menten and line Weaver-Burk diagrams are used to depict PC substitution in ethanol.

Table (3-11): The K_m and V_{max} values for the enzymatic reaction of PS with ethyl substitution.

kinetic Parameters	Michaels Menten plot	line weaver Burk plot
V_{max} (min^{-1})	0.234	0.234
K_m	0.730	0.730

3.9.2. Finding the Enzymatic Activity of the Substitution Reaction of PS with Ethanol

The experiments for finding the appropriate enzyme activity for the substitution reaction of PS with the ethanol in presence of PLD exhibited that the best activity for enzyme is 1.46 U/mg, as shown in (Fig. 3-50) which display the relationship between enzymatic activity and velocity of the substitution reaction.

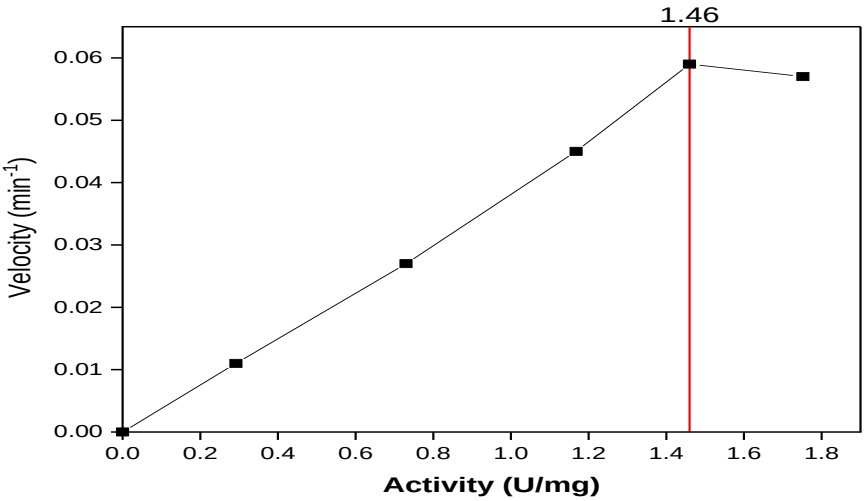

Figure (3-50): For the PS substitution reaction, a speed versus enzyme activity plot was created.

3.9.3. Determination of pH Value for the Enzymatic Substitution Reaction of PS with Ethanol in Presence of PLD.

By plotting the velocity of the substitution reaction against the corresponding acidity functions that were used in the enzymatic reactions, it was found that (pH = **6**) is the best suitable acidity function for this enzymatic reaction (Fig. 3-51).

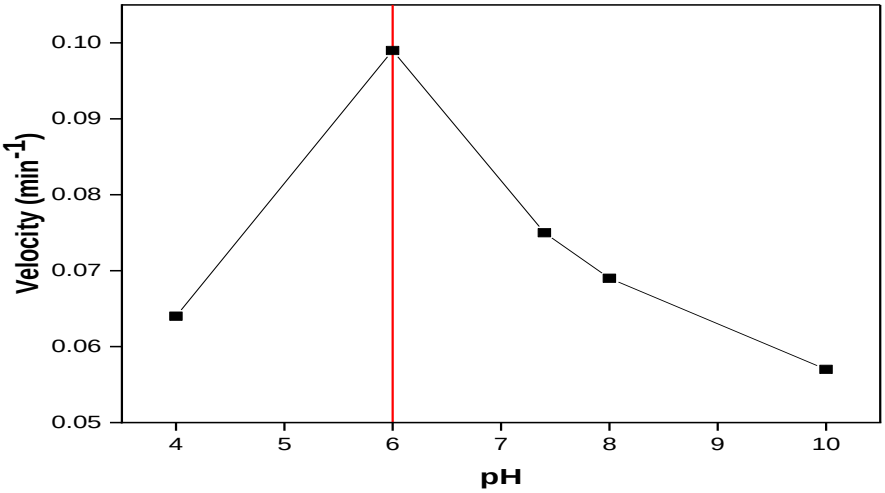

Figure (3-51): Illustrating the reaction's optimal pH for the PS ethyl substitution reaction.

3.9.4. Determination of Appropriate Temperature for the Enzymatic Substitution Reaction of PS with Ethanol.

The diagram between the velocity of the enzymatic substitution reaction between the PS and ethanol showed that the degree of 37 °C is the

optimal temperature to activate the enzymatic reaction as presented in (Fig. 3-52).

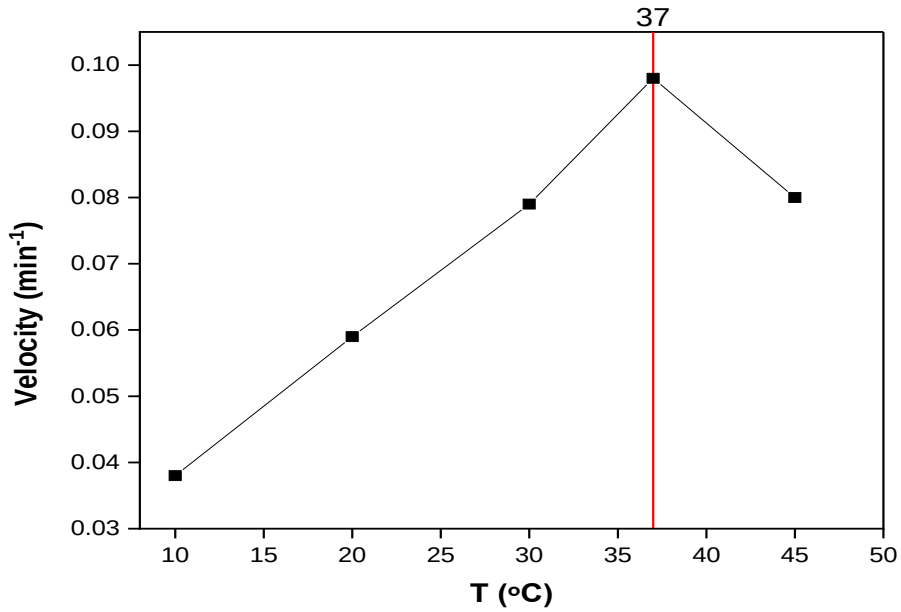

Figure (3-52): The diagram for determine of the optimum temperature for the substitution reaction of PS with ethanol in presence of PLD.

3.9.4.1. Determination of the Thermodynamic Parameters for the Substitution Reaction of PS with Ethanol in Presence of PLD

The Van't Hoff equation was applied to measure the thermodynamic parameters which include ΔH, ΔS, and ΔG as presented at in Table (3-11) and in Fig. 3-53.

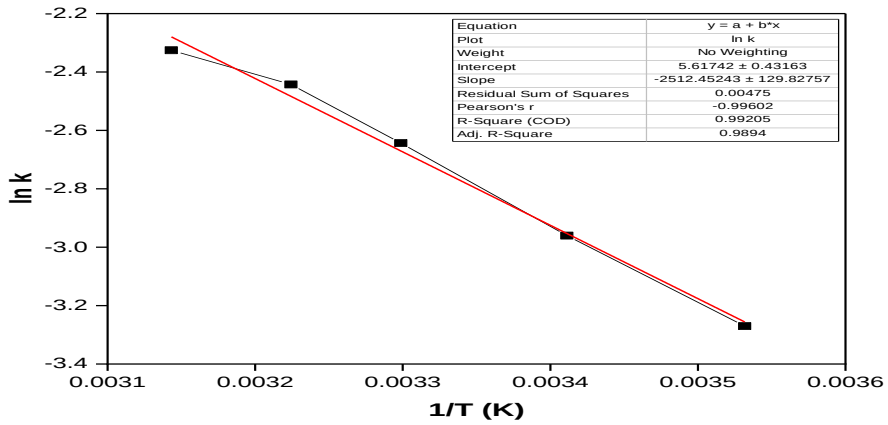

Figure (3-53): Plot of Van't Hoff equation for the substitution reaction of PS with ethanol in presence of PLD.

Table (3-12): The thermodynamic parameters for the substitution reaction of PS with ethanol in presence of PLD.

ΔH(kJ/mole)	ΔS (J/K)	ΔG (J)
302.195	0.675	92.843

It can be noted the enzymatic reaction occurs non- spontaneously due to the positive value for the free Gibbs energy. In addition, it is non-random because it has a positive entropy value.

3.10. Characteristics of the Products for Enzymatic Substitution Reaction between PS and Ethanol

3.10.1. FTIR of L-Serine:

The L-serene is the first product when its dissociative from PS in presence of PLD. The FTIR spectrum for this product appeared the peaks at 1014 cm^{-1}, 1060 cm^{-1}, and 1084 cm^{-1} that refer to (C-O) alcoholic bond. In addition, the peak at 3012 cm^{-1} indicate to the (O–H) group associated with the carboxyl group, and it got shifted towards lower frequencies because of the presence of the electron-donating amine group, a sharp peak of medium

intensity at 1739 cm^{-1} that belonged to the carbonyl group. The presence of two peaks at (3456 and 3090) cm^{-1} that are N–H bonds from the primary amine, as well as the compound's anticipated chemical structure of the serine group linked to the hydroxyl group.

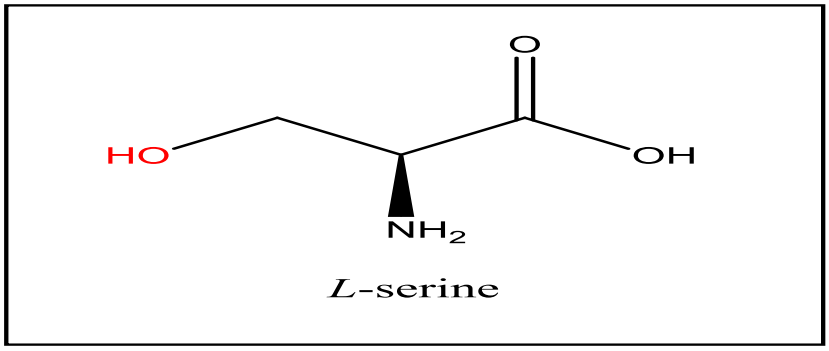

Figure (3-54): The expected structural formula for the first product of the enzymatic substitution reaction for PS with ethanol.

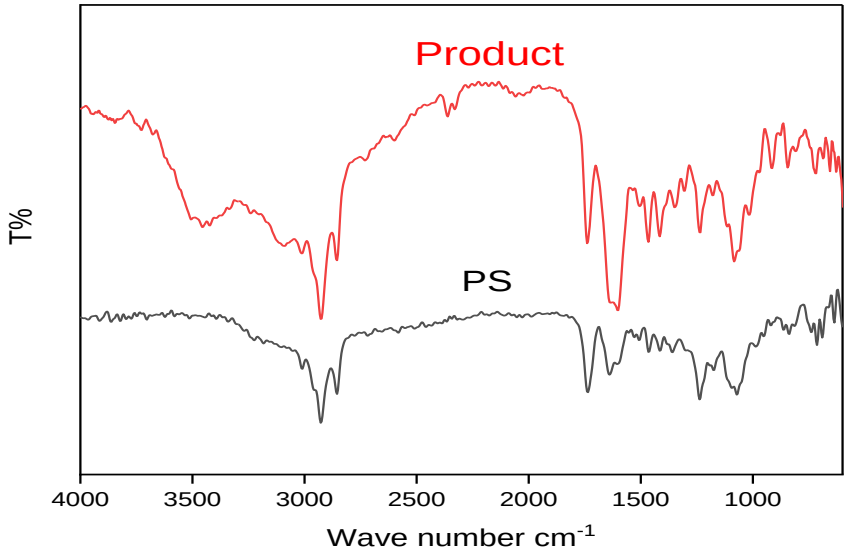

Figure (3-55): Infrared radiation from a PS (black curve) and L-serine (red curve).

3.10.2. FTIR for Phosphatidyl Derivative:

The Phosphatidyl derivative which is shown in Fig. 3-57 is the second product for the enzymatic substitution reaction between the PS and ethanol in presence of PLD. The FTIR spectrum for this derivative exhibited a strong and broad peak at 3209 cm^{-1} due attributed to the

hydroxyl group (OH) that bind with the phosphate group. In addition, the peak at 1735 cm^{-1} refer to the carbonyl group in the compound. The further two peaks at (1076 and 1114) cm^{-1} refer to alcoholic (C–O) bond. The presence of a strong and sharp peak at 1195 cm^{-1} attributed to the etheric (C–O) bond as a result of the binding of ethyl with the phosphate group at the backbone of glycerol (Fig.4.31), and therefore this compound is the expected main product of this reaction.

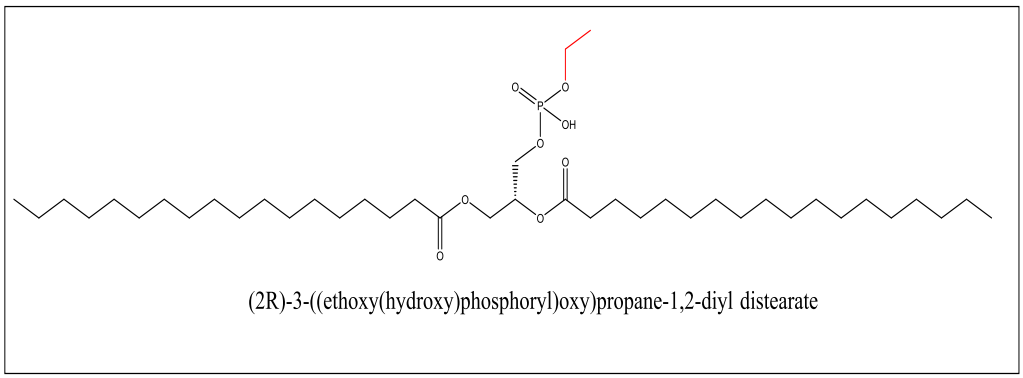

Figure (3-56): The predicted structure for the PS derivative as product for the enzymatic substitution reaction with ethanol in presence of PLD.

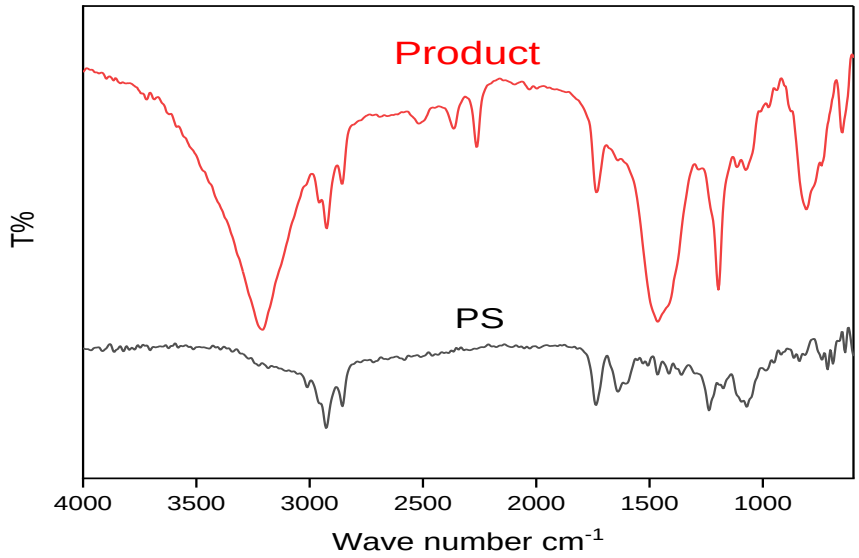

Figure (3-57): FTIR spectra for the PS (black spectrum) and its derivative (red spectrum) as main product for the substitution reaction of PS with ethanol in presence of PLD.

Conclusions

1- The degradation of PC in both solvents (water and ethanol) without use of PLD follows the same mechanism of reaction.

2- The variations in the substituted groups caused a small difference in the final products of these reactions. Thus, glycerol-3-phosphate was the primary product of PC hydrolysis in water, with free fatty acids and choline chloride emerging as byproducts. The hydrolysis of PC in ethanol produced the ethyl fatty ester.

3- The variations in the byproducts may give us a clear picture of how the solvent will affect this process, even though the mechanics of the hydrolysis in both solvents are similar.

4- The variations in the nitrogen bases that bind to the phosphate groups in PC or PS are responsible for the variations in the conditions for PC and PS.

5- The affinity between the substrate PC and the enzyme PLD in PC substitution reaction is the least value 3.664 among other reactions that mentioned.

6- In comparison to the other three reactions, the PC substitution process with ethanol requires a lower activation energy (ΔEa).

Recommendations

1. Using other phospholipids from components of the cell membrane and studying the effect of the alcoholic environment on them.

2. Applying this study to blood samples of alcoholics or ketoacidosis and following up the effect of alcohol on cell membrane components and a study of the harmful concentration of ethanol that leads to liver damage.

3. Owing to the wide range of uses for phosphatidylcholine, pharmaceutical, cosmetic, and food manufacturers can plan experiments that minimize the effects of alcoholic environments on the yield and efficiency of their primary products by taking into account the effects of these byproducts.

4. Studying other kinetics of the reaction, such as enzyme activity, or studying the use of other enzymes for the reaction, such as phospholipase A, phospholipase B and phospholipase C.

References

References:

1. Kiousi D-E. Anti-viral potential of marine and plant-derived bioactive molecules. 2022.

2. Bogojevic O, Nygaard JV, Wiking L, Arrevång C, Guo ZJBA. Designer phospholipids–structural retrieval, chemo-/bio-synthesis and isotopic labeling.*Biotechnology Advances*. https://doi.org/10.1016/j.biotechadv.2022.108025.

3. Parchem K, Sasson S, Ferreri C, Bartoszek AJFRR. Qualitative analysis of phospholipids and their oxidised derivatives–used techniques and examples of their applications related to lipidomic research and food analysis.*Free Radical Research*.2019;53(sup1):1068-100. https://doi.org/10.1080/10715762.2019.1657573.

4. Lupette J, Benning CJB. Human health benefits of very-long-chain polyunsaturated fatty acids from microalgae.*Biochimie*. 2020;178:15-25. https://doi.org/10.1016/j.biochi.2020.04.022.

5. Panda C, Varadharaj S, Voruganti VS. PUFA, genotypes and risk for cardiovascular disease. *Prostaglandins Leukot Essent Fatty Acids***.** 2022;176:102377. https://doi.org/10.1016/j.plefa.2021.102377.

6. Christie WW, Harwood JL. Oxidation of polyunsaturated fatty acids to produce lipid mediators. *Essays Biochem*. 2020;64(3):401-21. https://doi.org/10.1042/EBC20190082.

7. Guo Z, Vikbjerg AF, Xu X. Enzymatic modification of phospholipids for functional applications and human nutrition. *Biotechnol Adv*. 2005;23(3):203-59. https://doi.org/10.1016/j.biotechadv.2005.02.001.

8. Mashima R, Okuyama T, Ohira M. Biosynthesis of long chain base in sphingolipids in animals, plants and fungi. *Future Sci OA*. 2019;6(1):FSO434. https://doi.org/10.2144/fsoa-2019-0094.

9.Vargová K, Martinková M, Raschmanová JŠ, Pilátová MB, Kešeľáková A, Jáger DJCR. Straightforward access to novel cytotoxic phytosphingosine-like aminotriols from l-erythrose chiron.*Carbohydrate Research*. 2023;526:108789. https://doi.org/10.1016/j.carres.2023.108789.

10. Carreira ACN. Sphingosine-induced alterations in membrane biophysical properties: biological relevance in the pathophysiology of human disease: *Universidade de Lisboa (Portugal)*; 2019.

11. Floch V, Loisel S, Guenin E, Herve AC, Clement JC, Yaouanc JJ, et al. Cation substitution in cationic phosphonolipids: a new concept to improve transfection activity and decrease cellular toxicity. *J Med Chem*. 2000;43(24):4617-28. https://doi.org/10.1021/jm000006z.

12. De kkok NA, Exterkate M, Andringa RL, Minnaard AJ, Driessen AJJC, lipids po. A versatile method to separate complex lipid mixtures using 1-butanol as eluent in a reverse-phase UHPLC-ESI-MS system.*Chemistry and Physics of lipids.* https://doi.org/10.1016/j.chemphyslip.2021.105125.

13. Yang X, Lin C, Chen X, Li S, Li X, Xiao B. Structure deformation and curvature sensing of PIEZO1 in lipid membranes. *Nature*. 2022;604(7905):377-83. https://doi.org/10.1038/s41586-022-04574-8.

14. Bhavsar KV, Jagtap Upjuiisf. ENZYMES AND THEIR APPLICATIONS IN MEDICAL SCIENCES. 2021:265.

15. Gürkök SJIJSER. Microbial enzymes in detergents: a review. *International Journal of Scientific & Engineering Research*. 2019;10(9):75-81. http://www.ijser.org/.

16. Khandbahale SV, Pagar KR, Khankari RVJAJoRiPS. Introduction to Enzymes. *Asian Journal of Research in Pharmaceutical Science*.2019;9(2):123-30. http://dx.doi.org/10.5958/2231-5659.2019.00018.3.

17. Ramesh A, Harani Devi P, Chattopadhyay S, Kavitha MJMer, industries ai. *Commercial applications of microbial enzymes*. Enzymes: Roles and Applications in Industries. Microorganisms for Sustainability, vol 11. Springer, Singapore.2020:137-84. https://doi.org/10.1007/978-981-15-1710-5_6.

18. Bhardwaj D, Bharadvaja NJJoWPE. Phycoremediation of effluents containing dyes and its prospects for value-added products: A review of opportunities.*Journal of WaterProcessEngineering.*2021;41:102080.https://doi.org/10.1016/j.jwpe.2021.102080.

19. Sharma V, Tsai M-L, Nargotra P, Chen C-W, Kuo C-H, Sun P-P, et al. Agro-Industrial Food Waste as a Low-Cost Substrate for Sustainable

Production of Industrial Enzymes: A Critical Review. 2022;12(11):1373. https://doi.org/10.3390/catal12111373.

20. Zhang H, Han L, Dong HJR, reviews se. An insight to pretreatment, enzyme adsorption and enzymatic hydrolysis of lignocellulosic biomass: Experimental and modeling studies. *Catalysts* . 2021;140:110758. https://doi.org/10.3390/catal12111373.

21. Liu K-G, Sharifzadeh Z, Rouhani F, Ghorbanloo M, Morsali AJCCR. Metal-organic framework composites as green/sustainable catalysts.*Coordination Chemistry Reviews*. 2021;436:213827. https://doi.org/10.1016/j.ccr.2021.213827.

22. Bermejo P, Capelo J, Mota A, Madrid Y, Cámara Cjttiac. Enzymatic digestion and ultrasonication: a powerful combination in analytical chemistry.*TrAC Trends in Analytical Chemistry*. 2004;23(9):654-63. https://doi.org/10.1016/j.trac.2004.06.007.

23. Kent JA. Kent and Riegel's *Handbook of industrial chemistry and biotechnology*. Springerlink. 2007.

24. Sahu S, Agrawal S, Sahu A. *Regulatory policies on use of food enzymes*. Enzymes Beyond Traditional Applications in Dairy Science and Technology: Elsevier; 2023. p. 519-35. Academic Press. https://doi.org/10.1016/B978-0-323-96010-6.00021-7.

25.Christopher LP, Kumar H, Zambare VPJAE. Enzymatic biodiesel: Challenges and opportunities.*Applied Energy*. 2014;119:497-520. https://doi.org/10.1016/j.apenergy.2014.01.017.

26. De Koning AJ, McMullan KB. Hydrolysis of phospholipids with hydrochloric acid. *Biochim Biophys Acta*. 1965;106(3):519-26. https://doi.org/10.1016/0005-2760(65)90068-8.

27. Mangmee S, Adisakwattana P, Tipthara P, Simanon N, Sonthayanon P, Reamtong O. Lipid profile of Trichinella papuae muscle-stage larvae. *Sci Rep*. 2020;10(1):10125. https://doi.org/10.1038/s41598-020-67297-8.

28. Jové M, Mota-Martorell N, Obis È, Sol J, Martín-Garí M, Ferrer I, et al. Lipid Adaptations against Oxidative Challenge in the Healthy Adult Human Brain.*Antioxidants*. 2023;12(1):177. https://doi.org/10.3390/antiox12010177.

29. Nishimura S, Matsumori N. Chemical diversity and mode of action of natural products targeting lipids in the eukaryotic cell membrane. *Nat Prod Rep*. 2020;37(5):677-702. https://doi.org/10.1039/C9NP00059C.

30. Maertens JM, Scrima S, Lambrughi M, Genheden S, Trivellin C, Eriksson LA, et al. Molecular-dynamics-simulation-guided membrane engineering allows the increase of membrane fatty acid chain length in Saccharomyces cerevisiae. *Sci Rep.* 2021;11(1):17333. https://doi.org/10.1038/s41598-021-96757-y.

31. Beeler T, Fu D, Rivera J, Monaghan E, Gable K, Dunn T. SUR1 (CSG1/BCL21), a gene necessary for growth of Saccharomyces cerevisiae in the presence of high Ca^{2+} concentrations at 37℃, is required for mannosylation of inositolphosphorylceramide. *Molecular and General Genetics MGG*. 1997;255(6):570-9. https://doi.org/10.1007/s004380050530.

32. Ali AH, Zou X, Abed SM, Korma SA, Jin Q, Wang X. Natural phospholipids: Occurrence, biosynthesis, separation, identification, and beneficial health aspects. *Crit Rev Food Sci Nutr.* 2019;59(2):253-75. https://doi.org/10.1080/10408398.2017.1363714.

33. Haq M, Suraiya S, Ahmed S, Chun B-SJJoFF. Phospholipids from marine source: Extractions and forthcoming industrial applications.*Journal of functional Foods.* 2021;80:104448. https://doi.org/10.1016/j.jff.2021.104448.

34.Shahgholian NJHoN, Natural Products: Biological M, Properties N, Applications. *Encapsulation and Delivery of Nutraceuticals and Bioactive Compounds by Nanoliposomes and Tocosomes as Promising Nanocarriers*. Handbook of Nutraceuticals and Natural Products: Biological, Medicinal, and Nutritional Properties and Applications. 2022;1:403-39. https://doi.org/10.1002/9781119746843.ch17.

35. Li Y, Dai L, Liu D, Du WJC. Progress & Prospect of Enzyme-Mediated Structured Phospholipids Preparation.*Catalysts*. 2022;12(7):795. https://doi.org/10.3390/catal12070795.

36. Nessel I, Michael-Titus AT, editors. Lipid profiling of brain tissue and blood after traumatic brain injury: A review of human and experimental studies. *Seminars in Cell & Developmental Biology*. 2021: Elsevier. https://doi.org/10.1016/j.semcdb.2020.08.004.

37. Stubbs CD, Smith AD. The modification of mammalian membrane polyunsaturated fatty acid composition in relation to membrane fluidity and

function. *Biochim Biophys Acta*. 1984;779(1):89-137. https://doi.org/10.1016/0304-4157(84)90005-4.

38. Cvačka J, Vrkoslav V, Strnad ŠJMSfLM, Applications. *Structural Characterization of Lipids Using Advanced Mass Spectrometry Approaches*. Spectrometry for Lipidomics: Methods and Applications. Wiley Online Library. 2023;1:183-226. https://doi.org/10.1002/9783527836512.ch7.

39. Zia-Ul-Haq MJCS, Body FitH. *Historical and introductory aspects of carotenoids*. Carotenoids: structure and function in the human body. Springer. 2021:1-42.

40. Colin LA, Jaillais YJCoipb. Phospholipids across scales: lipid patterns and plant development. *Current opinion in plant biology*. 2020;53:1-9. https://doi.org/10.1016/j.pbi.2019.08.007.

41. Espinosa-Salinas I, Rodríguez-Casado A, Molina S, Rodríguez-González A, M Ordovas J, Ramirez de Molina AJCN, et al. Beneficial effects of bioactive phospholipids: genomic bases.*Current Nutrition & Food Science*. 2011;7(3):145-54. https://doi.org/10.2174/157340111797264859.

42. Lordan R, Redfern S, Tsoupras A, Zabetakis I. Inflammation and cardiovascular disease: are marine phospholipids the answer?. *Food Funct*. 2020;11(4):2861-85. https://doi.org/10.1039/C9FO01742A.

43. Ortega-Anaya J, Jiménez-Flores RJJods. Symposium review: The relevance of bovine milk phospholipids in human nutrition—Evidence of the effect on infant gut and brain development .*Journal of dairy science*. 2019;102(3):2738-48. https://doi.org/10.3168/jds.2018-15342.

44. Allegretti C, Denuccio F, Rossato L, D'Arrigo PJC. Polar Head Modified Phospholipids by Phospholipase D-Catalyzed Transformations of Natural Phosphatidylcholine for Targeted Applications: An Overview. *Catalysts*. 2020;10(9):997. https://doi.org/10.3390/catal10090997.

45. Niezgoda N, Gliszczyńska A, Gładkowski W, Kempińska K, Wietrzyk J, Wawrzeńczyk CJAJoC. Phosphatidylcholine with cis-9, trans-11 and trans-10, cis-12 conjugated linoleic acid isomers: synthesis and cytotoxic studies. *Australian Journal of Chemistry*. 2015;68(7):1065-75. https://doi.org/10.1071/CH14606.

46. Wu Y, Chen K, Xing G, Li L, Ma B, Hu Z, et al. Phospholipid remodeling is critical for stem cell pluripotency by facilitating mesenchymal-to-epithelial

transition. *Science Advances*.2019;5(11):eaax7525. https://doi.org/10.1126/sciadv.aax7525.

47. D'Arrigo P, Scotti M. Lysophospholipids: synthesis and biological aspects. *Current Organic Chemistry*. 2013;17(8):812-30.

48. Wang Y, Zhang P, Wei Y, Shen K, Xiao L, Miron RJ, et al. Cell-Membrane-Display Nanotechnology. *Adv Healthc Mater*. 2021;10(1):e2001014. https://doi.org/10.1002/adhm.202001014.

49. Wu P, Zhang B, Ocansey DKW, Xu W, Qian H. Extracellular vesicles: A bright star of nanomedicine. *Biomaterials*. 2021;269:120467. https://doi.org/10.1016/j.biomaterials.2020.120467.

50. Wäldchen F, Spengler B, Heiles SJJotacs. Reactive matrix-assisted laser desorption/ionization mass spectrometry imaging using an intrinsically photoreactive Paterno–Buchi matrix for double-bond localization in isomeric phospholipids. *Journal of the american*. 2019;141(30):11816-20. https://doi.org/10.1021/jacs.9b05868.

51. Javaid S, Farooq T, Rehman Z, Afzal A, Ashraf W, Rasool MF, et al. Dynamics of Choline-Containing Phospholipids in Traumatic Brain Injury and Associated Comorbidities. *International Journal of Molecular Sciences*. 2021 Oct 20;22(21):11313. https://doi.org/10.3390/ijms222111313.

52. Quan X, Bakovic MJOG. Regulation of membrane phospholipid homeostasis in neurodegenerative diseases. *OBM Geriatrics*. 2021 Jul;5(3):1-49. http://dx.doi.org/10.21926/obm.geriatr.2103176.

53. Schverer M, O'Mahony SM, O'Riordan KJ, Donoso F, Roy BL, Stanton C, et al. Dietary phospholipids: Role in cognitive processes across the lifespan. Neuroscience & Biobehavioral Reviews. *Neuroscience & Biobehavioral Reviews*. 2020 Apr 1;111:183-93. https://doi.org/10.1016/j.neubiorev.2020.01.012.

54. Yadav S, Sharma AK, Kumar P. Nanoscale Self-Assembly for Therapeutic Delivery. Front Bioeng Biotechnol. *Frontiers in Bioengineering and Biotechnology*. 2020 Feb 25;8:127. https://doi.org/10.3389/fbioe.2020.00127.

55. Chudasma MP, Shah SA, Qureshi MHN, Shah N, Shah D, Trivedi R, et al. Brief Insight on Nanovesicular Liposomes as Drug-delivery Carriers for

Medical Applications. *Journal of Exploratory Research in Pharmacology*. 2023 Apr 27(000):0-. https://dx.doi.org/10.14218/JERP.2022.00086.

56. Drescher S, van Hoogevest PJP. The phospholipid research center: Current research in phospholipids and their use in drug delivery. *Pharmaceutics*. 2020 Dec 18;12(12):1235. https://doi.org/10.3390/pharmaceutics12121235.

57. Chacko IA, Ghate VM, Dsouza L, Lewis SA. Lipid vesicles: A versatile drug delivery platform for dermal and transdermal applications. *Colloids Surf B Biointerfaces*. 2020 Nov 1;195:111262. https://doi.org/10.1016/j.colsurfb.2020.111262.

58. Safaeian Laein S, Katouzian I, Mozafari M, Farnudiyan-Habibi A, Akbarbaglu Z, Shadan MR, et al. Biological and thermodynamic stabilization of lipid-based delivery systems through natural biopolymers; controlled release and molecular dynamics simulations. *Critical Reviews in Food Science and Nutrition*. 2023 Mar 17:1-20. https://doi.org/10.1080/10408398.2023.2191281.

59. Maleki G, Woltering EJ, Mozafari MJTiFS, Technology. Applications of chitosan-based carrier as an encapsulating agent in food industry. *Trends in Food Science & Technology*. 2022 Feb 1;120:88-99. https://doi.org/10.1016/j.tifs.2022.01.001.

60. Jampilek J, Kos J, Kralova K. Potential of Nanomaterial Applications in Dietary Supplements and Foods for Special Medical Purposes. *Nanomaterials (Basel)*. 2019 Feb 19;9(2):296. https://doi.org/10.3390/nano9020296.

61. Sałek K, Euston SRJPB. Sustainable microbial biosurfactants and bioemulsifiers for commercial exploitation. *Process Biochemistry*. 2019 Oct 1;85:143-55. https://doi.org/10.1016/j.procbio.2019.06.027.

62. Schlame M, Xu YJJomb. The Function of Tafazzin, a Mitochondrial Phospholipid–Lysophospholipid Acyltransferase. Journal of molecular biology. 2020 Aug 21;432(18):5043-51. https://doi.org/10.1016/j.jmb.2020.03.026.

63. Alhajj MJ, Montero N, Yarce CJ, Salamanca CHJC. Lecithins from vegetable, land, and marine animal sources and their potential applications for cosmetic, food, and pharmaceutical sectors. *Cosmetics*. 2020 Nov 9;7(4):87. https://doi.org/10.3390/cosmetics7040087.

64. Allegretti C, Bono A, D'Arrigo P, Denuccio F, De Simeis D, Di Lecce G, et al. Valorization of Corn Seed Oil Acid Degumming Waste for Phospholipids Preparation by Phospholipase D-Mediated Processes. *Catalysts*. 2020 Jul 21;10(7):809. https://doi.org/10.3390/catal10070809.

65. Morris-Paxton A. *An Introduction to Concepts of Nutrition: Facilitator's Handbook* . A Facilitated Coursebook Designed for Further Education and Entry Level Higher Education/Adult and Community Learning: Xlibris Corporation; ; 2019 Feb 13..

66. Vance JE. Inter-organelle membrane contact sites: implications for lipid metabolism. *Biol Direct*. 2020;15(1):24. https://doi.org/10.1186/s13062-020-00279-y.

67. Zhao X, Xia Y. Characterization of Fatty Acyl Modifications in Phosphatidylcholines and Lysophosphatidylcholines via Radical-Directed Dissociation. *Journal of the American Society for Mass Spectrometry*. 2021 Jan 14;32(2):560-8. https://doi.org/10.1021/jasms.0c00407.

68. Kundu S, Malik S, Ghosh M, Nandi S, Pyne A, Debnath A, et al. A comparative study on DMSO-induced modulation of the structural and dynamical properties of model bilayer membranes. *Langmuir*. 2021 Feb 2;37(6):2065-78. https://doi.org/10.1021/acs.langmuir.0c03037.

69. Maleš P, Pem B, Petrov D, Jurašin DD, Bakarić DJSM. Deciphering the origin of the melting profile of unilamellar phosphatidylcholine liposomes by measuring the turbidity of its suspensions. *Soft Matter*. 2022;18(35):6703-15. https://doi.org/10.1039/D2SM00878E.

70. Tian CA, Chiu CC. Importance of Hydrophilic Groups on Modulating the Structural, Mechanical, and Interfacial Properties of Bilayers: A Comparative Molecular Dynamics Study of Phosphatidylcholine and Ion Pair Amphiphile Membranes. *International journal of molecular sciences*. 2018 May 23;19(6):1552. https://doi.org/10.3390/ijms19061552.

71. Lordan R, Blesso CN. Editorial: Phospholipids and sphingolipids in nutrition, metabolism, and health. *Frontiers in Nutrition*. 2023 Feb 7;10:1153138. https://doi.org/10.3389/fnut.2023.1153138.

72. Bot F, Cossuta D, O'Mahony JAJTiFS, Technology. Inter-relationships between composition, physicochemical properties and functionality of lecithin ingredients. *Trends in Food Science & Technology*. 2021 May 1;111:261-70. https://doi.org/10.1016/j.tifs.2021.02.028.

73. Kozakiewicz E, Cossuta D. *Emulsions: Lecithin*. Handbook of Molecular Gastronomy: CRC Press; 2021. p. 249-56.

74. Singh SJAotRSfCB. Comparative Study Ofsynthesis and Nutritional Aspects of Lecithin Fromsoya and Sunflower Oil. *Annals of the Romanian Society for Cell Biology*. 2021 Jul 10;25(6):16356-76. http://www.annalsofrscb.ro/index.php/journal/article/view/8884

75. Robert C, Couëdelo L, Vaysse C, Michalski M-CJB. Vegetable lecithins: A review of their compositional diversity, impact on lipid metabolism and potential in cardiometabolic disease prevention. *Biochimie*. 2020 Feb 1;169:121-32. https://doi.org/10.1016/j.biochi.2019.11.017.

76. Morita S-y, Ikeda YJBp. Regulation of membrane phospholipid biosynthesis in mammalian cells, *Biochemical pharmacology*. 2022:115296. https://doi.org/10.1016/j.bcp.2022.115296.

77. Al-Mutairi AA. Preparation, *Preparation, characterization and antitumor activity evaluation of oxaliplatin and gemcitabine encapsulated in a solid lipid nanoparticle* (Doctoral dissertation, (KING ABDULAZIZ UNIVERSITY JEDDAH). 2021.

78. Liu R. *Water-insoluble drug formulation*. CRC press; 2000. https://doi.org/10.1201/9781420026054.

79. Souza LMP, Lima MC, Bezerra LFS, Pimentel ASJCP. Transposition of polymer-encapsulated small interfering RNA through lung surfactant models at the air-water interface. *Chemical Physics*. 2022 Nov 1;563:111704. https://doi.org/10.1016/j.chemphys.2022.111704.

80. Mohammed RUR. RHEOLOGICAL BEHAVIOR OF DSPC-, DBPC-, AND DPPC-OXYGEN MICROBUBBLES AND THEIR EFFECTIVENESS IN IMPROVING SURVIVAL IN A RAT MODEL OF LIPOPOLYSACCHARIDE-INDUCED ACUTE RESPIRATORY DISTRESS SYNDROME. 2022.

81. Ma Y, Hong J, Ding YJAHM. Biological behavior regulation of gold nanoparticles via the protein corona. Advanced Healthcare Materials. 2020 Mar;9(6):1901448. https://doi.org/10.1002/adhm.201901448.

82. van Hoogevest P, Tiemessen H, Metselaar JM, Drescher S, Fahr AJEjols, technology. The use of phospholipids to make pharmaceutical form

line extensions. *European journal of lipid science and technology*. 2021 Apr;123(4):2000297. https://doi.org/10.1002/ejlt.202000297.

83. Boldyreva LV, Morozova MV, Saydakova SS, Kozhevnikova EN. Fat of the Gut: Epithelial Phospholipids in Inflammatory Bowel Diseases. *International Journal of Molecular Sciences*. 2021 Oct 28;22(21):11682. https://doi.org/10.3390/ijms222111682.

84. Kuksis A, Pruzanski W. Destruction of polyunsaturated alkyl/acyl and alkenyl/acyl glycerophosphocholine of plasma lipoproteins during incubation with group V and X secretory phospholipase A(2) s. *Lipids*. 2022 Mar;57(2):91-104. https://doi.org/10.1002/lipd.12333.

85. Kadokawa H, Kotaniguchi M, Mawatari S, Saito R, Fujino T, Kitamura SJSR. Ethanolamine plasmalogens derived from scallops stimulate both follicle-stimulating hormone and luteinizing hormone secretion by bovine gonadotrophs. *Scientific Reports*. 2022 Oct 6;12(1):16789. https://doi.org/10.1038/s41598-022-20794-4.

86. Diagne A, Fauvel J, Record M, Chap H, Douste-Blazy LJBeBA-L, Metabolism L. Studies on ether phospholipids: II. Comparative composition of various tissues from human, rat and guinea pig. *Biochimica et Biophysica Acta (BBA)-Lipids and Lipid Metabolism*. 1984 Apr 18;793(2):221-31. https://doi.org/10.1016/0005-2760(84)90324-2.

87. Tang L, Chi H, Li W, Zhang L, Zhang L, Chen L, et al. FgPsd2, a phosphatidylserine decarboxylase of Fusarium graminearum, regulates development and virulence. *Fungal Genetics and Biology*. 2021 Jan 1;146:103483. https://doi.org/10.1016/j.fgb.2020.103483.

88. Iwai M, Yamada-Oshima Y, Asami K, Kanamori T, Yuasa H, Shimojima M, et al. Recycling of the major thylakoid lipid MGDG and its role in lipid homeostasis in Chlamydomonas reinhardtii. *Plant physiology*. 2021 Nov 1;187(3):1341-56. https://doi.org/10.1093/plphys/kiab340.

89. St Germain M, Iraji R, Bakovic M. Phosphatidylethanolamine homeostasis under conditions of impaired CDP-ethanolamine pathway or phosphatidylserine decarboxylation. *Frontiers in Nutrition*. 2023 Jan 5;9:1094273. https://doi.org/10.3389/fnut.2022.1094273.

90. Lands WJBeba. Stories about acyl chains. *Biochimica et Biophysica Acta (BBA)-Molecular and Cell Biology of Lipids*. 2000 Jan 3;1483(1):1-14. https://doi.org/10.1016/S1388-1981(99)00177-8.

91. Fernandes Silva L. *Phenotypic characterization of genetic variants associated with the risk of type 2 diabetes and non-alcoholic fatty liver disease* (Doctoral dissertation, Itä-Suomen yliopisto); 2020.

92. Kwarteng DO, Gangoda M, Kooijman EEJBC. The effect of methylated phosphatidylethanolamine derivatives on the ionization properties of signaling phosphatidic acid. *Biophysical Chemistry*. 2023 May 1;296:107005. https://doi.org/10.1016/j.bpc.2023.107005.

93. Bogdanov M, Sun J, Kaback HR, Dowhan WJJoBC. A Phospholipid Acts as a Chaperone in Assembly of a Membrane Transport Protein (∗).*Journal of Biological Chemistry*. 1996 May 17;271(20):11615-8. https://doi.org/10.1074/jbc.271.20.11615.

94. Yao Z, Vance DEJJoBC. The active synthesis of phosphatidylcholine is required for very low density lipoprotein secretion from rat hepatocytes. *Journal of Biological Chemistry*. 1988 Feb 25;263(6):2998-3004. https://doi.org/10.1016/S0021-9258(18)69166-5.

95. Pandey SK, Paul A, Shteinfer-Kuzmine A, Zalk R, Bunz U, Shoshan-Barmatz V. SMAC/Diablo controls proliferation of cancer cells by regulating phosphatidylethanolamine synthesis. *Molecular Oncology*. 2021 Nov;15(11):3037-61. https://doi.org/10.1002/1878-0261.12959.

96. Menon A, Stevens VJJoBC. Phosphatidylethanolamine is the donor of the ethanolamine residue linking a glycosylphosphatidylinositol anchor to protein. *Journal of Biological Chemistry*. 1992 Aug 5;267(22):15277-80. https://doi.org/10.1016/S0021-9258(19)49529-X.

97. Piomelli D, Mabou Tagne A. Endocannabinoid-Based Therapies. *Annual Review of Pharmacology and Toxicology*. 2022 Jan 6;62:483-507. https://doi.org/10.1146/annurev-pharmtox-052220-021800.

98. El Itawi H. Impact of periodontal inflammation on the cardiac splenic axis: study of Neutrophils Extracellular Traps (NETs) and splenic microvesicles as mediators of procoagulant and inflammatory responses (Doctoral dissertation, Université de Strasbourg). 2022.

99. Callahan MK, Popernack PM, Tsutsui S, Truong L, Schlegel RA, Henderson AJJTJoI. Phosphatidylserine on HIV envelope is a cofactor for infection of monocytic cells. *The Journal of Immunology*. 2003 May 1;170(9):4840-5. https://doi.org/10.4049/jimmunol.170.9.4840.

100. Wanderley JLM, DaMatta RA, Barcinski MAJCC, Signaling. Apoptotic mimicry as a strategy for the establishment of parasitic infections: parasite-and host-derived phosphatidylserine as key molecule. *Cell Communication and Signaling*. 2020 Dec;18 (1):1-10. https://doi.org/10.1186/s12964-019-0482-8.

101. Leventis PA, Grinstein S. The distribution and function of phosphatidylserine in cellular membranes. *Annual review of biophysics*. 2010 Jun 9;39:407-27. https://doi.org/10.1146/annurev.biophys.093008.131234.

102. Rani MH, Liu Q, Yu N, Zhang Y, Wang B, Cao Y, et al. ES5 is involved in the regulation of phosphatidylserine synthesis and impacts on early senescence in rice (Oryza sativa L.). *Plant molecular biology*. 2020 Mar;102:501-15. https://doi.org/10.1007/s11103-019-00961-4.

103. Randolph CE. *Gas-phase Ion/Ion Reactions For Enhanced Lipid Analysis* (Doctoral dissertation, Purdue University); 2020.

104. Blunsom NJ, Cockcroft SJBEBA-M, Lipids CBo. Phosphatidylinositol synthesis at the endoplasmic reticulum. Biochimica et Biophysica Acta (BBA)-Molecular and Cell Biology of Lipids. 2020 Jan 1;1865(1):158471. https://doi.org/10.1016/j.bbalip.2019.05.015.

105. Hughes WE, Cooke FT, Parker Pjjbj. Sac phosphatase domain proteins. *Biochemical Journal* ,2000;350(2):337-52. https://doi.org/10.1042/bj3500337.

106. Allegretti C, Denuccio F, Rossato L, D'Arrigo P. Polar Head Modified Phospholipids by Phospholipase D-Catalyzed Transformations of Natural Phosphatidylcholine for Targeted Applications: An Overview. *Catalysts*. 2020 Sep 1;10(9):997. https://doi.org/10.3390/catal10090997.

107. Mazela J, Merritt TA, Gadzinowski J, Sinha S. Evolution of pulmonary surfactants for the treatment of neonatal respiratory distress syndrome and paediatric lung diseases. *Acta Paediatr*. 2006;95(9):1036-48. https://doi.org/10.1080/08035250600615168.

108. Allegretti C, Gatti FG, Marzorati S, Rossato LAM, Serra S, Strini A, et al. Reactive Deep Eutectic Solvents (RDESs): A new tool for phospholipase D-catalyzed preparation of phospholipids. *Catalysts*. 2021 May 22;11(6):655. https://doi.org/10.3390/catal11060655.

109. Piazza GJ, Marmer WNJJotAOCS. Conversion of phosphatidylcholine to phosphatidylglycerol with phospholipase D and glycerol. *Journal of the*

American Oil Chemists' Society. 2007 Jul;84:645-51. https://doi.org/10.1007/s11746-007-1081-1.

110. Semproli R, Robescu MS, Cambò M, Mema K, Bavaro T, Rabuffetti M, et al. Chemical and Enzymatic Approaches to Esters of sn-Glycero-3-Phosphoric Acid. *European Journal of Organic Chemistry*. 2021 Aug 6;2021(29):4027-37. https://doi.org/10.1002/ejoc.202100235.

111. Zhou H, Huo Y, Yang N, Wei T. Phosphatidic acid: from biophysical properties to diverse functions. *The FEBS Journal*. 2023 Apr 27. https://doi.org/10.1111/febs.16809.

112. Rodas-Junco BA, Nic-Can GI, Muñoz-Sánchez A, Hernández-Sotomayor STJIJoMS. Phospholipid signaling is a component of the salicylic acid response in plant cell suspension cultures. *International journal of molecular sciences*. 2020 Jul 25;21(15):5285. https://doi.org/10.3390/ijms21155285.

113. Showalter MR, Berg AL, Nagourney A, Heil H, Carraway KL, 3rd, Fiehn O. The Emerging and Diverse Roles of Bis(monoacylglycero) Phosphate Lipids in Cellular Physiology and Disease. *International journal of molecular sciences*. 2020 Oct 29;21(21):8067. https://doi.org/10.3390/ijms21218067.

114. Jennings W, Epand RMJC, Lipids Po. CDP-diacylglycerol, a critical intermediate in lipid metabolism. *Chemistry and Physics of Lipids*. 2020 Aug 1;230:104914. https://doi.org/10.1016/j.chemphyslip.2020.104914.

115. Thakur R, Naik A, Panda A, Raghu P. Regulation of Membrane Turnover by Phosphatidic Acid: Cellular Functions and Disease Implications. *Frontiers in Cell and Developmental Biology*. 2019 Jun 4;7:83. https://doi.org/10.3389/fcell.2019.00083.

116. Shulga YV, Topham MK, Epand RM. Regulation and functions of diacylglycerol kinases. *Chemical reviews*. 2011 Oct 12;111(10):6186-208. https://doi.org/10.1021/cr1004106.

117. Chow WY, De Paepe G, Hediger S. Biomolecular and Biological Applications of Solid-State NMR with Dynamic Nuclear Polarization Enhancement. *Chemical Reviews*. 2022 Apr 21;122(10):9795-847. https://doi.org/10.1021/acs.chemrev.1c01043.

118. Palfey B, Switzer RL. *Kinetics of Enzyme Catalysis*: American Chemical Society; 2022 Apr 20.

119. Vesely SLL. The Chemical Reactions Involving Radiation. 2021. https://hal.science/hal-03373189.

120. Meisenberg G, Simmons WH. *Enzymatic Reactions*. Principles of Medical Biochemistry. 2012. p. 39-54.diacylglycerol, a critical intermediate in lipid metabolism. 2020;230:104914.

121. Yadav M. *Enzymes: Classification and catalysis*. Institute of Lifelong Learning, University of Delhi, India. 2016. http://vle.du.ac.in/file.php/549/Development_Biology/Ch_Enzymes_classification_and_catalysis.pdf.

122. Huang L, Sun DW, Pu H, Wei Q. Development of Nanozymes for Food Quality and Safety Detection: Principles and Recent Applications. *Comprehensive Reviews in Food Science and Food Safety*. 2019 Sep;18(5):1496-513. https://doi.org/10.1111/1541-4337.12485.

123. Kumar A, Gudiukaite R, Gricajeva A, Sadauskas M, Malunavicius V, Kamyab H, et al. Microbial lipolytic enzymes–promising energy-efficient biocatalysts in bioremediation. *Energy*. 2020 Feb 1;192:116674. https://doi.org/10.1016/j.energy.2019.116674.

124. Maghraby YR, El-Shabasy RM, Ibrahim AH, Azzazy HME. Enzyme Immobilization Technologies and Industrial Applications. *ACS omega*. 2023 Jan 31;8(6):5184-96. https://doi.org/10.1021/acsomega.2c07560.

125. Garske AL, Kapp G, McAuliffe JC. *Industrial enzymes and biocatalysis*. Handbook of industrial chemistry and biotechnology: Springer; 2017. p. 1571-638. https://doi.org/10.1007/978-3-319-52287-6_28.

126. McAuliffe JC, Aehle W, Whited GM, Ward DE. Industrial enzymes and biocatalysis. Kent and Riegel's Handbook of Industrial Chemistry and Biotechnology: Boston, MA: Springer US; 2007(p. 1375-420). https://doi.org/10.1007/978-0-387-27843-8_31.

127. Szadkowska DJAoWUoLSS. Change in hydrolytic enzyme efficiency over time. *Annals of Warsaw University of Life Sciences SGGW (Forestry and Wood Technology)*. 2020;212:79-84. https://fwt.sggw.edu.pl/article/download/96/63.

128. Wang D, Yan L, Ma X, Wang W, Zou M, Zhong J, et al. Ultrasound promotes enzymatic reactions by acting on different targets: Enzymes, substrates and enzymatic reaction systems. *International journal of biological macromolecules*. 2018 Nov 1;119:453-61. https://doi.org/10.1016/j.ijbiomac.2018.07.133.

129. Bell EL, Finnigan W, France SP, Green AP, Hayes MA, Hepworth LJ, et al. Biocatalysis. *Nature Reviews Methods Primers*. 2021 Jun 24;1(1):46. https://doi.org/10.1038/s43586-021-00044-z.

130. Panawala L. What is the Active Site of an Enzyme. 25/05/2017. http://pediaa.com/what-is-the-active-site-of-an-enzyme/

131. Manoj KM, Gideon DA, Parashar AJCB, Biophysics. What is the role of lipid membrane-embedded quinones in mitochondria and chloroplasts? Chemiosmotic Q-cycle versus murburn reaction perspective. *Cell Biochemistry and Biophysics*. 2021 Mar;79(1):3-10. https://doi.org/10.1007/s12013-020-00945-y.

132. Raizner AE. Coenzyme Q(10). *Methodist DeBakey cardiovascular journal*. 2019 Jul;15(3):185-91. https://doi.org/10.14797%2Fmdcj-15-3-185.

133. Raizner AE, Quinones MA. Coenzyme Q(10) for Patients With Cardiovascular Disease: JACC focus seminar. *Journal of the American College of Cardiology*. 2021 Feb 9;77(5):609-19. https://doi.org/10.1016/j.jacc.2020.12.009.

134. Pastor-Maldonado CJ, Suarez-Rivero JM, Povea-Cabello S, Alvarez-Cordoba M, Villalon-Garcia I, Munuera-Cabeza M, et al. Coenzyme Q(10): Novel Formulations and Medical Trends. *International Journal of Molecular Sciences*. 2020 Nov 10;21(22):8432. https://doi.org/10.3390/ijms21228432.

135. López-Pedrera C, Villalba JM, Patiño-Trives AM, Luque-Tévar M, Barbarroja N, Aguirre MÁ, et al. Therapeutic potential and immunomodulatory role of coenzyme q10 and its analogues in systemic autoimmune diseases. *Antioxidants*. 2021 Apr 13;10(4):600. https://doi.org/10.3390/antiox10040600.

136. Rius R, Bennett NK, Bhattacharya K, Riley LG, Yuksel Z, Formosa LE, et al. Biallelic pathogenic variants in COX11 are associated with an infantile-onset mitochondrial encephalopathy. *Human Mutation*. 2022 Dec;43(12):1970-8. https://doi.org/10.1002/humu.24453.

137. Hargreaves I, Heaton RA, Mantle D. Disorders of Human Coenzyme Q10 Metabolism: An Overview. *International journal of molecular sciences*. 2020 Sep 13;21(18):6695. https://doi.org/10.3390/ijms21186695.

138. Gao M, Fan K, Chen Y, Zhang G, Chen J, Zhang Y. Understanding the mechanistic regulation of ferroptosis in cancer: the gene matters. *Journal of Genetics and Genomics*. 2022 Jun 10.49(10):913-26. https://doi.org/10.1016/j.jgg.2022.06.002.

139. Drauz K, Gröger H, May O. *Enzyme catalysis in organic synthesis*, 3 volume set. John Wiley & Sons; 2012 Mar 26.

140. Pradhan D, Sahoo B, Misra BB, Padhy SJASC. A multiclass SVM classifier with teaching learning based feature subset selection for enzyme subclass classification. *Applied Soft Computing*. 2020 Nov 1;96:106664. https://doi.org/10.1016/j.asoc.2020.106664.

141. Gagler DC. *Universal Biochemistry Within and Across Biological Domains and Levels of Organization on Earth* (Doctoral dissertation, Arizona State University); 2020.https://search.proquest.com/openview/2b57ac1884c51bc4b6e0b6db3007a4f9/1?pq-origsite=gscholar&cbl=44156.

142. Almonacid DE, Babbitt PC. Toward mechanistic classification of enzyme functions. *Current opinion in chemical biology*. 2011 Jun 1;15(3):435-42. https://doi.org/10.1016/j.cbpa.2011.03.008.

143. García-Cano I, Rocha-Mendoza D, Kosmerl E, Zhang L, Jiménez-Flores RJAm, biotechnology. Technically relevant enzymes and proteins produced by LAB suitable for industrial and biological activity. *Applied microbiology and biotechnology.* 2020 Feb;104:1401-22. https://doi.org/10.1007/s00253-019-10322-2.

144. Melis S, Delcour JA. Impact of wheat endogenous lipids on the quality of fresh bread: Key terms, concepts, and underlying mechanisms. *Comprehensive Reviews in Food Science and Food Safety*. 2020 Nov;19(6):3715-54. https://doi.org/10.1111/1541-4337.12616.

145. Marvi MV, Neri I, Evangelisti C, Ramazzotti G, Asioli S, Zoli M, et al. Phospholipases in Gliomas: Current Knowledge and Future Perspectives from Bench to Bedside. *Biomolecules*. 2023 May 7;13(5):798. https://doi.org/10.3390/biom13050798.

146. Fan R, Zhao F, Gong Z, Chen Y, Yang B, Zhou C, et al. Insights into the mechanism of phospholipid hydrolysis by plant non-specific phospholipase C. *Nature communications*. 2023 Jan 12;14(1):194. https://doi.org/10.1038/s41467-023-35915-4.

147. Booth LA, Smith TK. Lipid metabolism in Trypanosoma cruzi: A review. *Molecular and biochemical parasitology*. 2020 Nov 1;240:111324. https://doi.org/10.1016/j.molbiopara.2020.111324.

148. Cerminati S, Paoletti L, Aguirre A, Peirú S, Menzella HG, Castelli ME. Industrial uses of phospholipases: current state and future applications. *Applied Microbiology and Biotechnology*. 2019 Mar 15;103:2571-82. https://doi.org/10.1007/s00253-019-09658-6.

149. Bott E, López MG, Lammel EM, Carfagna IE, de Isola ELD, Ruybal P, et al. Cellular localization, cloning and expression of Leishmania braziliensis Phospholipase A1. *Microbial pathogenesis*. 2020 Apr 1;141:104010. https://doi.org/10.1016/j.micpath.2020.104010.

150. Nakagawara C, Arioka MJB, Communications BR. Distinct enzymatic and cellular characteristics of two phospholipases A1 in Aspergillus oryzae. *Biochemical and Biophysical Research Communications*. 2019 Oct 22;518(4):644-50. https://doi.org/10.1016/j.bbrc.2019.08.087.

151. Hayakawa Y, Nakayama R, Namiki N, Imai MJAS. Promising Immobilization of Industrial-Class Phospholipase A1 to Attain High-Yield Phospholipids Hydrolysis and Repeated Use with Optimal Water Content in Water-in-Oil Microemulsion Phase. *Applied Sciences*. 2021 Feb 5;11(4). https://doi.org/10.3390/app11041456.

152. Csáki KF, Sebestyén ÉJFS, Wellness H. Who will carry out the tests that would be necessary for proper safety evaluation of food emulsifiers? *Food Science and Human Wellness*. 2019 Jun 1;8(2):126-35. https://doi.org/10.1016/j.fshw.2019.04.001.

153. Zhang H, Zhang Y, Xu N, Rui C, Fan Y, Wang J, et al. Genome-wide expression analysis of phospholipase A1 (PLA1) gene family suggests phospholipase A1-32 gene responding to abiotic stresses in cotton. *International Journal of Biological Macromolecules*. 2021 Dec 1;192:1058-74..

154. Sonkar K, Ayyappan V, Tressler CM, Adelaja O, Cai R, Cheng M, et al. Focus on the glycerophosphocholine pathway in choline phospholipid

metabolism of cancer. *NMR in Biomedicine*. 2019 Oct;32(10):e4112. https://doi.org/10.1002/nbm.4112.

155. Nakajima K, Sonoda H, Mizoguchi T, Aoki J, Arai H, Nagahama M, et al. A novel phospholipase A1 with sequence homology to a mammalian Sec23p-interacting protein, p125. *Journal of Biological Chemistry*. 2002 Mar 29;277(13):11329-35. https://doi.org/10.1074/jbc.M111092200.

156. Shimoi W, Ezawa I, Nakamoto K, Uesaki S, Gabreski G, Aridor M, et al. p125 is localized in endoplasmic reticulum exit sites and involved in their organization. *Journal of Biological Chemistry*. 2005 Mar 18;280(11):10141-8. https://doi.org/10.1074/jbc.M409673200.

157. Lu Y, Zhang A, Wang X, Hao N, Chen K, Ouyang P. Surfactant enhancedl-α-glycerylphosphorylcholine production from phosphatidylcholine using phospholipase A1in the aqueous phase. *Biocatalysis and Biotransformation*. 2019 Sep 3;37(5):361-6. https://doi.org/10.1080/10242422.2019.1568413.

158. Cheng S, Guo Z, Liang C, Shi Y, Geng P, Xin Y, et al. Heterologous expression, refolding, and characterization of a calcium-independent phospholipase A1 from Streptomyces albidoflavus. *Systems Microbiology and Biomanufacturing*. 2022 Jul:1-1. https://doi.org/10.1007/s43393-021-00070-8.

159. Nakawatari K, Kurano M, Araki O, Nishikawa M, Shimamoto S, Igarashi K, et al. Elevated phosphatidylserine-specific phospholipase A1 level in hyperthyroidism. *Clinica Chimica Acta*. 2020 Apr 1;503:99-106. https://doi.org/10.1016/j.cca.2020.01.011.

160. Murakami M, Sato H, Taketomi Y. Updating Phospholipase A(2) Biology. *Biomolecules*. 2020;10(10). https://doi.org/10.3390/biom10101457

161. Khan SA, Ilies MA. The Phospholipase A2 Superfamily: Structure, Isozymes, Catalysis, Physiologic and Pathologic Roles. *International Journal of Molecular Sciences*. 2023 Jan 10;24(2):1353. https://doi.org/10.3390/ijms24021353.

162. Murakami M, Sato H, Taketomi Y. Modulation of immunity by the secreted phospholipase A(2) family. *Immunological Reviews*. 2023 Apr 10;317(1):42-70. https://doi.org/10.1111/imr.13205.

163. Jarc E, Petan T. A twist of FATe: Lipid droplets and inflammatory lipid mediators. *Biochimie*. 2020 Feb 1;169:69-87. https://doi.org/10.1016/j.biochi.2019.11.016.

164. Murakami M. Novel functions of phospholipase A(2)s: Overview. *Biochim Biophys Acta Mol Cell Biol Lipids*. 2019 Jun 1;1864(6):763-5.. https://doi.org/10.1016/j.bbalip.2019.02.005.

165. Durrani R, Khan FI, Ali S, Wang Y, Yang B. A Thermolabile Phospholipase B from Talaromyces marneffei GD-0079: Biochemical Characterization and Structure Dynamics Study. *Biomolecules*. 2020;10(6). https://doi.org/10.3390/biom10020231.

166.Durrani R, Khan FI, Ali S, Wang Y, Yang BJB. A thermolabile phospholipase B from Talaromyces marneffei GD-0079: biochemical characterization and structure dynamics study. *Biomolecules.* 2020 Feb 4;10(2):231. https://doi.org/10.3390/biom10020231

167. Borrelli GM, Trono DJIjoms. Recombinant lipases and phospholipases and their use as biocatalysts for industrial applications. *International journal of molecular sciences*. 2015 Sep 1;16(9):20774-840. https://doi.org/10.3390/ijms160920774.

168. Wei Y, Liu X, Ge S, Zhang H, Che X, Liu S, et al. Involvement of Phospholipase C in Photosynthesis and Growth of Maize Seedlings. *Genes*. 2022 Jun 3;13(6):1011. https://doi.org/10.3390/genes13061011.

169. Cerminati S, Paoletti L, Aguirre A, Peiru S, Menzella HG, Castelli ME. Industrial uses of phospholipases: current state and future applications. *Applied microbiology and biotechnology*. 2019 Mar 15;103:2571-82. https://doi.org/10.1007/s00253-019-09658-6.

170. Ramrakhiani L, Chand S. Recent progress on phospholipases: different sources, assay methods, industrial potential and pathogenicity. *Applied Biochemistry and Biotechnology*. 2011 Aug;164:991-1022. https://doi.org/10.1007/s12010-011-9190-6

171. Nakamura Y, Ngo AHJJopr. Non-specific phospholipase C (NPC): an emerging class of phospholipase C in plant growth and development. *Journal of plant research*. 2020 Jul;133(4):489-97. https://doi.org/10.1007/s10265-020-01199-8.

172. Bill CA, Vines CMJCS. Phospholipase C. *Adv Exp Med Biol*. 2020;1131:215-242. doi: 10.1007/978-3-030-12457-1_9.

173. Bill CA, Vines CM. Phospholipase C. In: Islam, M. (eds) *Calcium Signaling*. Advances in Experimental Medicine and Biology, vol 1131. Springer, Cham. 2020:215-42. https://doi.org/10.1007/978-3-030-12457-1_9

174. Xiang M, Wang L, Yan Q, Jiang Z, Yang S. High-level expression and characterization of a novel phospholipase C from Thielavia terrestris suitable for oil degumming. *International journal of biological macromolecules*. 2020 Aug 1;156:740-8. https://doi.org/10.1016/j.ijbiomac.2020.04.104.

175. Szumiło M, Rahden-Staroń IJPHiMD. Biological role of phosphatidylcholine-specific phospholipase C in mammalian cells. *National library of medicine*. 2008 Nov 3;62:593-8. Polish. PMID: 19002082..

176. Zhang Z, Chen M, Xu W, Zhang W, Zhang T, Guang C, et al. Microbial phospholipase D: Identification, modification and application. *Trends in Food Science & Technology*. 2020 Feb 1;96:145-56. https://doi.org/10.1016/j.tifs.2019.12.020.

177. Liu Y, Huang L, Fu Y, Zheng D, Ma J, Li Y, et al. A novel process for phosphatidylserine production using a Pichia pastoris whole-cell biocatalyst with overexpression of phospholipase D from Streptomyces halstedii in a purely aqueous system. *Food chemistry*. 2019 Feb 15;274:535-42. https://doi.org/10.1016/j.foodchem.2018.08.105.

178. Deepika D, Singh A. Plant phospholipase D: novel structure, regulatory mechanism, and multifaceted functions with biotechnological application. *Critical Reviews in Biotechnology*. 2022 Jan 2;42(1):106-24. https://doi.org/10.1080/07388551.2021.1924113.

179. Yao Y, Li J, Lin Y, Zhou J, Zhang P, Xu YJPiLR. Structural insights into phospholipase D function. *Progress in Lipid Research*. 2021 Jan 1;81:101070. https://doi.org/10.1016/j.plipres.2020.101070.

180. Zhang H, Yu Y, Wang S, Yang J, Ai X, Zhang N, et al. Genome-wide characterization of phospholipase D family genes in allotetraploid peanut and its diploid progenitors revealed their crucial roles in growth and abiotic stress responses. *Frontiers in Plant Science*. 2023 Jan 20;14:1102200. https://doi.org/10.3389/fpls.2023.1102200.

181. Tao X, Zhao M, Zhang Y, Liu M, Liu Q, Wang W, et al. Comparison of the expression of phospholipase D from Streptomyces halstedii in different hosts and its over-expression in Streptomyces lividans. *FEMS microbiology letters*. 2019 Mar;366(5):fnz051. https://doi.org/10.1093/femsle/fnz051.

182. Mendanha MIM. *Exploring the role of phospholipase D2 in mediating neuroinflammation in Alzheimer's Disease* (Doctoral dissertation). 2023. https://hdl.handle.net/1822/84701.

183. Bocckino SB, Blackmore P, Wilson P, Exton J. Phosphatidate accumulation in hormone-treated hepatocytes via a phospholipase D mechanism. *Journal of Biological Chemistry*. 1987 Nov 5;262(31):15309-15. https://doi.org/10.1016/S0021-9258(18)48176-8.

184. Baradaran M, Salabi F. Identification, classification and characterization of the dermonecrotic toxins in venom glands of Hottentotta saulcyi, Androctonus crassicauda and Hemiscorpius lepturus using transcriptome analysis.*Research sequre*. 2023. https://doi.org/10.21203/rs.3.rs-2501970/v1.

185. Arhab Y, Bessaa K, Abla H, Aydin M, Rahier R, Comte A, et al. Phospholipase D inhibitors screening: Probing and evaluation of ancient and novel molecules. *International Journal of Biological Macromolecules*. 2021 Jan 1;166:1131-40. https://doi.org/10.1016/j.ijbiomac.2020.10.268.

186. Arhab Y, Abousalham A, Noiriel A. Plant phospholipase D mining unravels new conserved residues important for catalytic activity. *Biochimica et Biophysica Acta (BBA)-Molecular and Cell Biology of Lipids*. 2019 May 1;1864(5):688-703. https://doi.org/10.1016/j.bbalip.2019.01.008.

187. Arhab Y, Abousalham A, Noiriel AJBeBA-M, Lipids CBo. Plant phospholipase D mining unravels new conserved residues important for catalytic activity. *National library of medicin.* 2019;1864(5):688-703.

188. Zhang Z, Chen M, Xu W, Zhang W, Zhang T, Guang C, et al. Microbial phospholipase D: Identification, modification and application. *Trends in Food Science & Technology*. 2020 Feb 1;96:145-56. https://doi.org/10.1016/j.tifs.2019.12.020.

189. Arhab Y, Bessaa K, Abla H, Aydin M, Rahier R, Comte A, et al. Phospholipase D inhibitors screening: Probing and evaluation of ancient and novel molecules. *International Journal of Biological Macromolecules*. 2021 Jan 1;166:1131-40. https://doi.org/10.1016/j.ijbiomac.2020.10.268.

190. Kattan RE, Han H, Seo G, Yang B, Lin Y, Dotson M, et al. Interactome Analysis of Human Phospholipase D and Phosphatidic Acid-Associated Protein Network. *Molecular & Cellular Proteomics*. 2022 Feb 1;21(2):100195. https://doi.org/10.1016/j.mcpro.2022.100195.

191. Bumpus TW, Baskin JMJACIE. A chemoenzymatic strategy for imaging cellular phosphatidic acid synthesis. *Angewandte Chemie International Edition.* 2016 Oct 10;55(42):13155-8. https://doi.org/10.1002/anie.201607443.

192. Selvy PE, Lavieri RR, Lindsley CW, Brown HA. Phospholipase D: enzymology, functionality, and chemical modulation. *Chemical reviews*. 2011 Oct 12;111(10):6064-119. https://doi.org/10.1021/cr200296t.

193. Goursot A, Mineva T, Krishnamurty S, Salahub DRJCJoC. Structural analysis of phosphatidyl choline lipids and glycerol precursors.*Canadian Journal of Chemistry*, 2009;87(10):1261-7. https://doi.org/10.1139/V09-056.

194. Yu B-Y, Cronholm TJBeBA-L, Metabolism L. Coupling of ethanol metabolism to lipid biosynthesis: labelling of the glycerol moieties of sn-glycerol-3-phosphate, a phosphatidic acid and a phosphatidylcholine in liver of rats given [1, 1-2H2] ethanol. *Biochimica et Biophysica Acta (BBA)-Lipids and Lipid Metabolism* 1997;1344(2):165-70. https://doi.org/10.1016/S0005-2760(96)00140-3.

195. Mulia K, Krisanti E, Terahadi F, Putri SJIJT. Selected natural deep eutectic solvents for the extraction of α-mangostin from mangosteen (Garcinia mangostana L.) pericarp. 2015;6(7):1211-20. DOI: http://dx.doi.org/10.14716/ijtech.v6i7.1984.

196. Christy AA, Egeberg PKJC, Systems IL. Quantitative determination of saturated and unsaturated fatty acids in edible oils by infrared spectroscopy and chemometrics. 2006;82(1-2):130-6. https://doi.org/10.1016/j.chemolab.2005.06.019.

197. Hassabo AG, Sharaawy S, Mohamed ALJJMI. *Saturated Fatty Acids Derivatives as Assistants Materials for Textile Processes*. J Textile Sci & Fashion Tech. 1 (4): 2018.516. DOI: 10.33552/JTSFT.2018.01.000516.

198. White EM, Holland AR, MacDonald GJB. Infrared Studies Reveal Unique Vibrations Associated with the PGK− ATP− 3-PG Ternary Complex. 2008;47(1):84-91. https://doi.org/10.1021/bi701723c.

Appendixes

Appendixes:

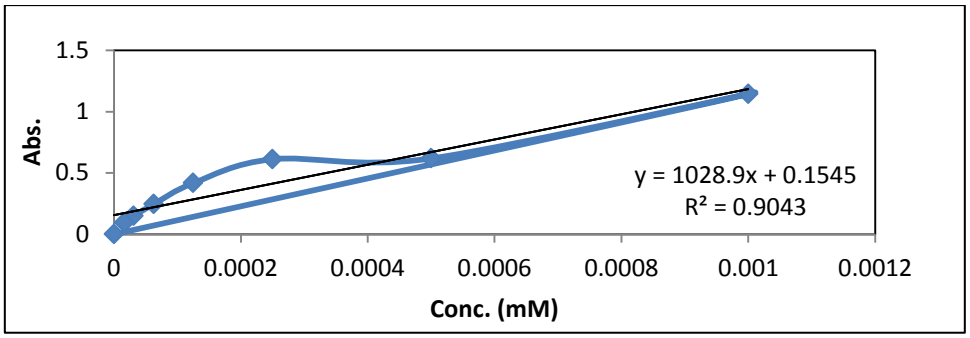

Appendix (1): Diagram of the PC hydrolysis reaction's calibration curve.

Appendix (2): represents the values used to draw the Michaelis-Menten and Line Weaver-Burk equations for the enzymatic hydrolysis reaction of PC.

[S] mM	K=V (min^{-1})	1/[S] mM^{-1}	1/V (min)
0.040	0.035	25.000	28.571
0.05	0.09	20.000	11.111
0.06	0.09	16.667	11.111
0.07	0.107	14.286	9.3458
0.08	0.052	12.500	19.231
0.09	0.079	11.111	12.658
0.1	0.063	10.000	15.873
0.12	0.02	8.333	50
0.14	0.543	7.143	1.8416
0.18	0.083	5.556	12.048
0.2	0.008	5.000	125
0.6	0.083	1.667	12.048
0.8	0.143	1.250	6.993

Appendix (3): Values for PC hydrolysis reaction's velocity plot against enzymatic activity.

Velocity (min^{-1})	Activity (U/mg)
0.013	0.146
0.026	0.292
0.056	0.584
0.072	0.73
0.087	0.876
0.117	1.168
0.145	1.46
0.175	1.752

Appendix (4): Values of the velocity versus temperature plot and the Arrhenius equation, respectively for hydrolysis reaction of PC.

T(C̊)	Velocity (min^{-1})
10	0.126
20	0.13
30	0.149
37	0.195
45	0.165

$1/T(K^{-1})$	ln k
0.00353	-2.07
0.00341	-2.04
0.0033	-1.90
0.00322	-1.63
0.00314	-1.80

Appendix (5): Show the data of velocity as an acidic function plot for the hydrolysis of PC.

pH	Velocity (min^{-1})
5	0.137
6	0.181
7	0.307
7.4	0.195
8	0.092
9	0.061
10	0.059

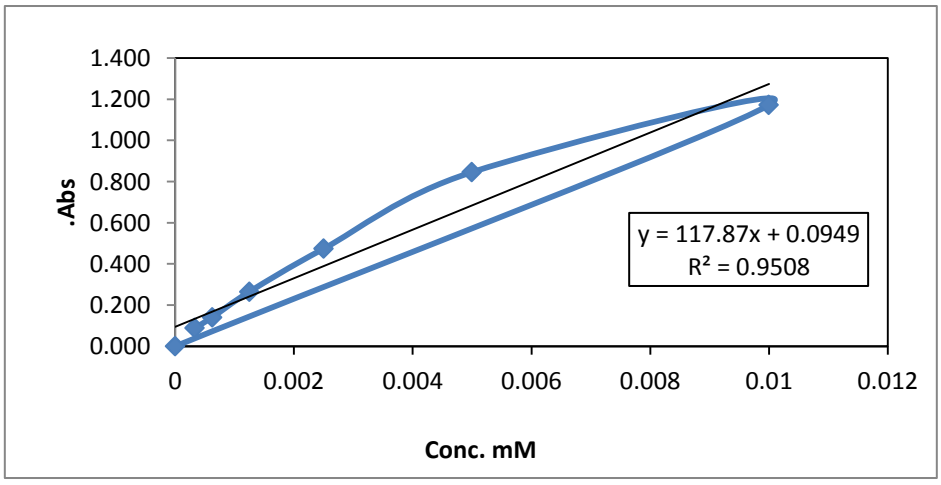

Appendix (6): Calibration curve diagram for the PS hydrolysis reaction.

Appendix (7): the parameters that were used to create the Line Weaver-Burk and Michaelis-Menten equations for PS's enzymatic hydrolysis process.

[S] M	V (min^{-1})	1/[S] mM $^{-1}$	1/V min
0.002	0.038	500.000	26.31578947
0.004	0.07	250.000	14.28571429
0.005	0.093	200.000	10.75268817
0.006	0.104	166.667	9.615384615
0.008	0.111	125.000	9.009009009

Appendix (8): Plotting the velocity values of the PS enzymatic hydrolysis reaction against enzymatic activity.

K=V (min^{-1})	Activity (U/mg)
0.026	0.584
0.0148	0.73
0.031	0.876
0.078	1.022
0.111	1.168
0.085	1.46
0.052	1.752

Appendix (9): The data for the enzymatic hydrolysis reactions of PS for the velocity versus temperature plot and the Arrhenius equation, respectively.

T(°C)	Velocity (min^{-1})
10	0.039
15	0.05
20	0.065
25	0.078
30	0.1
37	0.145
40	0.118
45	0.089

1/T(K^{-1})	ln k
0.0035	-3.24
0.0035	-3.00
0.0034	-2.73
0.0034	-2.55
0.0033	-2.30
0.0032	-1.93
0.0032	-2.14
0.0031	-2.42

Appendix (10): Display the velocity data in opposition to the pH for PS enzymatic hydrolysis reaction.

pH	Velocity (min^{-1})
4	0.019
5	0.026
6	0.034
7.4	0.049
8	0.06
9	0.083
10	0.073

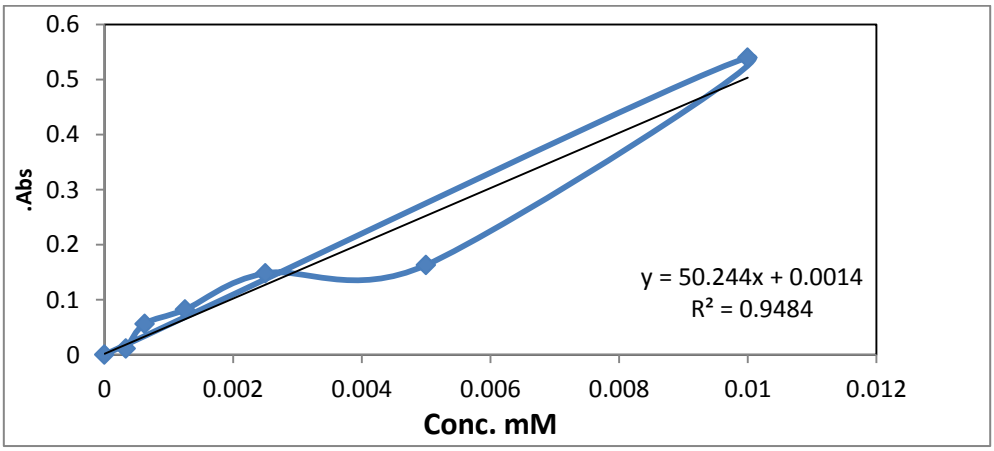

Appendix (11): PC ethyl substitution reaction calibration curve diagram.

Appendix (12): reflects the values that were utilised to create the Line weaver-Burk and Michaelis-Menten equations for the PC enzymatic ethyl substitution reaction.

[S] mM	K=V (min^{-1})	1/[S] mM^{-1}	1/V (min)
1	0.0536	1.00	18.6567
1.25	0.09	0.80	11.1111
1.5	0.075	0.67	13.3333
2	0.089	0.50	11.236

Appendix (13): Values for the velocity plot of the PC enzymatic hydrolysis reaction by ethanol vs. its enzymatic activity.

Velocity (min^{-1})	Activity (U/mg)
0.103	0.292
0.109	0.730
0.134	1.168
0.079	1.46
0.09	1.752

Appendix (14): The values of the velocity versus temperature plot and the Arrhenius equation, respectively for PC ethyl substitution reaction.

T(°C)	Velocity (min^{-1})
10	0.085
20	0.09
30	0.092
37	0.095
45	0.075

1/T(K^{-1})	ln k
0.0035	-2.4651
0.0034	-2.40795
0.0033	-2.38597
0.0032	-2.35388
0.0031	-2.59027

Appendix (15): Present the velocity data against the pH plot for PC ethyl substitution reaction.

pH	Velocity(min^{-1})
4	0.092
6	0.112
7.4	0.01
8	0.095
10	0.091

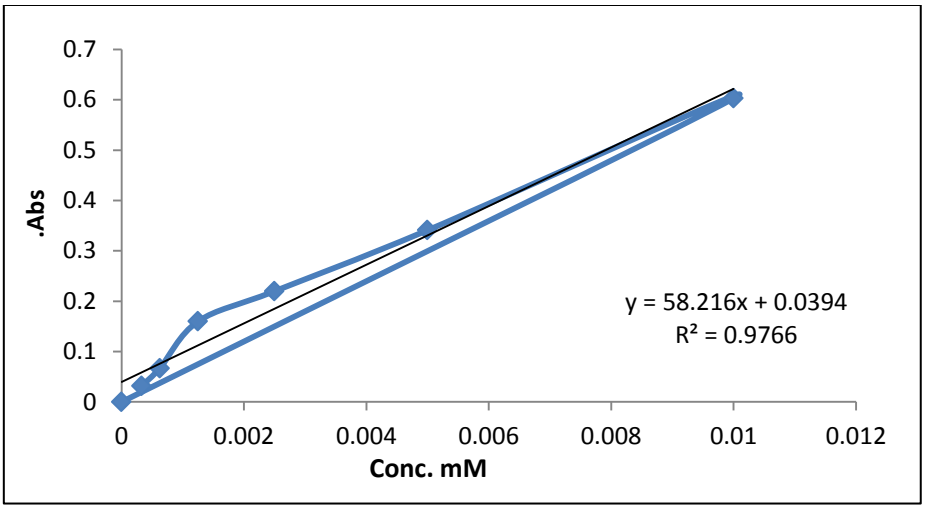

Appendix (16): PS ethyl substitution reaction calibration curve diagram.

Appendix (17): The values for the enzymatic hydrolysis reaction of PS with ethanol that were used to draw the Michaelis-Menten and Line Weaver-Burk equations.

[S] mM	V (min^{-1})	1/[S] mM $^{-1}$	1/V min
1	0.131	1	7.63359
1.25	0.151	0.80	6.62252
1.5	0.16	0.67	6.25
2	0.174	0.50	5.74713
2.5	0.178	0.40	5.61798

Appendix (18): The values of velocity plot against enzymatic activity for the ethyl substitution reaction of PS.

Velocity (min^{-1})	Activity (U/mg)
0.083	0.292
0.07	0.73
0.041	1.168
0.059	1.46
0.015	1.752

Appendix (19): The Values of the velocity versus temperature plot and the Arrhenius equation, respectively for enzymatic hydrolysis reaction of PS by ethanol.

T(°C)	Velocity (min^{-1})
10	0.038
20	0.059
30	0.096
37	0.098
45	0.08

1/T(K^{-1})	ln k
0.004	-3.270
0.003	-2.830
0.003	-2.343
0.003	-2.323
0.003	-2.526

Appendix (20): Show the PS ethyl substitution reaction velocity data versus the pH plot.

pH	Velocity(min^{-1})
4	0.064
6	0.099
7.4	0.069
8	0.066
10	0.057

الخلاصـــــــــــــــــــة

تلعب الدهون الفوسفاتية دورًا مهمًا في بناء جميع أغشية الخلايا لدى الحيوانات. بالإضافة إلى ذلك، فإن الدهون الفوسفاتية عبارة عن مركبات أمفيفيلية توجد على نطاق واسع في النظام الحي. بشكل عام، يمكن تقسيم الدهون الفوسفاتية إلى مجموعتين: سفينغوميالين وجليسيروفوسفوليبيد، والتي تشمل فوسفاتيديل كولين، فوسفاتيديل سيرين، فوسفاتيديل إيثانولامين، فوسفاتيديل جليسيرول وفوسفاتيديل اينوسيتول.

التحلل المائي للدهون الفوسفاتية هو التفاعل الرئيسي لتحلل الدهون الذي يحفز في وجود إنزيمات محددة تعرف باسم الفسفولييباز. في المختبر، هناك العديد من الدراسات لفهم آلية تحلل الفوسفات وما هو تأثير المحيط على هذا التفاعل.

ركزت الدراسة الحالية على مراقبة تفاعل التحلل المائي للـ فوسفاتيديل كولين، في الوسط الحامضي ومقارنته بنفس التفاعل في الوسط الكحولي لمعرفة تأثير البيئة الكحولية على هذا التفاعل. تم فصل جميع نواتج التحلل المائي ل فوسفاتيديل كولين في كل من البيئة الحامضية والكحولية وتشخيصها باستخدام تقنيات التحليل الطيفي للكتلة والرنين المغناطيسي وتقنية الاشعة تحت الحمراء.

اعتماداً على النتائج تم اقتراح ميكانيكيات التحلل المائي فوسفاتيديل كولين في كل من المحيط الحامضي والكحولي. كانت النواتج النهائية للتحلل المائي فوسفاتيديل كولين في الوسط الحامضي هي كلوريد الكولين وحامض البالمتيك وحامض أوكتاديكا-9،12-دينويك والجلسرين-3-فوسفات. ومع ذلك، فإن التحلل المائي فوسفاتيديل كولين في الإيثانول اعطى النواتج التالية: كلوريد الكولين، وإيثيل بالميتات، وإيثيل أوكتاديكا-9,12-دينوات، والجلسرين-3-فوسفات. يمكن ملاحظة أن الجلسرين -3-فوسفات يتكون في كلا التفاعلين باعتباره العمود الفقري فوسفاتيديل كولين، كما تم إنتاج كلوريد الكولين أثناء التفكك من مجموعة الفوسفات فوسفاتيديل كولين.

تم اعادة نفس التفاعلات المذكورة أعلاه لأثنين من الدهون الفوسفاتية، وهما فوسفاتيديل كولين وفوسفاتيديل سيرين، على التوالي، في وجود فسفولييباز D (PLD) كعامل محفز. وتمت دراسة حركية تفكك الكولين من مجموعة الفوسفات في وجود PLD من خلال تطبيق معادلة ميكايليس-مينتن. تم تحديد السرعة القصوى (Vmax) وثابت Michaelis-Menten (Km) لجميع تفاعلات التحلل المائي الإنزيمي فوسفاتيديل كولين ولفوسفاتيديل سيرين في وجود PLD في البيئات الحامضية والكحولية. كان مستوى الالفة بين فوسفاتيديل كولين والإنزيم في حالة استخدام

الإيثانول كمذيب هو الأقل بين التفاعلات الأخرى لأنه كان له أعلى قيمة كم تبلغ 3.664. ومع ذلك، كان تفاعل التحلل المائي الإنزيمي لـ لفوسفاتيديل سيرين هو الأعلى الفة من بين التفاعلات الأخرى من خلال الحصول على أقل قيمة ثابت مكاليس منتن.

بالإضافة إلى ذلك، تم إجراء تحديد الظروف المثلى لتفاعلات التحلل المائي الأنزيمي التي شملت تحديد تركيز المادة الاساس، والنشاط الأنزيمي، ودرجة الحموضة، ودرجة الحرارة للتأكد من أن هذا التحلل المائي الإنزيمي يحاكي ما يحدث في النظام الحيوي. تم ايجاد الدوال الديناميكية الحرارية والتي تشمل التغير في المحتوى الحراري (ΔH) وتغير الطاقة الحرة لجيبس (ΔG)وتغير الإنتروبي (ΔS). كانت جميع تفاعلات التحلل المائي الإنزيمي للفوسفاتيديل كولين، والفوسفاتيديل سيرين في وجود PLD مواتية من الناحية الديناميكية الحرارية .

أظهرت هذه الدراسة أن جميع تفاعلات التحلل المائي للدهون الفوسفاتية في غياب الإنزيم تكون أبطأ من تفاعلات التحلل في وجود.PLD ونتيجة لذلك، تم عزل وتمييز جميع منتجات التحلل المائي فوسفاتيديل كولين بدون وجود الإنزيم بسلاسة. ومع ذلك، لم يتمكن من عزل المنتجات الخاصة بالتحلل المائي الإنزيمي للفوسفاتيديل كولين والفوسفاتيديل سيرين نظرًا لأن التفاعلات سريعة جدًا.

على الرغم من التشابه في آليات تفاعل التحلل المائي للدهون الفوسفاتية (فوسفاتيديل كولين، والفوسفاتيديل سيرين) في بيئات مختلفة (الحامضية والكحولية)، فإن الاختلافات في المنتجات الثانوية قد توفر لنا رؤية جيدة للتنبؤ بتأثير المذيب على هذه العملية. نظرًا للتطبيقات المختلفة للفوسفاتيديل كولين والفوسفاتيديل سيرين، فإن فهم تأثير البيئة الكحولية يمكن أن يساعد مصانع الأدوية ومستحضرات التجميل والأغذية على تصميم تجارب مناسبة لتقليل تأثير هذه المنتجات الثانوية على كفاءة المنتج الرئيسي وإنتاجيته.

جامعة كربلاء

كلية العلوم

قسم الكيمياء

دراسة تفاعلات الاستبدال الإنزيمي لمشتقات الفوسفاتيديل في الوسط الكحولي والحامضي

رسالة مقدمة الى

مجلس كلية العلوم – جامعة كربلاء

كجزء من استكمال متطلبات نيل درجة الماجستير في الكيمياء

من قبل

إكرام سالم حسين خشان

بكالوريوس علوم في الكيمياء (2012) / جامعة كربلاء

بأشراف

أ.م. د. ثائر مهدي مدلول

كانون الأول \ ٢٠٢٣ م **جمادى الاخرة \ ١٤٤٥ هـ**